

Design of a Standardized *in vitro* Model of Skeletal Muscle Regeneration For Implantable Fibrin Microthread Scaffolds

A Major Qualifying Project Report

Submitted to the Faculty

of

Worcester Polytechnic Institute

In partial fulfillment of the requirements for the

Degree of Bachelor Science

By

Erin Heinle

Emily Morra

Emily Mossman

Alyssa Paul

Advisors:

Professor George Pins

Professor Catherine Whittington

25 April 2019

Table of Contents

Table of Contents	1
Authorship	8
Table of Figures	14
Table of Tables	16
Acknowledgements	17
1.0 Introduction	18
2.0 Literature Review	24
2.1 Volumetric Muscle Loss (VML)	24
2.2 Skeletal Muscle	25
2.2.1 Anatomy and Physiology	25
2.2.2 Wound Healing	26
2.2.3 Current Treatments for VML	28
2.2.4 Clinical Need	29
2.3 Tissue Engineering Scaffolds	30
2.3.1 Decellularized Extracellular Matrix Scaffolds	31
2.3.2 Hydrogel Scaffolds	34
2.3.3 Fibrin Based Microthread Scaffolds	35
2.3.4. Need for Tissue Engineered Scaffolds for VML	39

2.4 <i>In Vitro</i> Assays for Tissue Regeneration	40
2.4.1 2-Dimensional (2D) Assays	41
2.4.2 Need for 3D <i>in vitro</i> Assays	43
2.4.3 3-Dimensional Assays	44
2.4.3.1 Scaffold-Based Approaches	44
2.4.3.2 Non-scaffold Based Approaches	46
2.4.3.3 Current 3D <i>in vitro</i> Fibrin Microthread Scaffold Model	47
3.0 Project Strategy	49
3.1 Stakeholders	49
3.2 Initial Client Statement	50
3.3 Objectives	51
3.4 Constraints	56
3.4.1 Design Dimension Constraints	56
3.5 Quantitative Analysis of Objectives	57
3.6 Functions and Specifications	59
3.6.1 Six or more sufficient fibrin microthread - C2C12 cell gel interfaces	59
3.6.2 Fixturing mechanism of fibrin microthreads onto PDMS frame	60
3.6.3 Support cell culture environment	60
3.6.4 Data capture and imaging of six or more thread-gel interfaces	61
3.7 Engineering Standards	61

3.8 Revised Client Statement	62
4.0 The Design Process	64
4.1 Needs Analysis	64
4.2 Design Alternatives	66
4.2.1 Thread-Gel Interface	67
4.2.2 Fixturing System	72
4.2.3 Data Collection Throughput	76
4.3 Means Analysis	77
4.4 Feasible Designs	79
4.5 Final Design	82
5.0 Design Development and Validation Plan	83
5.1 Three-Dimensional <i>in vitro</i> Assay Development and Analysis	83
5.1.1 Mold for PDMS Frame	83
5.1.2 Cutting Tool and Guide for Fibrin Microthread Fixturing Slits	87
5.2 Three-Dimensional <i>in vitro</i> Assay Verification Studies	89
5.2.1 Assembly Testing	89
5.2.1.1 Pins Lab Model Assembly Test	90
5.2.1.2 ML Model Assembly Test	93
5.2.2 Reproducibility Testing and Sustainability Analysis	97
5.2.2.1 Pins Lab Model Reproducibility and Sustainability Tests	98

5.2.2.2 ML Model Reproducibility and Sustainability Tests	99
5.2.3 Cell Viability Research	100
5.2.4 Sterilization Method	102
5.2.4.1 Ethylene Oxide Sterilization	102
5.2.5 Cellular Outgrowth Assay Validation	102
6.0 Final Design and Results of Validation Testing	104
6.1 Overview of Final Design	104
6.2 Objectives Achieved	105
6.2.1 Ease of Use: Assembly	105
6.2.1.1 Mold for PDMS Frame	105
6.2.1.2 Cutting Guide and Cutting Tool for Fibrin Microthread Fixation Slits	109
6.2.2 Reproducibility: Frame Fabrication	109
6.2.2.1 Mold for PDMS Frame	109
6.2.2.2 Cutting Guide and Cutting Tool for Fibrin Microthread Fixation Slits	111
6.2.3 Cost Efficient	113
6.2.3.1 Mold for PDMS Frame	113
6.2.3.2 Cutting Guide and Cutting Tool for Fibrin Microthread Fixation Slits	114
6.2.4 Interface with 3D Scaffold	115
6.2.4.1 Mold for PDMS Frame	115
6.2.4.2 Cutting Guide and Cutting Tool for Fibrin Microthread fixation slits	116

6.2.5 Support of Cellular Outgrowth on 3D Scaffold	116
6.2.5.1 Cellular Outgrowth Assay Validation Experiment 1	116
6.2.5.2 Cellular Outgrowth Assay Validation Experiment 2	117
6.2.5.3 Cellular Outgrowth Assay Validation Experiment 3	117
6.2.5.4 Cellular Outgrowth Assay Validation Experiment 4	118
6.2.5.5 Cellular Outgrowth Assay Validation: 96hr Outcome	119
6.3 Impact Analysis of PDMS Frame	119
6.3.1 Economic Impact	120
6.3.2 Environmental Impact	121
6.3.3 Health and Safety Impact	122
6.3.4 Societal Impact	122
6.3.5 Political Impact	123
6.3.6 Ethical Impact	123
6.3.7 Manufacturing Impact	124
6.3.8 Sustainability	124
7.0 Discussion of Results	126
7.1 Development of 3D <i>in vitro</i> Assay	126
7.1.1 Mold for PDMS Frame	126
7.1.2 Cutting Guide and Cutting Tool for Fibrin Microthread Fixturing Slits	126
7.2 Assembly Testing	127

7.3 Reproducibility and Sustainability Analysis	127
7.3.1 Reproducibility Testing	128
7.3.2 Sustainability Analysis	128
7.4 Cell Outgrowth Assay Viability	129
7.5 Cost Analysis	130
7.6 Comparison to Existing Research	130
8.0 Conclusions and Future Work	132
8.1 Conclusions	132
8.2 Future Work	132
References	135
Appendices	139
Appendix A: Fibrin Microthread Protocol	139
Appendix B: User Interview Notes	141
Appendix C: Industry/Company Interview Notes	143
Appendix D: Client Interview Notes	145
Appendix E: Research Team Pairwise Comparison Chart	147
Appendix F: Decision Matrix Criteria	148
Appendix G: User Variability Assembly Testing: Pins Lab Model	150
Appendix H: User Variability Assembly Testing: ML Model	153
Appendix I: Frame Reproducibility Testing Protocol	157

Appendix J: Sustainability Analysis Protocol	159
Appendix K: “OG” Outgrowth Assay Protocol	160
Appendix L: ML Model Outgrowth Assay Protocol	163
Appendix M: PDMS Mold Drawing for Machining	172
Appendix N: PDMS Mold Drawing for Machining	173
Appendix O: Cutting Guide Drawing	174
Appendix P: Imaging Exposure Settings	175
Appendix Q: Outgrowth Images: 24-96hr	176
Appendix R: Gantt Chart	177
A Term	177
B Term	178
C Term	179
D Term	180
Appendix S: Expense Report/Budget Analysis	181
Appendix T: Bill of Materials	182

Authorship

1.0 Introduction	Alyssa and Emily Mossman
2.0 Literature Review	Erin and Emily Mossman
2.1 Volumetric Muscle Loss (VML)	Erin
2.2 Skeletal Muscle	Erin
2.2.1 Anatomy and Physiology	Erin
2.2.2 Wound Healing	Erin
2.2.3 Current Treatments for VML	Erin
2.2.4 Clinical Need	Erin
2.3 Tissue Engineering Scaffolds	Emily Mossman
2.3.1 Decellularized ECM Scaffolds	Emily Mossman
2.3.2 Hydrogel Scaffolds	Emily Mossman
2.3.3 Fibrin Based Microthread Scaffolds	Emily Mossman
2.3.4 Need for Tissue Engineered Scaffolds for VML	Emily Mossman
2.4 Assays for Tissue Regeneration	Emily Morra
2.4.1 2-Dimensional Assays	Emily Morra
2.4.2 Need for 3D <i>in vitro</i> Assays	Emily Morra
2.4.3 3-Dimensional Assays	Emily Morra
3.0 Project Strategy	Team
3.1 Stakeholders	Alyssa
3.2 Initial Client Statement	Alyssa
3.3 Objectives	Alyssa and Emily Morra
3.4 Constraints	Alyssa and Emily Morra
3.4.1 Design Dimension Constraints	Emily Morra

3.5 Quantitative Analysis of Objectives	Alyssa
3.6 Functions and Specifications	Alyssa
3.6.1 Thread-gel interface	Alyssa
3.6.2 Fixturing mechanism	Alyssa
3.6.3 Cell culture environment	Alyssa
3.6.4 Data capture	Alyssa
3.7 Engineering Standards	Erin
3.8 Revised Client Statement	Alyssa
4.0 The Design Process	Team
4.1 Needs Analysis	Alyssa
4.2 Design Alternatives	Emily Mossman
4.2.1 Thread-Gel Interface	Emily Mossman
4.2.2 Fixturing System	Emily Mossman
4.2.3 Data Collection Throughput	Emily Mossman
4.3 Means Analysis	Erin
4.4 Feasible Designs	Emily Morra
4.5 Final Design	Emily Morra
5.0 Design Verification	Emily Morra and Emily Mossman
5.1 3D <i>in vitro</i> Assay Development and Analysis	Emily Morra
5.1.1 Mold for PDMS Frame	Emily Morra
5.1.2 Cutting Guide for Fibrin Microthread Fixturing Slits	Emily Morra
5.2 3D <i>in vitro</i> Assay Verification Studies	Emily Mossman
5.2.1 Assembly Testing	Emily Mossman
5.2.2 Reproducibility Testing	Emily Morra and Emily Mossman

5.2.3 Cell Viability Research	Emily Mossman
5.2.4 Sterilization Method	Alyssa
5.2.5 Cellular Outgrowth Validation	Emily Mossman
6.0 Final Design and Validation	Team
6.1 Overview of Final Design	Emily Morra
6.2 Objectives Achieved	Alyssa
6.2.1 Ease of Use: Assembly	Alyssa
6.2.1.1 Mold for PDMS Frame	Alyssa and Emily Mossman
6.2.1.2 Cutting Guide and Cutting Tool for Fibrin Microthread fixation slits	Alyssa
6.2.2 Reproducibility: Frame Fabrication	Emily Mossman
6.2.2.1 Mold for PDMS Frame	Emily Mossman
6.2.2.2 Cutting Guide and Cutting Tool for Fibrin Microthread fixation slits	Emily Mossman
6.2.3 Cost Efficient	Emily Mossman
6.2.3.1 Mold for PDMS Frame	Emily Mossman
6.2.3.2 Cutting Guide and Cutting Tool for Fibrin Microthread fixation slits	Emily Mossman
6.2.4 Interface with 3D Scaffold	Alyssa
6.2.4.1 Mold for PDMS Frame	Alyssa
6.2.4.2 Cutting Guide and Cutting Tool for Fibrin Microthread fixation slits	Alyssa
6.2.5 Support of Cellular Outgrowth on 3D Scaffold	Emily Mossman
6.2.5.1 Cellular Outgrowth Assay Validation Experiment 1	Emily Mossman

6.2.5.2 Cellular Outgrowth Assay Validation Experiment 2	Emily Mossman
6.2.5.3 Cellular Outgrowth Assay Validation Experiment 3	Emily Mossman
6.2.5.4 Cellular Outgrowth Assay Validation Experiment 4	Emily Mossman
6.2.5.5 Cellular Outgrowth Assay Validation: 96hr Outcome	Emily Mossman
6.3 Impact Analysis of PDMS Frame	Erin and Alyssa
6.3.1 Economic Impact	Alyssa
6.3.2 Environmental Impact	Alyssa
6.3.3 Health and Safety Impact	Alyssa
6.3.4 Societal Impact	Erin
6.3.5 Political Impact	Erin
6.3.6 Ethical Impact	Erin
6.3.7 Manufacturing Impact	Erin
6.3.8 Sustainability	Erin
7.0 Discussion of Results	
7.1 Development of 3D in vitro Assay	Alyssa and Emily Morra
7.1.1 Mold for PDMS Frame	Alyssa and Emily Morra
7.1.2 Cutting Guide and Cutting Tool for Fibrin Microthread Fixturing Slits	Alyssa and Emily Morra
7.2 Assembly Testing	Alyssa and Emily Morra
7.3 Reproducibility and Sustainability Analysis	Alyssa and Emily Morra
7.3.1 Reproducibility Testing	Alyssa and Emily Morra

7.3.2 Sustainability Analysis	Alyssa and Emily Morra
7.4 Cell Outgrowth Assay Viability	Alyssa and Emily Morra
7.5 Cost Analysis	Emily Mossman
7.6 Comparison to Existing Research	Erin
8.0 Conclusions and Future Work	Alyssa
8.1 Conclusions	Alyssa
8.2 Future Work	Alyssa
Appendices	
Appendix A: Fibrin Microthread Protocol	Team
Appendix B: User Interview Notes	Team
Appendix C: Industry/Company Interview Notes	Team
Appendix D: Client Interview Notes	Team
Appendix E: Research Team Pairwise Comparison Chart	Team
Appendix F: Decision Matrix Criteria	Team
Appendix G: User Variability Assembly Testing: Pins Lab Model	Emily Morra
Appendix H: User Variability Assembly Testing: ML Model	Emily Morra
Appendix I: Frame Reproducibility Testing Protocol	Emily Morra
Appendix J: Sustainability Analysis Protocol	Emily Morra
Appendix K: “OG” Outgrowth Assay Protocol	Pins Lab
Appendix L: ML Model Outgrowth Assay Protocol	Emily Morra
Appendix M: PDMS Mold Drawing for Machining	Emily Morra

Appendix N: PDMS Mold Drawing for Machining (Section View)	Emily Morra
Appendix O: Cutting Guard Drawing	Emily Morra
Appendix P: Imaging Exposure Settings	Emily Mossman
Appendix Q: Outgrowth Images: 24-96hr	Emily Mossman and Alyssa
Appendix R: Gantt Chart	Alyssa
A Term	Alyssa
B Term	Alyssa
C Term	Alyssa
D Term	Alyssa
Appendix S: Expense Report/Budget Analysis	Team
Appendix T: Bill of Materials	Emily Morra

Table of Figures

Figure 1. Calf muscle VML injury	18
Figure 2. Structure of muscle tissue	25
Figure 3. Schematic of muscle regeneration	27
Figure 4. Healthy versus scarred muscle tissue	28
Figure 5. Histological sections of recovering muscle	36
Figure 6. Histological analysis of various treatments	39
Figure 7. 2D <i>in-vitro</i> scratch assay	42
Figure 8. 2D <i>in-vitro</i> cell exclusion zone assay	43
Figure 9. Current PDMS frame model in Pins Lab	47
Figure 10. Project objectives hierarchical tree	52
Figure 11. Means 1: thread-gel interface	68
Figure 12. Means 2: thread-gel interface	69
Figure 13. Means 3: thread-gel interface	71
Figure 14. Means 1: fixturing system	72
Figure 15. Means 2: fixturing system	74
Figure 16. Means 3: fixturing system	75
Figure 17. Location of data collection points for thread-gel interfaces	77
Figure 18. “The Grill” design	80
Figure 19. “The Sandwich” design	81
Figure 20. “The Grilled Cheese” design	81
Figure 21. Overview of final design	82
Figure 22. Durable resin mold	84
Figure 23. Biocompatible resin mold	85
Figure 24. Tough resin two-piece mold	86
Figure 25. Machined Delrin™ acetal plastic mold	87
Figure 26. PDMS frame made in Delrin™ mold	87
Figure 27. Cutting tool and PLA cutting guard	88
Figure 28. PDMS frames placed in PLA cutting guard	89
Figure 29. Steps taken to construct the 6 PDMS rings for Pins Lab Model	91

Figure 30. Steps taken to construct the Thermanox® stage for Pins Lab Model	92
Figure 31. Steps taken to construct place fibrin microthreads for the Pins Lab Model	93
Figure 32. Steps taken to construct 6 PDMS frames for ML Model	94
Figure 33. Steps taken to construct fixation slits for ML Model	95
Figure 34. Steps taken to place Thermanox® stage for ML Model	96
Figure 35. Steps taken to place fibrin microthreads in ML Model	97
Figure 36. Pins Lab Model PDMS frames for reproducibility testing	98
Figure 37. Side width measurement positions and slit distance for Pins Lab Model	99
Figure 38. Side width measurement positions and slit distance for ML Model	100
Figure 39. Setup steps for both the Pins and ML Model	106
Figure 40. Data: Assembly time (Pins vs ML Model)	108
Figure 41. Width measurements: Pins vs ML Model	110
Figure 42. Data: Width of PDMS frames (Pins vs ML Model)* (p<0.05)	111
Figure 43. Distance between fixturing slits: Pins vs ML Model	112
Figure 44. Data: Distance between fixturing slits on PDMS frames (Pins vs ML Model)* (p<0.05)	113
Figure 45. Cost of PDMS waste: Pins vs ML Model* (p<0.05)	114
Figure 46. Contamination seen in Exp 3	118
Figure 47. Outgrowth assay: 96hr observation	119

Table of Tables

Table 1. Main objective definitions	53
Table 2. Sub-objective definitions for Ease of Use	53
Table 3. Sub-objective definitions for Reproducible	54
Table 4. Sub-objective definitions for Interface with 3D Scaffolds	54
Table 5. Sub-objective definitions for Support Cellular Characterization	55
Table 6. Sub-objective definitions for Cost-Efficient	55
Table 7. Project constraints	56
Table 8. Pairwise comparison chart	58
Table 9. Objective weights	58
Table 10. Current assay setup and elapsed time	65
Table 11. Means for each function	67
Table 12. Pros and cons for means 1 (thread-gel interface)	68
Table 13. Pros and cons for means 2 (thread-gel interface)	70
Table 14. Pros and cons for means 3 (thread-gel interface)	71
Table 15. Pros and cons for means 1 (fixturing system)	73
Table 16. Pros and cons for means 2 (fixturing system)	74
Table 17. Pros and cons for means 3 (fixturing system)	75
Table 18. Decision Matrix	78
Table 19. Assembly time for four assembly steps: Pins Lab Model	107
Table 20. Assembly times for four assembly steps: ML Model	107
Table 21. Cost analysis for ML Model assembly kit	115

Acknowledgements

The team would like to acknowledge all of those who helped to make our project successful; the Biomedical Engineering (BME) Department for funding and providing academic grounds for this project, our advisors Dr. George Pins and Dr. Catherine Whittington for advising our project and teaching us along the way, and Ph.D. candidate Meagan Carnes for helping in the lab and providing user insight. The team would also like to acknowledge Leonard Polizzotto Ph.D., Distinguished Executive in Residence, for his commitment to assisting the team with project development and Value Creation. We would like to thank Victoria Huntress for her assistance in operating the imaging equipment. Additionally, thank you to Dr. Glenn Gaudette of the KEEN team for helping to make this project experience possible, to Lisa Wall for continued support in making sure laboratory products were readily available, as well as the BME department head, Kristen Billiar.

1.0 Introduction

During the recent Operation Iraqi Freedom and Operation Enduring Freedom, 82% of soldiers injured during battle suffered from a musculoskeletal extremity wound (Devore, 2011). Powerful bombs, Improvised Explosive Devices (IEDs), and firearms that cause these injuries remove soldiers from the battlefield surviving what were once non-survivable injuries just a couple of decades ago. The rapid triage, emergent medical evacuation and strategically placed Combat Army Surgical Hospitals providing immediate surgical intervention have significantly increased the survival rate of those soldiers who face large traumas, but this leads our injured military members into a new battle. Many recovering soldiers have to endure large functional and morphological damage, as many of these wounds can cause volumetric muscle loss (VML) (Figure 1).

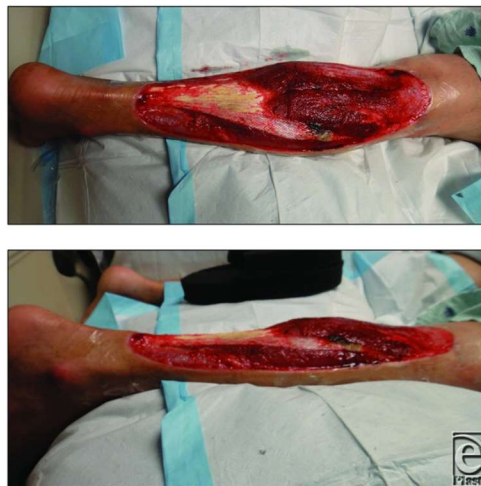


Figure 1. Left: Calf muscle VML (Sahar, 2013)

Skeletal muscle accounts for 45% of body mass and can heal itself and restore function when small-scale injuries occur to the myofibers (Tidball, 2010). VML occurs when the basement membrane that recruits and forms new muscle cells is damaged at the wound site. As a result, muscle cannot properly heal and form functional tissue. At the site of the wound, muscle

cells are not able to align uniaxially to restore function. Additionally, fibroblasts invade the wound site, forming disorganized scar tissue. Over 4.5 million reconstructive surgeries involving VML are performed annually which include burn victims, trauma patients, injured sports players, and maxillofacial reconstructive patients (Grasman, 2015). The most common reconstructive surgery performed to treat VML injuries is an autologous tissue transfer wherein healthy muscle tissue is taken from somewhere else in the body and is implanted at the wound site in an attempt to restore function. However, autologous tissue transfers have a high rate of failure, result in donor site morbidity, and are expensive (Sahar, 2013). Additionally, the average lifetime disability cost for veterans suffering from a VML injury is on average \$341,300 (Corona, 2015).

There is a need for an approach that provides biophysical and biochemical cues for the muscle cells to regrow functional tissue at the site of the wound. One approach is an implantable therapy which would provide biophysical and biochemical cues to signal for muscle cells to regrow and restore function to the damaged tissue. The Pins lab has shown promising results with fibrin microthreads as an implantable scaffold for VML. The fibrin microthreads provide a uniaxially aligned scaffold for myoblasts (muscle cell precursors) to grow out onto while also functioning as a delivery vehicle for growth factors to increase cell proliferation (Litvinov, 2016). *In vitro* studies can be carried out to test these factors in order to maximize the structural, mechanical, biological, and chemical properties of the fibrin microthreads to predict and improve *in vivo* results (Grasman, 2015 & 2017).

There currently exists no reproducible *in vitro* 3D modeling system that fully predicts the interactions cells have with the scaffold *in vivo*. Therefore, the design team worked to design, develop, and test a more reproducible 3D *in vitro* model for fibrin microthreads as a treatment for skeletal muscle regeneration. The overarching goal of this project is to develop a

standardized model that will provide researchers with reproducible, higher throughput *in vitro* results, which will increase overall confidence in study results for tested treatments in advance of *in vivo* studies. The team developed an initial set of objectives, but refined those objectives (and detailed sub-objectives) upon client and user interviews and further background research. Each objective was further broken down to define sub-objectives for the project. A list of constraints was created and utilized to remain within the scope of the project.

Using an objectives tree, the team developed a decision matrix that was used to make pairwise comparison charts for the design of the assay. It was determined that the model must be **easy to use, reproducible** between users, **interface with 3D scaffolds** (fibrin microthreads), **support cellular characterization**, and remain **cost efficient**. The results of the pairwise comparison led the team to focus on which objectives were of highest priority, and their respective functions. Reproducibility, ability to interface with 3D scaffolds, and cellular characterization/efficient data collection were the highest priority of all of the clients, users, and team. The team then used the prioritized objectives to develop a series of functions for the model:

1. Six or more sufficient fibrin microthread - C2C12 cell gel interfaces
2. Fixturing mechanism of fibrin microthreads
3. Support cell culture environment
4. Data capture and imaging of six or more thread-gel interfaces

From these initial functions, multiple design iterations were created and researched. Each design iteration combined several methods of the above functions, guiding the team to determine which method for each function was most ideal. The team determined that a Thermanox® coverslip was the best surface for the cell gel to be deposited onto, as it has the ideal properties to maintain

surface tension for the gel to interact with the fibrin microthreads. For the fixturing method, it was determined that manually cut slits into the PDMS with a razor blade were most effective at securing the thread without disrupting the sterilization process. It was determined that in order to standardize the dimensions of the PDMS frames, a mold which would create PDMS frames with a groove for Thermanox® placement could be used. Additionally, a cutting guide 3D printed out of acrylonitrile butadiene styrene (PLA), and a cutting tool of three equidistantly spaced razor blades, were made to minimize user variability when cutting slits while increasing data throughput.

Once the final design for making the frames was selected, experimentation was performed to validate and optimize the design. The final design is composed of 3 separate components: a mold for making PDMS frames, a cutting guide, and cutting tool. Potential materials for the mold were heat tested to ensure they could withstand being in the oven for at least one hour at 60°C which is necessary for complete PDMS curing. The team tested molds made from biocompatible, flexible, tough, and durable resins, in addition to Delrin™, manufactured by DuPont, plastic by placing each mold in the oven for 2 hours and observing the material for deformation or breakage. It was determined by the team that any observable deformation was unacceptable. Each material was tested to ensure it could properly cure and release the PDMS frames. Out of the available 3D resins and machining materials, it was observed that only Delrin™ plastic passed both heat testing and PDMS curing testing.

Through these experiments, the team was able to confirm that Delrin™ plastic was the optimal material to create the mold for the PDMS frames. Additional research was done, and it was found in the literature that experiments had been performed which determined that Delrin™ is not cytotoxic and would therefore not leach any chemicals into the PDMS frames that would

affect the viability of the cells during the assay (Penick et al., 2005). Therefore, cell viability testing on the frames was not needed.

To validate that this design improved standardization of the frames, assembly testing was done to compare the model created by the design team to the current Pins Lab Model. Initial assembly testing for the Pins Model included the cutting and shaping of six PDMS rings, cutting slits into the PDMS using a razor blade, placing three fibrin microthreads per ring, and constructing six Thermanox® cell-gel stages. This was then compared to the six PDMS frames that the team removed from the mold. Using the rapid prototyped PLA cutting guide, razor slits were made into the PDMS frames. The assembly time for each model was compared, and the team determined their model decreased assembly from fifteen to eight steps.

To validate the reproducibility of the design, the team created 48 models using the Pins Lab method and 24 models using the Muscle Ladies Model (ML Model). The wall thickness of each PDMS frame was measured using calipers and recorded. The distance between slits for fibrin microthread fixturing was also measured and recorded. It was determined that the ML Model decreased assembly time by 42.8%, reduced PDMS frame width variability by 94.4%, and reduced fibrin microthread fixation slit variability by 83.0%.

The ML Model is a reusable, cost-effective kit that can be used within the Pins Lab and other labs which investigate the use of scaffolds to achieve reproducible *in vitro* results capable of predicting *in vivo* response to the scaffold implanted in a wound site. This standardized design and protocol will provide more valid cellular outgrowth assay results, as the dimensions are the same for each frame, and each setup has negligible variability. Future studies could be used to quantify the reproducibility of outgrowth assay results, as preliminary testing confirmed that outgrowth is sustainable over 96 hours.

The team recognizes and discussed design changes that should be made to future iterations of this project, such as the depth of the Thermanox® groove on the PDMS frame. Future applications of this project include testing the ML Model with growth factor threads (HGF, etc.) and altering mechanical properties of the fibrin microthreads (UV treatment, bundling, etc.) to better reflect *in vivo* conditions. Additionally, we recommend the creation and study of a multicellular design incorporating muscle, nerve, and endothelial cells to better mimic native muscle tissue growth.

2.0 Literature Review

2.1 Volumetric Muscle Loss (VML)

Since the beginning of Operation Enduring Freedom and Operation Iraqi Freedom, more than 40,000 soldiers have suffered casualties (Wenke, 2011). While advancements in protective gear and medical care on the battlefield have led to reduced mortality, there is still significant morbidity resulting from injuries to the extremities. Eighty two percent of injuries on the battlefield have caused a musculoskeletal injury, many of which result in VML (Devore, 2011). This leads to a loss of muscle function and mobility due to the formation of a large amount of scar tissue (Grasman, 2015). The lifetime cost per person for this type of disability is \$341,300 (Pantelic, 2018). In addition to soldiers, VML injuries affect athletes, trauma victims, and cancer patients, with over 4.5 million reconstructive surgeries performed annually in cases of VML (Pollot, 2016).

VML is broken down into two categories: partial compartment loss and total compartment loss. Partial compartment loss occurs when the nerve remains intact. Total compartment loss is defined as the loss of the nerve that supplies the muscle compartment, depleting most ability for the muscle to function. Currently available treatments for VML fail to restore function to the damaged tissue at a level similar to the muscle before the injury (Grogan, 2011). The Medical Research Council (MRC) Scale for Muscle Strength provides a method of determining the level of function a muscle group has. An examiner provides resistance against the muscle and if the patient is able to contract the muscle against full resistance, then the muscle is determined to have full function. In order to restore full function to the damaged tissue after VML, surgical intervention is required as it is beyond the capacity of the muscle to heal itself

(Grogan, 2011). The current methods that are used to restore function to the damaged muscle include autologous tissue transfers, prosthetics and biological scaffolding (Liu, 2018).

2.2 Skeletal Muscle

In developing a treatment for VML, it is necessary to understand the structure and function of skeletal muscle, in addition to the natural healing process in cases of small injuries. Then it is possible to understand what is required by a new therapy in order to promote the proliferation of healthy, functional tissue.

2.2.1 Anatomy and Physiology

Muscle makes up as much as 45% of the body's mass and has a remarkable capacity to heal itself (Juhás, 2013). Muscle tissue is composed of grouped units, called fascicles, and the smallest unit, the myofibers which are multinucleated cells formed by the fusion of myoblasts (Figure 2).

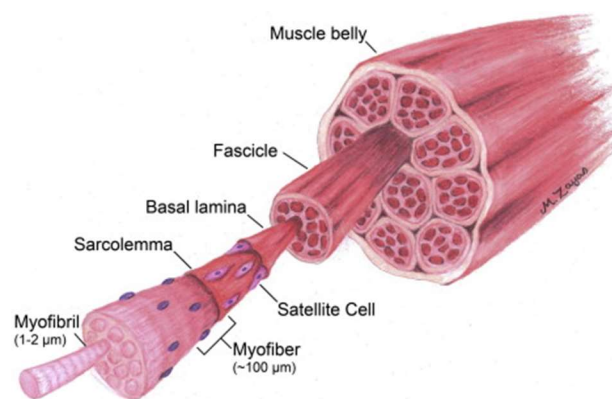


Figure 2. Structure of muscle tissue (Grasman, 2015)

Myofibers contain bundles of myofibrils made up of contracting units of actin and myosin filaments and are each enveloped by connective tissue known as the endomysium, also

referred to as the basement membrane (Grefte, 2007). Fascicles are made up of bundled together myofibers which are held together by the connective tissue of the perimysium. These fascicles are grouped together to form the whole muscle and are held together by the epimysium (Korthuis, 2011). The organized and uniaxial structure of muscle fascicles allows muscle to contract and produce resistance to force.

2.2.2 Wound Healing

Muscle tissue is a highly innervated and vascularized tissue, with each myofiber being innervated by an individual motor neuron which branches off from a larger nerve. This connection is where the muscle is signaled to contract. Additionally, the muscle tissue is vascularized by branching blood vessels which penetrate through the connective tissue of the muscle to the epimysium to provide blood flow to each myofiber (Segal, 2005). This high level of vascularization is what allows muscle to heal itself from smaller injuries. When a small muscular injury occurs, the smallest unit of the muscle (myofibrils) are torn. This triggers the three-phase healing process (Figure 3). The first phase is inflammation, during which the damaged tissue is cleared away by neutrophils and macrophages that release signals to amplify the inflammatory response and signal for satellite cells to invade (Figure 3B) (Tidball, 2010). Satellite cells reside between the cell membrane of myofibers and the basement membrane (Figure 3A) and proliferate in response to injuries (Morgan, 2003). The next step is the repair phase which includes the invasion of vascular, nerve, and muscle tissue to the wound area. Satellite cells begin to differentiate into myoblasts which fuse together to form new myofibers or build onto the damaged ones (Figure 3C). During this time, collagenous scar tissue is formed to stabilize the wound by connecting the damaged myofibers. In the third and final phase, the newly

formed portions of myofiber re-align uniaxially, healing the gap between the damaged myofibers while incorporating themselves into the extracellular matrix (Figure 3D) (Grasman, 2015).

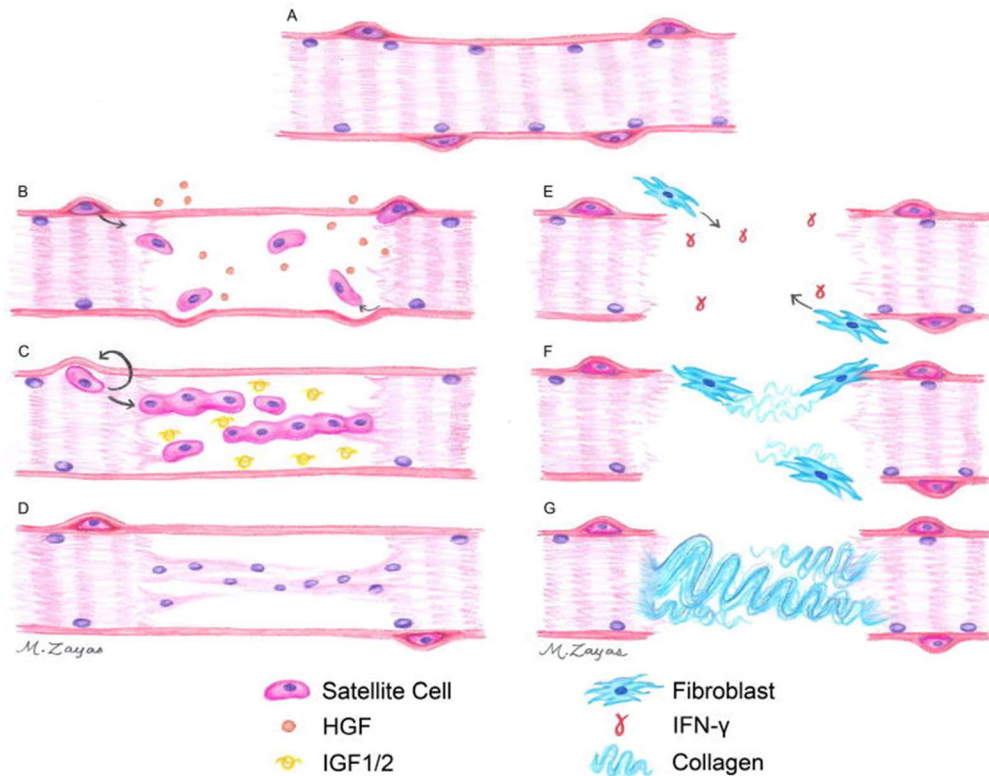


Figure 3: Schematic of muscle regeneration (Grasman, 2016)

Muscle healing occurs for a small-scale injury, so when the damage is too great, healing does not occur effectively. A large-scale muscle injury is defined as when enough muscle is lost that it is not able to be regenerated by the muscle's innate healing ability (Turner, 2012). In cases of VML, organized repair is not able to occur because such a large amount of muscle tissue, as well as connective tissue, nerve tissue, and vasculature, are lost. This lack of vasculature prevents the promotion of guided satellite cell infiltration to form myoblasts as the basement membrane has been destroyed (Jarvinen, 2005). This can be seen in the healing pathway depicted by Figure 3E-G. Since the basement membrane is gone, satellite cells cannot infiltrate the wound site (Grasman, 2016). Instead, fibroblasts invade the wound site and generate collagen that first

stabilizes the wound then remodels into nonfunctional scar tissue (Jarvinen, 2005). This dense scar tissue inhibits the infiltration of nerve tissue and vasculature, which further inhibits healthy muscular regrowth. The end result of this healing process is disorganized and low functioning muscle (Juhas, 2013). As shown in Figure 4, healthy muscle tissue is highly striated and uniaxial, whereas natural healing from a VML injury is disorganized and occurs multi directionally. This lack of uniaxial alignment means that the muscle cannot contract.

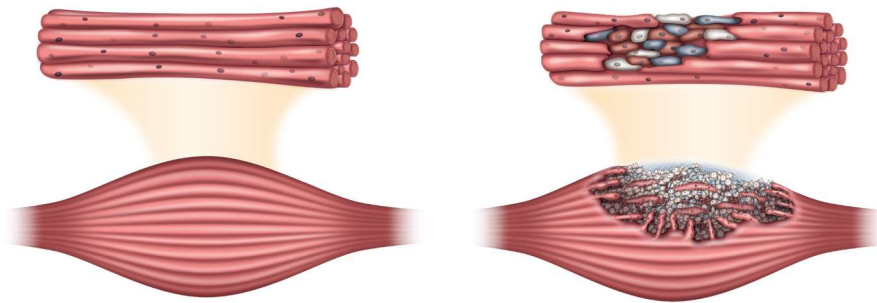


Figure 4. Healthy (left) versus scarred muscle tissue (right) (Grasman, 2015)

2.2.3 Current Treatments for VML

Autologous tissue transfers involve the surgical transfer of functional, innervated muscle from a different muscle group in the body to the site of the VML. This procedure is able to restore some function to the damaged muscle, but even the best-case outcome for this procedure is not able to restore full function to the muscle (Fischer, 2013). A high rate of failure can be attributed to infection and necrosis at the site of implantation, as well as morbidity at the donor site. Complications, such as total flap failure, can arise as a result of damage to the donor nerve (Bianchi, 2009). Yet another drawback of this procedure is the limited availability of donor muscle tissue. Depending on the severity of the injury, the patient may not have enough healthy muscle tissue available to transplant to the wound site. If the wound is so severe that the entire

limb portion is compromised, amputation and prosthetics are an option to provide the patient with limited use of that limb.

Another treatment for VML involves the use of biological scaffolds, specifically those comprised of decellularized extracellular matrix (dECM) (Liu, 2018). These scaffolds are formed by extracting biological tissue and removing all of the cells and living material, leaving behind the extracellular proteins that serve as a scaffold to direct the growth of cells and support muscle regeneration (Sicari, 2014). While decellularized ECM scaffolds direct muscle healing and restore some function, this type of treatment is not able to create architecturally accurate muscle tissue. The structure of the new muscle tissue does not fully mimic that of the native tissue because the decellularized ECM is not as highly uniaxial as native muscle tissue (Dziki, 2016). The uniaxial orientation of muscle is imperative to its proper function because that is the main characteristic that allows it to contract and resist force. The absence of a structure similar to native tissue means that the new muscle generated will not have the same level of strength and functionality as the tissue prior to the injury.

2.2.4 Clinical Need

While more research has been done investigating VML and its effects, there is still no consensus regarding how best to treat it. Currently available treatments are able to restore moderate strength, mobility, and function to the damaged tissue, but none of the available treatments fully restore function to a level comparable to that of the muscle before trauma (in animal subjects).

The best available treatment involves autologous tissue transfer of functional muscle to the site of VML. High rates of failure due to infection and donor site morbidity, as well as a limited availability of donor tissue, creates a large gap for improved treatment options for VML.

The gap in treatment success emphasizes the need for an implantable therapy to provide the necessary biophysical and biochemical cues to direct the uniaxial regeneration of healthy, functional muscle tissue.

2.3 Tissue Engineering Scaffolds

Tissue engineering is a broad and interdisciplinary field of research. One of the major goals of tissue engineering is to develop solutions to restore function to damaged tissues and organs. The most promising approach tissue engineers have discovered in order to overcome the limitations of current VML treatments are biomimetic scaffolds (Passipieri, 2017). A biomimetic scaffold is a 3D, tissue-similar structural framework that cells use as a guide to proliferate and migrate onto to promote regrowth of functional tissue. Biomimetic scaffolds for wound healing should emulate the environment of the extracellular matrix (ECM) and encourage cellular behavior to maintain, restore, or improve tissue function (Nigam, 2014). Tissue engineered scaffolds can be utilized as a partial muscle graft, as a whole muscle replacement, or as a drug screening device when developed *in vitro*. Key features of a successful biomimetic scaffold for skeletal muscle regeneration include (Lev, 2018):

1. The ability to provide an environment for the formation of functional muscle tissue.
2. The ability to construct densely-packed uniaxial myofibers
3. The ability to promote bioactive cell signaling
4. The ability to deliver regenerative growth factors

There are two major types of scaffolds used for tissue regeneration; synthetic and natural. Synthetic scaffolds can be classified as organic or inorganic and are often made from polymers such as Polylactic Acid (PLA), Polyglycolic Acid (PGA), nylon, and gelatin. Synthetic scaffolds

are considered beneficial because they have mechanical and physical properties that can be modified for specific applications. However, synthetic scaffolds are not as biocompatible as natural scaffolds, making it difficult for cells to adhere. Oftentimes, synthetic scaffolds are modified with bioactive molecules such as growth factors, enzyme sensitive peptides, and cell adhesive peptides to increase cells ability to migrate and proliferate onto the scaffold (Zhu, 2011). Additionally, as synthetic polymers degrade they increase the pH of the surrounding tissue and release toxins into the body. Natural scaffolds are typically derived from proteins, polysaccharides, and polynucleotides (DNA and RNA). Natural scaffolds are beneficial because of their high biocompatibility and bioresorbability (Nigam, 2014). Researchers have applied tissue engineered scaffolds alone or have paired them with drugs, cells, or growth factors as a treatment for VML in preclinical and clinical studies (Passipieri, 2017). Numerous types of biomimetic scaffolds have been investigated in the field such as dECM, hydrogel, and microthread scaffolds.

2.3.1 Decellularized Extracellular Matrix Scaffolds

A commonly investigated scaffold as a therapy for VML is dECM. Biologic scaffold materials composed of dECM are typically produced by decellularization of mammalian tissues. Successful dECM scaffolds provide a supportive environment for cells that influence endogenous cell behavior at the target site (Dziki, 2016). Proper cell function and behavior is achieved for muscle regeneration when the dECM scaffold is able to align itself with the surrounding muscle fibers to optimize recruitment of myogenic stem cells and fusion of new myotubes (Zhang, 2016). However, proper alignment of muscle fibers is often difficult to achieve using a dECM scaffold because the structure of the dECM does not mimic the highly uniaxial structure of skeletal muscle.

A study performed by Ma et al., investigated the ability of small intestinal submucosa (SIS) grafts to be utilized to repair and promote regeneration of skeletal muscle in VML injuries in rodent abdominal walls. The success of the scaffold was analyzed using tissue biopsies performed 16 weeks after surgery. Three to five 10 μm transverse cryosections were cut at 0.6-0.8 mm intervals throughout the defect and stained with hematoxylin and eosin to measure morphologic observations, and Herovici's polychromatic to visualize and quantify the VML defect. Researchers found after 16 weeks of implantation, only about 10% of the target site was vascularized muscle tissue. The lack of vascularized muscle tissue indicated that the SIS ECM scaffold did not provide an adequate environment for VML repair (Ma, 2015).

Sicari et al., performed a study illustrating the effects of xenogenic dECM scaffolds derived from a porcine urinary bladder as a treatment for VML injuries in a preclinical rodent model and in five male human patients. Histological analysis and immunolabeling were used to identify skeletal muscle and examine perivascular stem cells (PVSCs). The detection of PVSCs is an indication the newly formed tissue is beginning to vascularize, which is crucial for the development of functional skeletal muscle. Six months after the ECM scaffold was implanted in the rodent models, VML defects exhibited evidence of striated skeletal muscle tissue throughout the target area. PVSCs were identified outside of their normal niche and were present among the degrading ECM scaffold in both rodent and human biopsies. At 24 to 28 weeks after scaffold implantation in human patients, three out of the five male patients showed at least a 20% improvement of muscle strength. At six months, all patients exhibited signs of new muscle and blood vessel formation at the target site with improved strength after physical therapy (Sicari, 2014).

Dziki et al., completed a larger scale cohort study where they implanted porcine ECM scaffolds into a VML wound in 13 human patients. The scaffold was analyzed using histology and immunolabeling to observe the structure of the formed tissue and identify the cellular interactions. Three different scaffolds derived from porcine tissues were used. However, there was no measurable difference in skeletal muscle regeneration based on scaffold origin. Force production, strength improvement, and degradation rate of the scaffold were monitored throughout the duration of the study. After 24-28 weeks, the average increase in force production for the 13 patients was $37.3\% \pm 12.4\%$. Seven out of thirteen patients had an improvement in strength at the injury site with an average increase of $21.1\% \pm 12.2\%$. After an average of 7 months, the scaffold had completely degraded and been replaced with new muscle tissue. Additionally, the bulk tissue density increased by an average of 27.2% after 8 months (Dziki, 2016).

Although these studies do exhibit moderate improvements in muscle structure and function, the scaffold could still be improved. The low level of muscle fiber regeneration observed in each study is predicted to be a result of the decellularization process of the scaffold. Naturally, ECM materials contain bioactive proteins and growth factors which are involved in complex interactions between the regenerative elements in skeletal muscle. When the ECM is decellularized, these elements are damaged and wound healing is inhibited (Greising, 2016). However, acellular biological scaffolds still remain a vital tool for VML injuries and should continue to be modified in combination with other biological and rehabilitative therapeutic strategies.

2.3.2 Hydrogel Scaffolds

Another popular scaffold for muscle regeneration is a hydrogel scaffold. Hydrogels act as cell delivery vehicles to promote the differentiation and maturation of skeletal muscle cells. Ideal hydrogel scaffolds encourage cellular integration onto the scaffold, support cell survival, and protect the cells upon implantation into the body (Lev, 2018). Natural hydrogels can be made out of materials such as alginate, collagen, and keratin.

The Christ lab has recently focused their work on creating a keratin hydrogel as a treatment for VML injuries. Keratin is a fibrous protein that is responsible for forming hair. It has been investigated as a scaffold material because of its ability to promote cell adhesion and release drugs and growth factors (Passipieri, 2017). Keratin hydrogels alone were placed into a surgically induced VML wounds in mice. Force analysis and histological analysis were performed on the injury site two months post-surgery. Researchers discovered the maximum force exerted by the muscle treated with the keratin hydrogel was about 70% of the maximum force exerted by the control group, which was native muscle tissue. The histological analysis revealed that the tissue at the wound site repaired with varying amounts of collagen, adipose, and neomuscle tissue. Collagen and adipose tissue do not allow for functional repair of the muscle tissue because these tissues are not uniaxially aligned. Regenerated muscle tissue must be aligned uniaxially in order to be able to produce forces similar to forces exerted by native muscle tissue. Compared to native tissue, the keratin hydrogels provided a much less structural organization of muscle fibers (Passipieri, 2017). Future work is needed to further enhance the wound healing mechanisms of hydrogel systems to provide more aligned formation of muscle fibers *in vivo* and improve functional outcomes.

2.3.3 Fibrin Based Microthread Scaffolds

Fibrin is a natural provisional matrix protein that is vital in the clotting of blood at a wound site. When tissue damage that results in bleeding occurs, thrombin, a clotting enzyme, polymerizes fibrinogen into fibrin at the wound site (O'Brien, 2016). Fibrin is made up of long fibrous chains that entangle platelets at the wound site to create a blood clot. Since fibrin is naturally found in the body and facilitates wound healing, it is a biocompatible material that supports cell adhesion and proliferation in the direction of the fibers. This makes fibrin a promising material to use as a biomimetic scaffold for wound healing. Fibrin scaffolds act as a delivery vehicle for growth factors to increase cell proliferation to the target site. As the adherent cells create new ECM, the fibrin scaffold degrades to allow the newly formed tissue to take over. Fibrin has been used to create multiple types of scaffolds including hydrogel scaffolds and microthread scaffolds (Litvinov, 2016).

Fibrin microthreads and fibrin bundles offer a number of benefits for skeletal muscle regeneration; they provide contact guidance for cell growth, act as a delivery vehicle for muscle-derived cells, promote functional skeletal muscle regeneration, and deliver necessary growth factors (O'Brien, 2016). Page et al. 2011, loaded fibrin microthread bundles with adult human cells harvested from an adult male's muscle tissue. The cell-loaded fibrin bundles were placed into a large wound in the tibialis anterior (TA) of a mouse. After 2 weeks, the fibrin threads were no longer individually visible by gross inspection and there was evidence of physical contact between the native tissue and the fibrin threads at the wound site. Thirty days after implantation, the wounds sites with fibrin implants (about 8%) had significantly less collagen than untreated controls (about 55%) (Figure 5), implying that the fibrin scaffolds prevent the formation of scar tissue (Page, 2011).

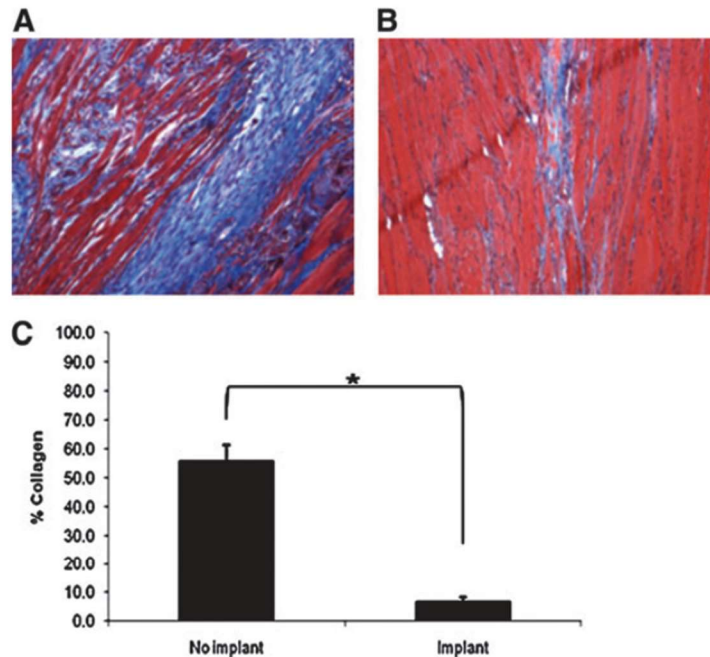


Figure 5. Histological sections of wound healing in untreated mouse tibialis anterior defect (A) and fibrin microthread implanted mouse tibialis anterior defect (B). Masson's Trichrome stain was used for collagen (blue) and muscle tissue (red). Quantification of collagen deposition at no implant (untreated) and implant wound site (C) (Page, 2011).

In addition, the cell-loaded fibrin microthread bundle implants improved the recovery of muscle strength 4 months after surgery. The tetanic intermittent and maximum force was measured on mice without a TA defect (baseline), on mice with an untreated TA defect (no implant), and mice with a TA defect treated with cell-loaded fibrin microthread implants (implant). After the injury was left to heal, the results of the maximum tetanic force indicated a positive linear trend of muscle function in implanted mice, reaching almost 100% recovery at 90 days post-surgery. No implant mice showed a negative linear trend of function and exhibited just over 50% of normal (baseline) muscle strength. These results reveal that cell-loaded fibrin microthreads promote functional skeletal muscle recovery in a large-scale muscle wound (Page, 2011).

Grasman et al. 2015, fabricated a biomimetic scaffold using fibrin microthreads and incorporated varying biochemical and biophysical cues to promote tissue regeneration. Researchers conducted a study using cell seeded microthreads as a scaffold in a rodent VML injury. Human muscle cells were seeded onto fibrin microthreads and then secured in bundles into a VML injury created in the tibialis anterior (TA) muscle of mice and examined after 90 days. Time-course examination of the maximum tetanic force revealed the fibrin microthread scaffolds helped restore strength to the injury site. The mean tetanic force of the uninjured muscle, non-innervated muscle, and treated muscle were 16 g, 10 g, and 14 g respectively. Histological analysis of the injury site indicated that the microthreads appeared to reduce scar formation at the wound site as well as promote myotube formation. Fibrin microthreads appear to be a promising therapy for VML injuries, but more *in vitro* studies need to be conducted in order to test alterations to structural, mechanical, biological, and chemical properties of the microthreads to improve results and better predict how the scaffold will perform in an *in vivo* wound healing environment (Grasman, 2015).

The Pins lab has continuously been working to enhance the biological, chemical, and physical properties of fibrin microthreads (Grasman, 2017). A study comparing fibrin hydrogel scaffolds and fibrin microthread scaffolds was conducted to determine which scaffolding material was able to best promote regeneration of functional tissue in a mouse VML model. A VML injury was created in the TA muscle of a mouse. After the formation of the injury one of 5 treatments was implanted into the wound site: no intervention (control), fibrin hydrogel, uncrosslinked (UNX) microthreads, crosslinked (EDCn) microthreads, or crosslinked and hepatocyte growth factor loaded (EDCn-HGF) microthreads. HGF is key signaling molecule for cell adhesion and wound healing found in the basal lamina of the body. In large skeletal muscle

injuries, the basal lamina is destroyed and HGF is removed. The fibrin gel treatment was used as a control to study the effect of the microthread architecture on wound healing. Pins lab performed force and histological experiments to determine which condition promoted functional wound healing.

Sixty days post injury, a tetanic force analysis and a histological and immunohistochemical analysis were performed on the animal subjects. Researchers concluded that crosslinked fibrin microthreads loaded with HGF (EDCn-HGF) were the most promising scaffold technology to promote skeletal muscle growth in a uniaxial direction. HGF stimulates the activation and migration of satellite cells from the wound margin onto the scaffold and to the injury site (O'Brien, 2016). EDCn-HGF microthreads were able to produce 200% the force of the injured muscle. Fibrin gels were only able to produce about 125% the force of the injured muscle. As indicated in the histological analysis (Figure 6), the no intervention treatment shows excess collagen tissue represented by the blue arrows, while the fibrin gel treatment resulted in the formation of adipose tissue represented by the yellow arrows. The EDCn-HGF resulted in regenerated muscle tissue with myofibers in direct contact with the threads (green arrows). Both adipose tissue deposition and collagen deposition at the wound site do not lead to functional muscle regrowth because the fat cells and collagen fibers do not align themselves uniaxially along the scaffold to allow for maximum contraction of the muscle.

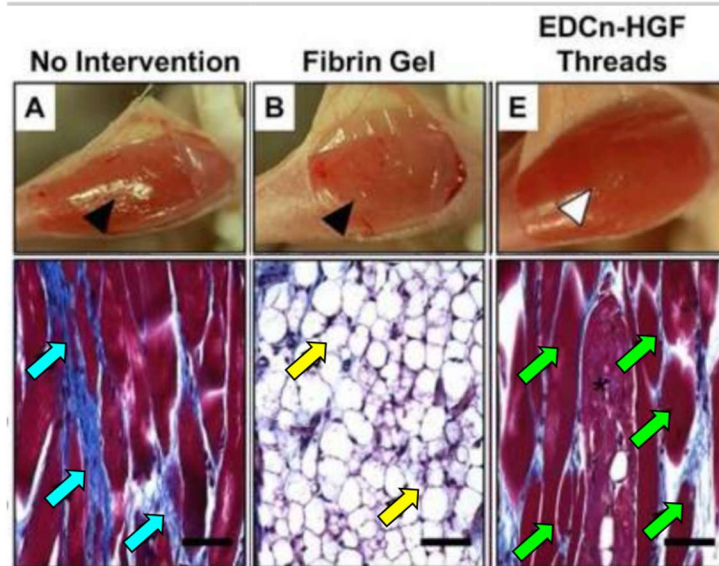


Figure 6: Histological analysis of no intervention (A), fibrin gel (B), and fibrin microthread (E) treatments. The bottom pictures are a cross section of the target site with blue arrows indicating fibrous tissue, yellow arrows indicating adipose tissue, and green arrows indicating aligned myofibers (Grasman, 2015).

Microthreads appear to be a successful method to facilitate cellular migration and proliferation of native muscle cells with reduced collagen and adipose deposition and increased muscle strength (Grasman, 2015). However, tissue engineers continuously strive to improve the clinical outcome of biomaterial-based therapies. The biological properties, strength, immune response, recruitment of cells, and infiltration of cells, of fibrin microthreads could be optimized and tested *in vitro* to improve the clinical results of fibrin microthreads as a treatment for VML. Therefore, a 3D *in vitro* model is needed to mimic the biological environment while testing the effectiveness of several scaffolds for muscle cell growth.

2.3.4. Need for Tissue Engineered Scaffolds for VML

Fibrin microthreads produce promising results that demonstrate their ability to be used as a potential scaffolding material and treatment for VML. Scaffolds are used as a tool to guide cells to specific areas of the body. Fibrin can be extruded into microthreads that mimic the

natural architecture of skeletal muscle tissue. Results with animal studies with scaffolds created out of fibrin microthreads increase confidence that a patient's cells will migrate to the wound site, proliferate in the correct direction, and regenerate functional muscle tissue. However, much more data needs to be collected before fibrin microthreads can be tested clinically.

Therefore, there is a need to develop a 3D *in vitro* model system to predict how human muscle cells will interact with a scaffold *in vivo*, specifically fibrin microthreads that have been altered by crosslinking and bundling or loaded with growth factors to promote functional muscle tissue regrowth. A 3D *in vitro* model system of cellular outgrowth, defined as cellular migration and proliferation, would allow for multiple thread conditions to be tested to determine which type of thread will provide regenerated muscle tissue with the highest degree of functionality. Successful *in vitro* results will provide researchers with more confidence in the scaffolding treatment as they move into *in vivo* studies. Ultimately, a 3D *in vitro* model of skeletal muscle cell outgrowth onto fibrin microthreads will expedite the testing process of scaffolds to be used clinically in VML injuries.

2.4 *In Vitro* Assays for Tissue Regeneration

Tissues and organs are complex three-dimensional (3D) structures. In order for advances in regenerative medicine to be made, researchers must fully understand their structures and functions as well as how they interact with scaffolds. Improving the understanding of tissue and organ function can be achieved through the use of experimental models and assays. Testing can be done using two-dimensional (2D) or 3D models. Two-dimensional models are often used for preliminary testing and consist of a monolayer of cells grown on a flat tissue culture plate. After preliminary testing is completed using *in vitro* 3D methods, scaffolds are most often tested in an

animal model. Although these two model types can provide valuable information, there is a need to better understand *in vivo* molecular mechanisms in a simplified 3D environment (Yamada, 2007). Three-dimensional *in vitro* models bridge this gap and provide opportunities to more accurately model complex structures in the in-vitro environment.

2.4.1 2-Dimensional (2D) Assays

2D cell culture has served as an invaluable tool for cell biology and preclinical biomedical research for decades. 2D cell migration models are an important device for investigating key physiological events which occur during wound healing. They model the movement of cells, allow researchers to easily study the effects of various stimulating factors, but are often expensive to use (Kramer, 2011).

Scratch assays (Figure 7) are one of the most widely used formats for studying cell migration. Cells are seeded onto a multiwell assay plate and allowed to form a confluent monolayer. A tool is then used to remove or “scratch” cells from an area and cell migration into the scratch is observed. Scratch assays are versatile and can be performed in any basic cell culture plate configuration without the need for a specialized assay setup. Prior to the experiment, the scratch assay surface can be coated with an ECM of choice, adding to its versatility. An additional advantage of the scratch assay is that cells along the scratch boundary move in a defined direction to try to close the wound, and the movement and morphology of these cells can be captured in real-time (Hulkower, 2007). Scratch assays can be useful in wound healing studies because the process of creating the scratch damages cells along the boundary. These damaged cells release growth factors and produce signals which facilitate wound repair and migration (Vogt, 2010). However, the scratch assay method can be inconsistent due to user variation in scratch technique. Additionally, it can be difficult to ensure that different treatment

groups are run under equivalent conditions of monolayer confluence and that the consistency of wound size is precise (Hulkower, 2007). There are a number of commercially available scratch assays, such as the CytoSelect Wound Healing Assay (Cell Biolabs) and the Cell Comb Scratch Assay (Millipore Sigma) which are designed to maximize standardization.

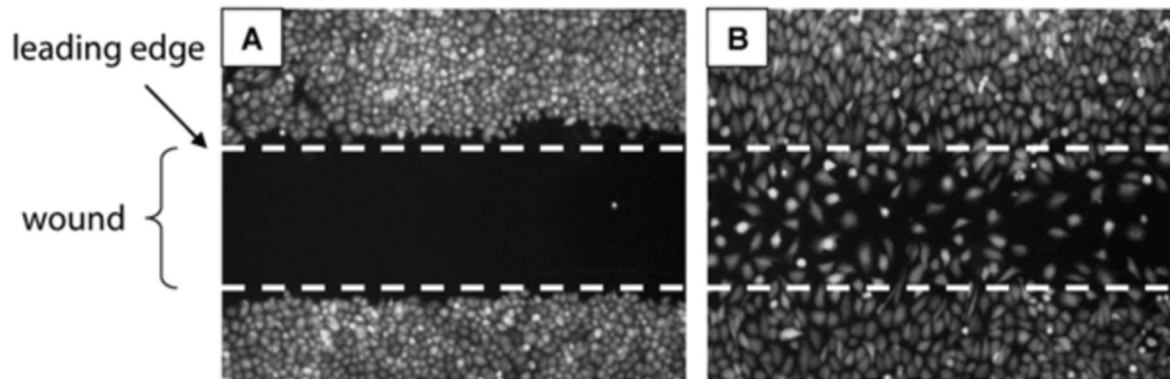


Figure 7. Example of a scratch assay showing (A) the wound created by the scratch, and (B) cells migrating into the wound site (Vogt, 2010).)

Another type of commonly used 2D *in vitro* model is the cell exclusion zone assay. Cell exclusion assays use stencils, such as small silicone stoppers to create an exclusion zone. The stencil is placed on the plate and then cells are seeded into the surrounding space and allowed to reach confluence. The stencil is then removed, allowing the cells to migrate into that area (Kramer, 2011). Figure 8 shows an example of a cell exclusion zone assay. Cell migration can be quantified using fluorescent cell stains and fluorescence plate readers or with other image analysis techniques such as microscopy. A commonly used cell exclusion zone assay which operates under these principles is the Orsis Cell Migration Assay (Platypus Technologies LLC). To eliminate the need for a microstencil which must be manually removed, assays with a chemically engineered cell exclusion zone have also been designed. Cells cannot penetrate the

area while being seeded, and once the cells have adhered, the exclusion zone dissolves to allow cell migration (Vogt, 2010).

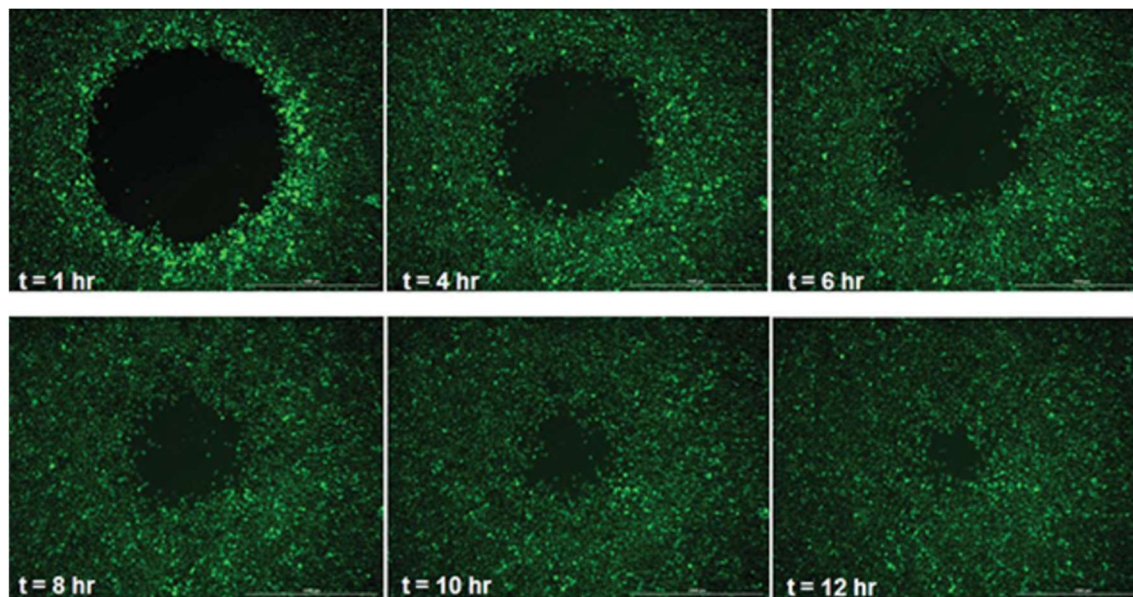


Figure 8. Cells growing into an exclusion assay over a 12-hour period. At $t=1$ hr, the clean border created by the exclusion zone stencil is still visible. Over the next 11 hours, the cells migrate into the exclusion zone. Cells were stained with CellTracker Green and imaged using wide field fluorescence microscopy (Brescia and Banks, 2013).

2.4.2 Need for 3D *in vitro* Assays

While 2D assays provide valuable information about basic cell migration and behavior, cells cultured in 2D on a flat surface are not representative of cells residing in the complex conditions and 3D architecture of tissue *in vivo*. In native tissue, cells reside in an ECM and interact with neighboring cells and the surrounding matrix through biochemical and mechanical cues. Intercellular interactions influence cell properties such as morphology, differentiation, proliferation, gene and protein expression, and response to stimuli. Because cells grown in 2D cell culture cannot achieve the same level of organization and connectivity, many of these properties are limited or diminished. When cells are placed in 2D culture they become progressively flatter, divide abnormally, and can lose their differentiated phenotypes (Sanyal, 2014).

3-Dimensional *in vitro* models offer an alternative which can provide a reproducible, controlled microenvironment which mimics conditions *in vivo* (Creative Bioarray, 2016). In 3D models, cell attachment occurs around the entire surface of the cell. Cells grown in a 3D environment exhibit similar morphology, signaling, and polarity to cells in native tissue (Sanyal, 2014). Additionally, 3D *in vitro* models can act as an intermediate assessment stage before moving to *in vivo* techniques, bridging the gap between 2D culture models and animal models. The designed microenvironment of the 3D *in vitro* model enables studies which would be difficult to address *in vivo*. Users can test cell responses to specific conditions in isolation from the full *in vivo* system. The 3D *in vitro* model also is conducive to continuous biochemical analysis and imaging (Creative Bioarray, 2016). Ultimately, using 3D *in vitro* modeling techniques allows researchers to accurately evaluate cellular responses in a more ethical, and more cost-effective way before proceeding to *in vivo* studies (Biogelx, 2018).

2.4.3 3-Dimensional Assays

There are a variety of existing 3D *in vitro* models which can be grouped into two categories; scaffold and non-scaffold based. Scaffold-based approaches include solid polymeric scaffolds, hydrogel-based scaffolds, and micropatterned surfaces. Non-scaffold-based approaches include cells only that assemble into 3D structures using hanging drop microplates, spheroid microplates, and microfluidic devices.

2.4.3.1 Scaffold-Based Approaches

3-Dimensional scaffold-based models can be created by culturing cells on pre-fabricated polymeric scaffolds designed to mimic the *in vivo* ECM. Scaffolds are used as a physical support system to which cells attach and fill the interstices within the scaffold to form a 3D culture

environment. Commonly used synthetic polymers include polystyrene (PS), polycaprolactone (PCL), poly(glycolic acid) (PGA), and poly(lactic-co-glycolic acid) (PLGA) which are then fabricated into scaffolds. Scaffold structures include electrospun fiber networks, porous materials, and orthogonal layered meshes (Larson, 2015) created by fabrication techniques including soft-lithography, electrospinning and bio-printing (Sanyal, 2014). 3D *in vitro* models made with synthetic polymer scaffolds are advantageous because they can be fabricated with strict control over mechanical, structural, and physicochemical properties. However, unlike naturally-derived polymers, synthetic polymer scaffolds lack adhesion motifs which promote optimal cell attachment and growth (Duda, 2015).

3D *in vitro* scaffold-based models can also be created using hydrogels that can be formed using proteins commonly found in the ECM such as fibronectin, collagen, laminin, and gelatin. In addition to providing a support matrix, naturally-derived scaffolds provide growth factors, hormones and other molecules that cells interact with in the *in vivo* environment (Larson, 2015). Cells can be encapsulated within or sandwiched between hydrogel layers. Synthetic hydrogels can also be used when naturally-derived biological matrices are unsuitable. These include poly(ethylene glycol) (PEG), poly (vinyl alcohol) and poly (2-hydroxyethyl methacrylate) . Synthetic hydrogels are biologically inert, but can be modified with appropriate biological components (Sanyal, 2014).

Another scaffold-based 3D *in vitro* modeling technique is micropatterned surface microplates. Each microplate well contains regularly arrayed, micrometer sized compartments. Wells can be various shapes and are created using micro-fabrication technology. Micropattern configuration is dependent on the cell type being used and can be optimized for spheroid or cell networking formation. Wells are selectively coated to create low adhesion surfaces in each

micro-space. This causes cells to aggregate together into spheroid structures at the bottom or form continuous cell networks (Larson, 2015). The transparent bottom of the plate allows for easy imaging and observation of *in vivo*-like cell activity (Creative Bioarray, 2016).

2.4.3.2 Non-scaffold Based Approaches

Scaffold-free 3D *in vitro* models use self-assembled 3D cells rather than a physical support system. Hanging drop microplates use gravity to encourage 3D growth of cells downward from where they were seeded in wells. Unlike traditional well plates, hanging drop plates have an open bottom. Cell media is dispensed on top of the well, and surface tension causes a small drop of media to hang from the aperture in the bottom (Creative Bioarray, 2016). This media drop is large enough for cellular aggregation into spheroids, but small enough that it will not dislodge when handled. Co-cultured spheroids can be created by adding multiple cell types sequentially. These hanging drop spheroids can also be transferred to a larger volume plate for long-term culturing (Larson, 2015). Hanging drop microplates are one of the most cost-effective methods for 3D cell culture because they only require cells and media, and are compatible with automated liquid handling devices (Creative Bioarray, 2016).

Spheroid microplates with an ultra-low attachment coating create a similar tissue model to hanging drop microplates. Each well has a typical shape and depth but has an ultra-low attachment coating on the bottom. This minimizes cell adherence and allows spheroid formation (Creative Bioarray, 2016). Well bottoms also have a round, tapered, or v-shaped geometry to ensure the creation of consistent sized spheroids positioned in the center of the well. Because of the larger well capacity, procedures can be carried out in the same plate and do not need to be transferred for long-term culturing (Larson, 2015).

Microfluidic devices simulate the 3D architecture of *in vivo* tissues and cell-ECM interactions while adding an additional layer of complexity by introducing fluid flow to the cellular environment. This allows for continuous nutrition and oxygen introduction as well as waste removal. Microfluidic devices are composed of polymers such as polydimethylsiloxane (PDMS), polymethylmethacrylate (PMMA), polycarbonate (PC) and polystyrene (PS), in addition to chromatographic or filter paper and hydrogels. (Larson, 2015). This type of technology was used to create an *in vitro* model of skeletal muscle to evaluate tissue formation and injury. The “muscle-on-a-chip” provided uniaxial cell alignment and was able to quantify strain as the tissue formed and matured (Varghese, 2017).

2.4.3.3 Current 3D *in vitro* Fibrin Microthread Scaffold Model

The Pins Lab is currently researching a 3D *in vitro* model of skeletal muscle regeneration.

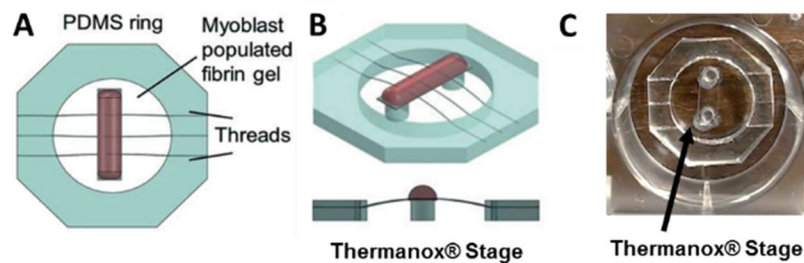


Figure 9. Current PDMS frame model: A - Top view, B - Thermanox® stage with fibrin microthreads stretched across, C - Ring and stage assembly in a well of a 6-well tissue culture plate. Adapted from (Grasman, 2015).

In order to create the PDMS ring in Figure 9A, the user must make rectangular sheets of PDMS. From one sheet of PDMS, a leather hole punch (19mm) is used to make 6 holes in the sheet. A razor blade is used to cut squares around the holes that are punched in the PDMS. These squares are shaped once more with the razor blade into an octagon. Then, the user must use the razor blade to cut three slits in parallel sides of the PDMS rings. The slits are estimated to be half of

the depth of the PDMS ring, however this is an estimated length, so it is subjected to user variability. Following the laboratory protocol for making fibrin microthreads (Appendix A), the user must make fibrin microthreads, a polymerization of fibrinogen and thrombin. Once the fibrin microthreads are extruded, dehydrated, and cut into ideal sizes, the user must use forceps and their fingers to open the PDMS slits and place the fibrin microthreads in each side. This step causes 25% failure in the rings, as the opening of the slits typically causes the PDMS to fully split. The user then constructs a Thermanox® stage by making small PDMS “posts” (Figure 9B, lower graphic), and gluing a small rectangle of Thermanox® to the top of the PDMS posts. The PDMS ring, with threads intact, is then laid over the Thermanox® stage, inside a single well of a 6-well plate. Vacuum grease is used to keep the PDMS ring and Thermanox® stage from moving during cellular characterization studies. The whole system must then be sterilized, which is currently done using 70% ethanol sterilization.

This assay is run in a 6-well plate for a total of 96 hours, with imaging done every 24 hours on a Zeiss inverted microscope in phase contrast and fluorescence mode. The cells are stained with Dioctadecyl-Tetramethylindocarbocyanine Perchlorate (DiI), a lipophilic, red-orange membrane stain and each fibrin microthread (or bundle of fibrin microthreads, collagen thread, etc.) and C2C12 myoblast populated fibrin gel interface is imaged. The phase contrast image is overlaid with the fluorescent image to measure cellular alignment and migration onto the fibrin microthreads.

3.0 Project Strategy

The project strategy chapter discusses the framework of the engineering design process and its application regarding the design of a 3D *in vitro* skeletal muscle outgrowth assay. The design team gathered information crucial to the engineering design process from the initial client statement, client interviews, user interviews, industry expert interviews, project objectives, constraints, and the revised client statement.

3.1 Stakeholders

In order to effectively frame the need, constraints, and expectations of the project, the team considered all of the stakeholders. These stakeholders include the design team, the clients, and the users. It is important to consider the opinions and needs of the clients, as they are funding the project. The users are also critical, as they are the researchers that will ultimately utilize the assay in the future. In order to meet the needs of the stakeholders, the design team must be able to apply the engineering design process to define the assigned project and determine a feasible solution.

The clients of this project include Dr. George D. Pins and Dr. Catherine F. Whittington, and the current user of this project is PhD candidate, Meagan Carnes. Other potential users include other researchers in the field of exploring scaffolds for use in directing repair of muscle or other tissues. The design team is composed of Erin Heinle, Emily Morra, Emily Mossman, and Alyssa Paul. The project objective was provided to the team by Dr. George D. Pins and Dr. Catherine F. Whittington due to the need for a 3D assay to more efficiently and reproducibly model cellular outgrowth onto fibrin microthread scaffolds to predict muscle healing. This assay

will assist Dr. George D. Pins and Meagan Carnes in their research by creating a 3D assay to model outgrowth, for increased detection and predictability of scaffold to succeed *in vivo*. It can also be implemented in other labs where it may be used to model cellular outgrowth onto various types of biological scaffolds compatible with the final system created by the design team.

The design team has determined through client and user interviews that there exists a need to design a new assay that will reduce current assay assembly time by 50%, allow for a 6-well imaging format, and has the ability to model reproducible cell proliferation, migration, and confluence of C2C12 cells onto a 3D fibrin microthread scaffold. Ultimately, this model should be able to support different types of scaffolds (e.g. collagen, bundles of fibrin microthreads) and multiple cell lines to better model skeletal muscle regrowth. Overall, there exists a need to bridge the research gap between the current 2D and 3D *in vitro* assays and the 3D *in vivo* testing of scaffolds, specifically for cellular outgrowth onto fibrin microthreads as a treatment for VML. A reproducible model will allow researchers to identify predict the *in vivo* response to the scaffold and enhance the rate of which scaffolds can be tested.

3.2 Initial Client Statement

The initial client statement provided to the team:

“Design, develop, and characterize a 3D in vitro model of skeletal muscle ingrowth”

In order to accomplish this goal, the design team would need to successfully develop a new assay or improve the existing 3D assays in order to effectively model cell confluence, migration, and proliferation onto the scaffold. It was important that the team identified and prioritized design objectives and constraints, which would be iterated as the stakeholders’ needs were understood in depth. A final set of objectives and constraints were formed to assist the team

in moving forward with a comprehensive project strategy and testing mechanisms throughout the design phase.

3.3 Objectives

A list of objectives was created based on the initial client statement. Client and user interviews, along with team assessments, were used to then tailor the objectives to the wants and needs of the present stakeholders and determine success (Appendix B-D).

The initial objectives determined by the team were evaluated once client and user interviews provided detailed information regarding goals of the project. The team decided to focus on developing a new model system that would be compatible with 3D models, and then test this assay using a 3D microthread scaffold. Once the design iteration process began, the objectives and sub-objectives were further investigated for importance to the assay design. Figure 10 shows a hierarchical structure of the project objectives and their relevance to the design.

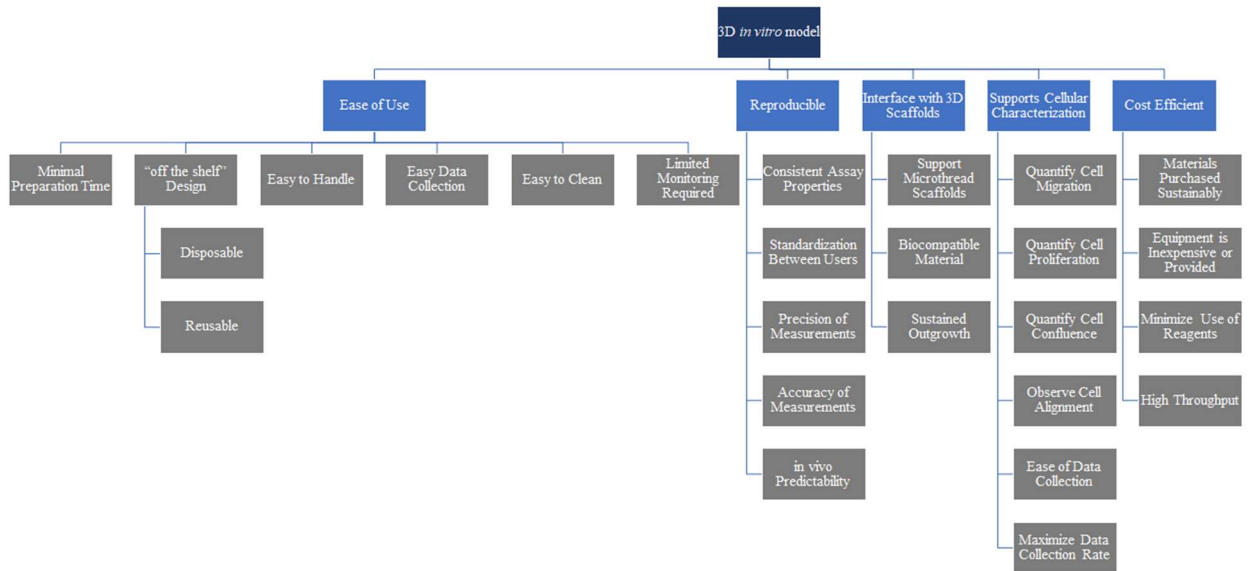


Figure 10. Project objectives hierarchical tree

The five high-level objectives specify that the assay will be **Easy to Use**, **Reproducible**, it will **Interface with 3D scaffolds** (e.g. fibrin microthreads), **Support Cellular Characterization**, and be **Cost Efficient**. These objectives are defined in Table 1 and the sub-objectives are defined in Tables 2 through 6.

Table 1. Main objective definitions

Objective	Definition
Easy to Use	Model must be easy to assemble, easy to handle and intuitive to use
Reproducible	Must produce results that are consistent across replicates and multiple users
Interface With 3D Scaffolds	Model needs to be biocompatible and conducive to C2C12 replication and migration onto the scaffold
Support Cellular Characterization	Must be able to obtain quantifiable results and be designed to allow the user to test multiple replicates at once and meet size constraints
Cost Efficient	Model needs to be productive relative to the cost of building and using it

Table 2. Sub-objective definitions for Ease of Use

Sub-Objective: Ease of Use	Definition
Minimal Preparation Time	Model assembly and testing setup must be intuitive and efficient for user
“Off the Shelf” Design	Components are prefabricated and minimal assembly is required
Easy to Handle	Model must be easy to work with during setup, testing, and imaging
Easy Data Collection	The user must be able to stain and image cells and analyze relevant throughput using available techniques
Easy to Clean	Assay can be sterilized using 70% Ethanol
Limited Monitoring Required	The assay will not come out of place once final assembly is complete (only media changes and imaging will be required)

Table 3. Sub-objective definitions for Reproducible

Sub-Objective: Reproducible	Definition
Consistent Assay Properties	Model must be able to show similar levels of cell outgrowth and confluence between replicates and between multiple tests
Standardization Between Users	Model must be designed to minimize variability between users
Precision of Measurements	Little variance between cellular outgrowth distance measurements of same conditions (consistent)
Accuracy of Measurements	Cellular confluence predictive of <i>in vivo</i> response (shows cellular alignment, comparable leading cell outgrowth, formation of ECM around thread-gel interface)
<i>in vivo</i> Predictability	Data provides benchmarks to recognize success and failure once the scaffold is tested <i>in vivo</i>

Table 4. Sub-objective definitions for Interface with 3D Scaffolds

Sub-Objective: Interface with 3D Scaffolds	Definition
Support Microthread Scaffolds	The model must be designed to test fibrin microthreads as the primary focus
Biocompatible Material	Materials used for the model must be compatible with C2C12 cells and non-cytotoxic
Sustained Outgrowth	The model must be able to sustain cells in order for proliferation to occur

Table 5. Sub-objective definitions for Supports Cellular Characterization

Sub-Objective: Supports Cellular Characterization	Definition
Quantify Cell Migration	Model must support cell migration onto the microthread scaffold
Quantify Cell Proliferation	Model must be able to distinguish if outgrowth is caused by cell division or cell migration
Quantify Cell Confluence	Model must be able to quantify cell confluence around the circumference of the microthread
Observe Cell Alignment	Model must support the cell alignment required for functional muscle tissue regrowth
Ease of Data Collection	Data collection must be efficient using microscopes and technology provided
Maximize Data Collection Rate	Efficient and intuitive set up leads to more assays being analyzed and more conditions being tested

Table 6. Sub-objective definitions for Cost-Efficient

Sub-Objective: Cost-Efficient	Definition
Materials Purchased Sustainably	The model must be made of materials which are available to the lab over time and affordable to purchase. Required consumables and disposable components must also be inexpensive.
Equipment is Inexpensive or Provided	Model must be compatible with technologies already present in the lab and any additional accessories must be inexpensive to purchase
Minimize Use of Reagents	Lower the cost of materials / amount of materials used
High Throughput	Device is able to provide a high volume of data in a short time

3.4 Constraints

In order to complete the MQP project requirements, certain criteria must be met. These criteria were identified as constraints because they had the potential to limit the ability for continuation of the project. Table 7 defines the constraints.

Table 7. Project Constraints

Constraint	Definition
Financials	Budget of \$1,000
Time	Project must be completed by April 19th, 2019
Resources	Materials must be available or attainable for the team
Materials	Must not be cytotoxic or harm users
Sterility	Must be able to be sterilized by lab standards or fabricated in a sterile environment.

The constraints provided the team with working limitations that must be met to design the assay. WPI provided a working budget of \$1,000 and the team had until April 19th, 2019 (Project Presentation Day) to complete the MQP. It is important that the materials used for the project be available to the team and the users within the Pins lab. Additionally, the materials used to produce the assay must not be cytotoxic or harmful to users of the model system. Finally, the team needed to ensure that the assay could be sterilized by laboratory standards.

3.4.1 Design Dimension Constraints

The design of the developed assay must also fit physical constraints. Each singular model system must fit into a 34.8 mm diameter well. The container in which PDMS is cured must fit into a vacuum chamber, measuring 25 cm in diameter. Additionally, the PDMS has to be cured

at 60°C for at least one hour. The container in which the PDMS is cured must not be cytotoxic or leach toxins into the PDMS.

3.5 Quantitative Analysis of Objectives

To identify the most important objectives directing the design specifications, the design team, clients, and users completed a pairwise comparison. A pairwise comparison is beneficial to the design process, because it allows each objective and sub-objective to be prioritized against the others. The objectives in a row and column that overlapped were compared and given a numerical score. A score of “1” indicates that the objective in the column position of the chart had priority over the objective in the row position of the chart. A score of “0.5” indicates that the two objectives were equally important. A score of “0” indicates that the objective in the column position had less priority than that of the objective in the row position. The scores were tallied for each objective, and compared among the design team, clients, and users. The pairwise comparison charts for each stakeholder can be found in Appendix E.

The scores of the two clients and one user were evaluated and used for final scoring. Table 8 shows the average scores for the design team, clients, and user. Each objective was then assigned a weight based on the total scores. The average of the clients’ responses was multiplied by 0.4, as were the user’s responses. The design team’s responses were multiplied by 0.2, giving more weight to the clients and users, as this project is ultimately for them. The final weighted objectives determined using the following equation are listed in Table 9.

$$\textit{Weight} = [(0.4 * \textit{user score}) + (0.4 * \textit{average of clients' score}) + (0.2 * \textit{average of design team score})]$$

Table 8. Pairwise comparison chart

Totals for Pairwise Comparison for 3D <i>in vitro</i> Skeletal Muscle Regeneration					
	Team	Pins	Whittington	Carnes	Total
Ease of Use	0.5	0.5	0.5	0.5	2
Reproducible	3	4	3.5	2	12.5
Interface with 3D Scaffolds	4.5	4	3.5	4.5	16.5
Data Collection	4.5	4	3.5	4.5	16.5
Multi-Well Format	2	2	3.5	1.5	9
Cost Efficient	0.5	0.5	0.5	0	1.5

Table 9. Objective weights

Objective	Weight
Ease of Use	0.5
Reproducible	2.7
Interface with 3D Scaffolds	3.7
Data Collection	3.7
Multi-Well Format	2.1
Cost Efficient	0.3

The customer, user, and design team pairwise comparison shows that interfacing with 3D scaffolds, and efficient and effective data collection were the two most important objectives. These objectives were prioritized moving forward with the design process. After the initial objectives were defined, the terms “Data Collection” and “Multi-Well Format” were merged into one category, called “Supports Cellular Characterization”.

3.6 Functions and Specifications

The design team worked with the clients and user to identify specific functions and specifications that would be evaluated throughout testing to determine if the assay is reaching an ideal standard. The assay was considered to consist of six supportive frames to fit into a 6-well plate. Each one of the six frames was required to have a successful fibrin microthread to gel interface, fixturing mechanism, supportive cell culture environment, and data capture and analysis. It was important to keep the objectives defined in Section 3.3 in mind, which these functions were created to satisfy. These key functions allowed for the creation of a successful assay and modeling system for 3D microthread scaffolds.

3.6.1 Six or more sufficient fibrin microthread - C2C12 cell gel interfaces

In order for the model to effectively be used to depict proliferation, migration, and alignment of cells along the scaffold, a C2C12 myoblast populated fibrin gel of C2C12 cells must be in contact with the fibrin microthreads. Our model must provide a sufficient area, 3 mm, on which the cell-gel will interface with the fibrin microthreads and a biocompatible material. In the past, Thermanox® has been used, as it does not disrupt the cellular proliferation. Additionally, the thread-gel interface must provide at least six data points that can be monitored and imaged by a Zeiss AxioVert 200M microscope.

. A minimum of six thread-gel interfaces implies that at least three fibrin microthreads must be able to be secured to the model.

3.6.2 Fixturing mechanism of fibrin microthreads onto PDMS frame

The fibrin microthreads must be stably fixtured to the PDMS frame in order to model cellular proliferation onto the fibrin microthreads. The current “gold standard” secures the threads to the PDMS by manually cutting slits in the side of the PDMS using a razor blade. The threads are then carefully slid into the “slits”, securing them in place (Grasman, 2017). It is crucial that the new design allows for user friendly and time efficient placement of threads. The fixturing mechanism must be able to be performed by one user and should not require significant experience. It is important that during media changes, a process that results in fluctuation of fluid level in the assay, the threads must remain in place. The team performed tests to determine whether slits or silicone glue would be the best fibrin microthread fixturing mechanism.

3.6.3 Support cell culture environment

The assay must be able to function in an ideal cell culture environment for an extended amount of time. Ideal cell culture environment for mammalian cells is 37°C, 5% carbon dioxide, and ~85% humidity. The environment must be robust for 96 hours. It must be compatible with the current media formulations used in the Pins Lab. To maintain ideal thread length and reduce stretching, the thread culture environment should be no longer than 1 cm within a 6-well plate format, with each well diameter measuring to be 35 mm. The height of the threads must be within the height range of the well plate, relative to the plate bottom, so that the media can surround the threads. The design team estimates this height to be 9.65 mm. However, the height of the model will be lower than this in order to be in the optimal range for imaging. The assay components must be biocompatible and support cellular outgrowth onto the fibrin microthreads.

3.6.4 Data capture and imaging of six or more thread-gel interfaces

The assay must be able to be imaged using an inverted Zeiss AxioVert 200M microscope currently available in the Pins Lab. Each system must fit in a well of a 6-well plate and within the vertical working distance of the microscope. Six or more data interface points must be visible for each singular assay system (a 6-well plate with six data points in each well) by the microscope and analyzing software.

3.7 Engineering Standards

In order to ensure that the final device functions properly, protocols set forth by the International Standardization Organization (ISO) and the American Society of Testing and Materials (ASTM) will be used.

The device must be tested for cytotoxicity. Because it is meant to support the growth of muscular cells, it must not create any toxic effects on the cells which would disrupt the data. This will be tested in two ways. A direct contact assay will be carried out per ASTM F813-07. This method calls for the incubation of mammalian cells in contact with the model. These results will be compared to those of cells incubated on latex as a positive control and high-density polyethylene (HDPE) as a negative control. This will allow the team to draw conclusions about whether contact with the device causes toxic effects to the cells. If there is research that supports that the material is not cytotoxic, then this test does not need to be conducted.

The leaching of the device model will also be tested using an extract cytotoxicity assay following ASTM F619-03. In this test, samples of the model are incubated in media for five days. This media then replaces media in which healthy cells were growing. The effect of this media on the cell morphology determines if the model leached anything harmful into the media.

The same procedure was performed with samples of latex as a positive control and high-density polyethylene (HDPE) as a negative control. If there is research that supports that the material does not leach, then this test does not need to be conducted.

To test that the chosen method of sterilization is effective, the device could be sterilized and submerged in media. It would then be stored in an incubator for five days, after which it would be examined under a microscope to determine microbial growth. If there is research that supports the effectiveness of the chosen method of sterilization, this test does not need to be done. CAD is being used to create the design for the model so ISO 16792, which dictates technical product documentation using CAD, must be followed. This standard which outlines methods for documenting the design drawings (ISO 16792, 2015).

3.8 Revised Client Statement

After weighting and evaluating the importance of the objectives, sub-objectives, and further specifications from the clients and user, the design team developed a revised client statement:

*“Design, develop, and characterize a **reproducible and standardized** 3D in vitro model of skeletal muscle tissue with less than 5% user variability. It must be **assembled in 50% of the time required in the current Pins Lab protocol** and must be able to be **imaged to quantify outgrowth of C2C12 cells in six, 35mm wells. Whilst maintaining structural integrity while submerged in media in a sterile environment for 96 hours.**”*

The revised client statement was iterated as the project progressed to ensure that the clients' and user's wants and needs are achieved by the objectives and specifications determined

by the design team. Once the design process became more detail oriented, it was important to reiterate and understand the wants and needs of the customer and user.

4.0 The Design Process

Once the team completed a thorough literature review and conducted interviews with both the client and user, the team formulated a project strategy. The project strategy began with identifying the stakeholders for the project. The objectives for the project design were formulated after a series of interviews with the stakeholders and were prioritized as stated in Section 3.5. The design team then determined the functions of the project design and formulated multiple means to fulfill each function. Each means was evaluated in terms of its ability to fulfill the specifications of the function. The final design was chosen after iterating the means of the assay and prioritizing functions using a decision matrix.

4.1 Needs Analysis

Based on the information gathered by the design team from the clients and users, all objectives were ranked based on their importance to the success of the project (Appendix E).

The design team observed the current setup process of the assay used now, while asking the user what improvements they would like to see in a new model. While observing the current assay assembly, the team recorded the number of steps and length of time each respective step took. Table 10 shows the PDMS and fibrin microthread ring assembly steps and corresponding elapsed time.

Table 10. Current assay setup and elapsed time

Task/Step	User's Time (Experienced User)
Making fibrin microthreads	1 hour, 30 minutes
Mixing and pouring PDMS	10 minutes
Vacuuming out air bubbles from PDMS	20 minutes
Cure PDMS in oven	12 hours (overnight)
Making six PDMS rings	5 minutes, 35 seconds
Make Thermanox® "stage"	12 minutes, 12 seconds
Place three threads in each (6) PDMS rings	18 minutes, 8 seconds

While several additional steps follow the placement in threads into each ring, the design team focused on the assembly time for the PDMS and microthread portion. In the design of the new model, a need was defined as an aspect of the assay that the stakeholders felt was crucial for the project and design to succeed. Table 9 shows how the objectives were ranked, which informed needs and wants. The top four ranked objectives were to **Interface with 3D Scaffolds**, **Support Cellular Characterization**, for the design to be **Reproducible** and standardized. The team determined the extent of these needs when observing the setup and cellular outgrowth assay completed by the user, and understanding which features they would like to see be improved with our design.

When evaluating the wants and needs of the user, client, and industry, a want was defined as an aspect of the assay that was desired to be included, but not entirely necessary for the success of the project. The two objectives labeled as wants were **Ease of Use** and **Cost Efficient**. These objectives would improve the final assay design/appeal, but are not crucial to the success

of the assay. The functions of the assay were developed and defined by further analyzing the clients' and user's rankings.

4.2 Design Alternatives

After each function was defined, the design team created a list of design alternatives (means) to satisfy each function. Each means was initially tested and evaluated based on its ability to pass the constraints test. If the means did not pass the constraints test, it was eliminated from the list of design alternatives. Table 11 contains all of the means that passed the constraints test. A list of pros and cons was created for each means in order to determine which means satisfies its corresponding function the best. The functions the model must meet to be successful are provide six or more fibrin microthread-C2C12 cell gel interfaces, fixture fibrin microthreads to a PDMS frame, support cell culture environment, and capture data by imaging six or more thread-gel interfaces. Once each means was evaluated, the team completed a feasibility study to determine whether the means could be used to create a successful assay.

Table 11. Means for each function

Thread-Gel Interface	Fixturing System	Data Collection Throughput
Thermanox® coverslip in the middle with threads resting on top	Slits created in frame of assay	Zeiss microscope
Two Thermanox® coverslips on the ends with threads resting on top	Silicone glue	Confocal microscope
Threads resting across a fibrin gel with another fibrin gel on top	Surface roughness as a gasket	Center orientation of threads
		Side orientation of threads

4.2.1 Thread-Gel Interface

Thermanox® coverslips are favorable surfaces for cell attachment and growth. They are resistant to all commonly used solvents. As a result, Thermanox® can be easily sterilized using techniques involving solvents such as ethanol or isopropanol. Additionally, Thermanox® can be cut into various shapes and sizes using sterile scissors. Because Thermanox® can be cut into different shapes and sizes, it allows the design team and user to be able to customize the shape and size of the thread-gel interface allowing for different numbers of fibrin microthreads to be tested with the assay system.

One means for the thread-gel interface is to have a piece of Thermanox® placed under the midline of the fibrin threads. A C2C12 myoblast populated fibrin gel would then be seeded

on top of the Thermanox® (Figure 11). Table 12 lists the pros and cons of this means to be used as a thread-gel interface.

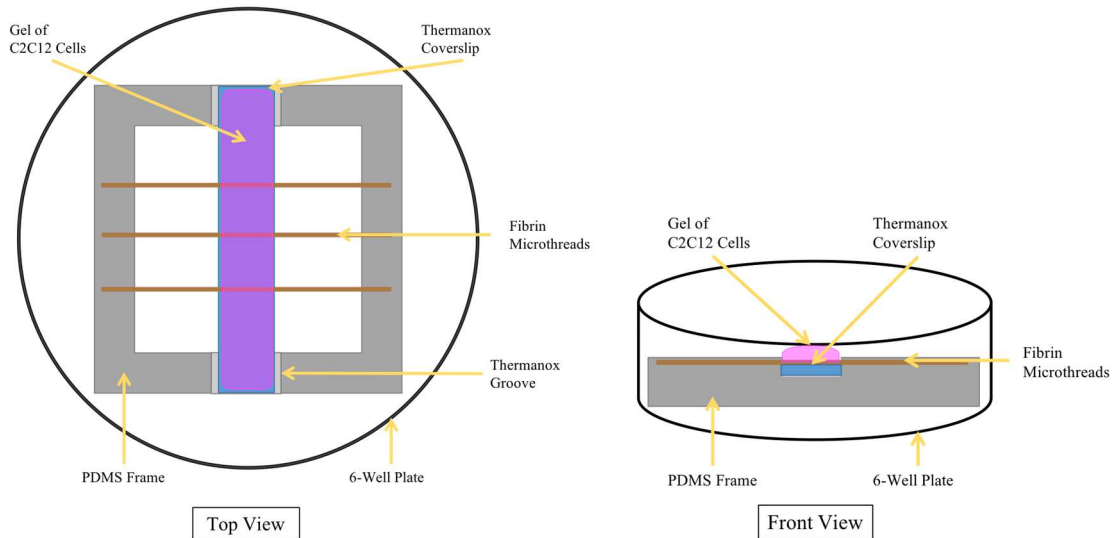


Figure 11. Means 1 for thread-gel interface (top view and front view)

Table 12. Pros and cons for means 1 (one centered thread-gel interface)

	Pros	Cons
One Thermanox® Coverslip Centered	Allows for a wider range of means to be used for fixturing method	Placement of Thermanox® may require additional assembly
	Mechanical support in the middle of the threads	Greater risk of threads bundling when gel is placed
	Only one gel needed	

By placing the piece of Thermanox® coverslip at the midline of the threads, there is a wider range of methods that can be used to fixture the threads to the assay system, increasing the flexibility of the overall assay design. A Thermanox® coverslip at the midline of the threads acts as a mechanical support for the threads. When media is applied to the well in the current configuration, the threads hydrate and will begin to sag. If the threads are too long, they will

touch the bottom of the well plate and compromise the experiment. Longer threads can be used when a mechanical support is present in the middle of the threads. Longer threads are easier to handle making the overall assay more user friendly. Lastly, only one gel needs to be seeded. This is beneficial because the gel needs to completely set before media can be added and only seeding one gel will decrease the amount of time needed to set up the assay as well as decrease the cost of reagents used.

However, additional assembly of a stage created out of PDMS in order to elevate the Thermanox® coverslip off of the bottom of the plate may be needed in order to place the Thermanox® at the midline of the threads, thus, increasing the difficulty of the set-up process as well as increasing the amount of time needed to set up the assay system. Another risk to consider is the threads may touch or bundle together when the gel is seeded. The threads may bundle because the threads are fixtured at the ends creating a wider range of movement of the threads at the center.

The second means for creating the thread-gel interface is to fixture a Thermanox® coverslip under each end of the fibrin microthreads with a gel of C2C12 cells seeded on top of the threads and the Thermanox® (Figure 12), and Table 13 lists the pros and cons for this means.

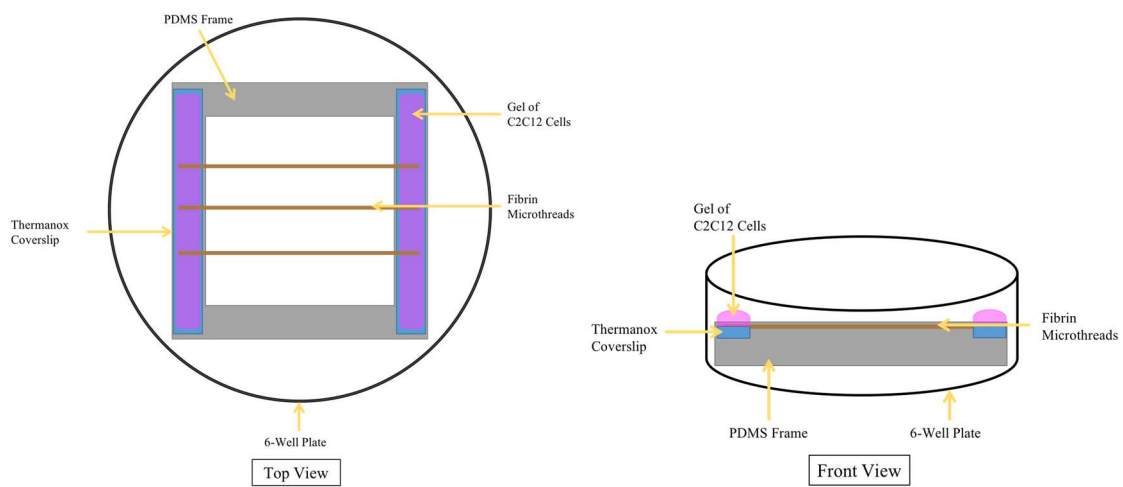


Figure 12. Means 2 for thread-gel interface (top view and front view)

Table 13. Pros and cons for means 2 (thread-gel interface)

	Pros	Cons
Two Thermanox® Coverslips on Sides	Easy to attach Thermanox® to frame	No mechanical support in the middle of the threads
		Fixturing method must account for presence of gel
		Multiple gels needed

The Thermanox® coverslip at the end of the threads will be easy to attach to the frame of the assay system decreasing the time needed to set up the system. Since the threads need to be fixtured to the system at the end of the threads, the fixturing method may interfere with the gel's interaction with the threads. Additionally, there is no mechanical support in between the threads increasing the risk the threads will sag to the bottom of the well. The threads will need to be cut shorter, no longer than 1 centimeter, to ensure they will not touch the well plate. Multiple gels are needed for this means, which increases the time it takes to set up the assay system and increases the volume of reagents needed.

The third means for thread-gel interface is to first seed a gel of C2C12 cells on either side of a well plate (Figure 13). For this configuration, a rubber stopper will be placed in the middle of the well to create a mold for the gel. Once the gel has set, the stopper will be removed and the threads will be placed over the gels with the ends resting on the gels. A second gel will then be seeded on the top of the first gel and the threads. Table 14 lists the pros and cons for the means.

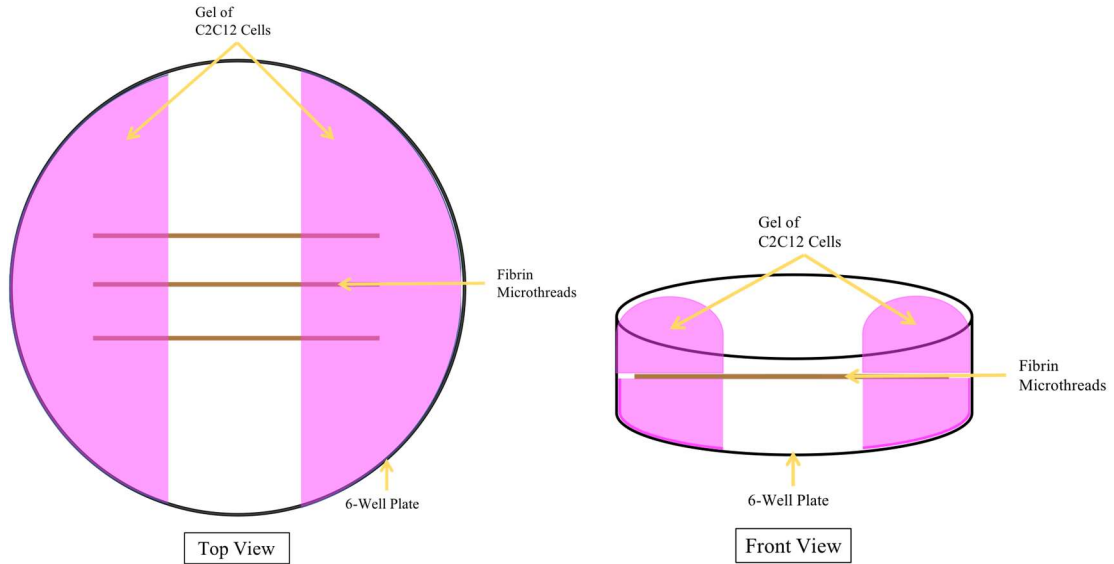


Figure 13. Means 3 for thread-gel interface (top view and front view)

Table 14. Pros and cons for means 3 (thread-gel interface)

	Pros	Cons
Two Gels Seeded on Sides of Well	Cells can migrate and proliferate onto the threads without interruption of the Thermanox®	Placement of gels may require additional assembly
		Complicates means of fixturing method
		No mechanical support in the middle of the threads
		Multiple gels and molds for gels needed

The most beneficial aspect of this design is that the threads will completely be surrounded by gels creating an assay that is a better representation of the environment the threads would experience *in vivo*. However, this means has the most difficult execution. Four gels will need to be seeded, which is a timely procedure that uses the greatest volume of reagents. There is also no mechanical support placed in the middle of the threads increasing the risk of the threads

touching the bottom of the well plate. The last drawback of this design is that it would be difficult to securely fix the threads in the gel as media is added to the well.

4.2.2 Fixturing System

Another function that was decided upon by the design team, users, and clients was a fixturing system to attach the fibrin microthreads to the assay system. Three means were brainstormed for this function including slits, glue, and a gasket.

Currently in the Pins lab, slits are manually made in PDMS using a razor blade, and the fibrin microthreads are placed into the slits using forceps (Figure 14). Once the fibrin microthreads are placed in the slits, the PDMS slit is closed and it is tightly pressed against the fibrin microthreads holding the threads taut in place. A list of the pros and cons to this method in Table 15.

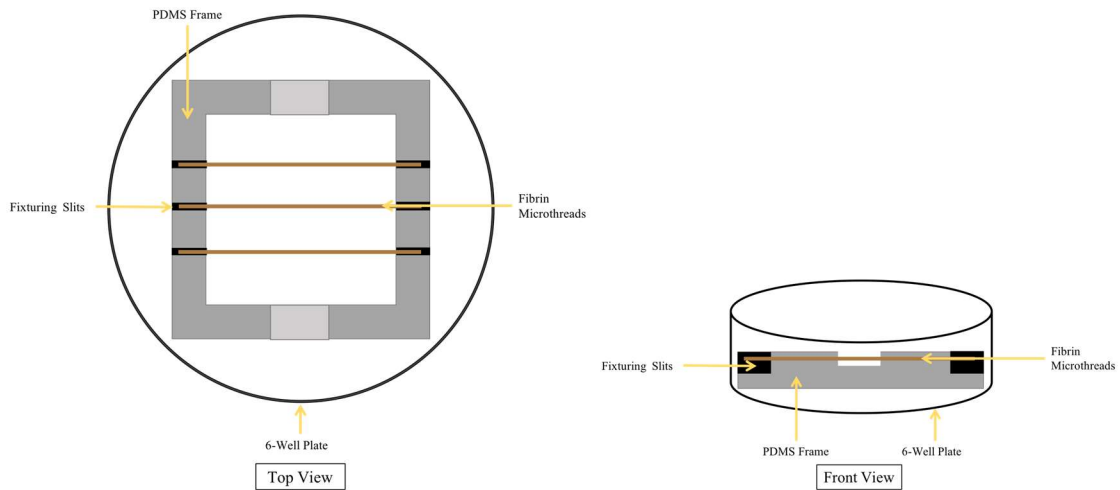


Figure 14. Means 1 for fixturing system (top view and front view)

Table 15. Pros and Cons for means 1 (fixturing system)

	Pros	Cons
Slits Created with a Razor Blade	Does not interfere with sterilization method	Can be difficult to place the threads
	Holds the threads taut	PDMS frame can break
	Quick procedure	Variable depth

By creating slits in PDMS, the assay system would easily be able to be sterilized using the currently used method in the Pins lab of 70% ethanol. Additionally, it is easy to readjust the threads when they are placed into the assay system and pull them taut so that they do not touch the bottom of the well. The slits method is also quick to assemble. The gels can be seeded and the system can be submerged in media on the same day. However, when slits are created in the PDMS, it decreases the mechanical strength of the material increasing the chance the PDMS will split as threads are placed.

Using silicone glue is another means to fixture the threads at the ends of the PDMS (Figure 15). Silicone glues are commonly used for biomedical laboratory research applications because they are non-toxic, adhere to organic and inorganic surfaces, and can be sterilized. A pros and cons list is shown in Table 16.

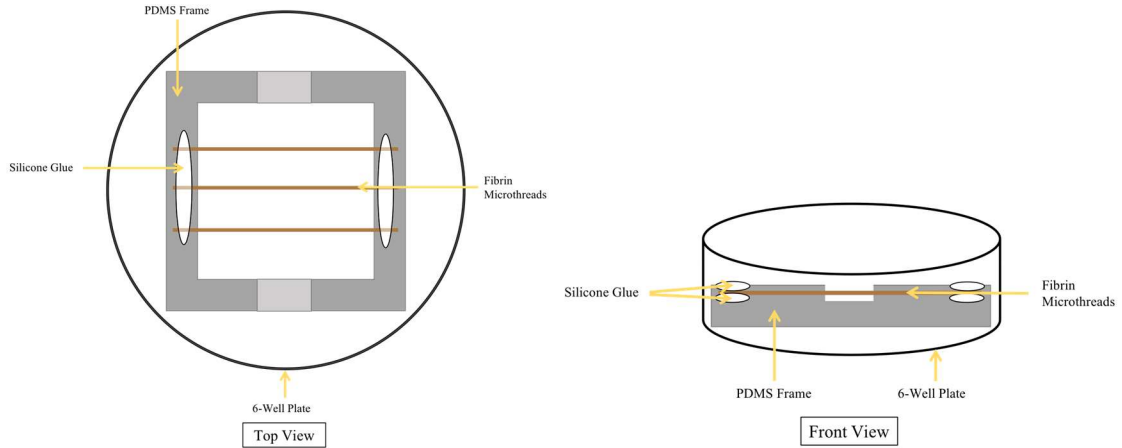


Figure 15. Means 2 for fixturing system (top view and front view)

Table 16. Pros and cons for means 2 (fixturing system)

	Pros	Cons
Silicone Glue	Simple procedure to place threads	Takes 24 hours to dry
	Can be done on top of the Thermanox® coverslips or on PDMS	Complicates sterilization

Using glue to fixture the threads is another commonly used fixturing method in the Pins lab. Glue is placed on the ends of the PDMS frame and the threads are placed on top of the glue. Then another layer of glue is placed on top of the threads. The glue is left to dry for at least 12 hours. Glue is beneficial because it is a simple procedure with minimal steps. In addition, this means can be used with multiple means for thread-gel interface. Thermanox® can be placed in the middle of the threads and the threads can be fixtured to the PDMS using glue, or the Thermanox® can be on the ends of the PDMS frame and the threads can be fixtured using glue on top of the Thermanox®.

The third means to fixture the threads is to create a gasket system. In order to create a gasket, two frames would be 3D printed. Three-dimensional printing naturally creates a

roughened surface on the material. This small degree of surface roughness would work to create a gasket. The threads would first be placed along one frame. Then a second frame would be placed on top and the two frames would be clamped together to hold the threads in place (Figure 16). A list of the pros and cons is in Table 17.

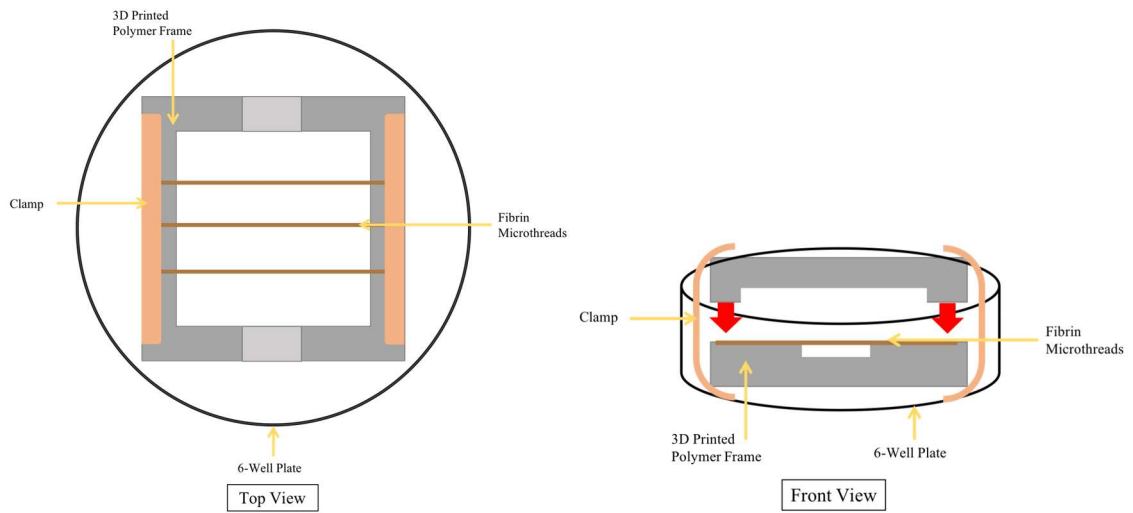


Figure 16. Means 3 for fixturing system (top view and front view)

Table 17. Pros and cons for means 3 (fixturing system)

	Pros	Cons
Gasket and Clamp	Multiple threads can be fixtured at once	Threads could slip out as clamp is placed
		Additional equipment needed for set up
		Gaskets are needed

Ideally, the gasket system would be a quick and efficient way to secure the threads. It would allow for all of the threads to be fixed at one-time. However, the threads tend to have static cling, and the movement of the top 3D printed frame could cause the threads to move out of place. There is also a need for a clamping mechanism to ensure the seal between the two

pieces of the 3D printed polymer frame will not break. Adding a clamping mechanism could increase the time needed to set up the system as well as increase the complexity of the design.

4.2.3 Data Collection Throughput

One of the microscopes available to the team is the Zeiss AxioVert 200M Microscope (Zeiss). The Zeiss is an inverted fluorescent microscope that can take images of living cells. An inverted microscope has a larger working distance than an upright microscope, which allows for a 6-well tissue culture plate to fit in the microscope and be imaged. Images taken with the Zeiss can be analyzed using ImageJ, the analysis software chosen by the team users and clients.

Another microscope available to the team is the Leica TCS SP5 Confocal Laser Scanning Microscope (confocal). Confocal microscopes also use fluorescence to image samples but do so by passing a laser beam through a light source to focus on a defined spot and specific depth within the sample, which increases the resolution of the image. However, the signal intensity is decreased, and the sample must be exposed for a long period of time which increases the overall time it takes to collect data from the assay. Images taken with the confocal microscope can be analyzed using ImageJ.

The location of the data collection points is dependent on the orientation of the Thermanox® coverslip seeded with the fibrin gel of C2C12 cells. Whether the gel is in the center of the PDMS frame (Figure 17A) or on the sides of the PDMS frame (Figure 17B), there will still be at least six data points to image per well.

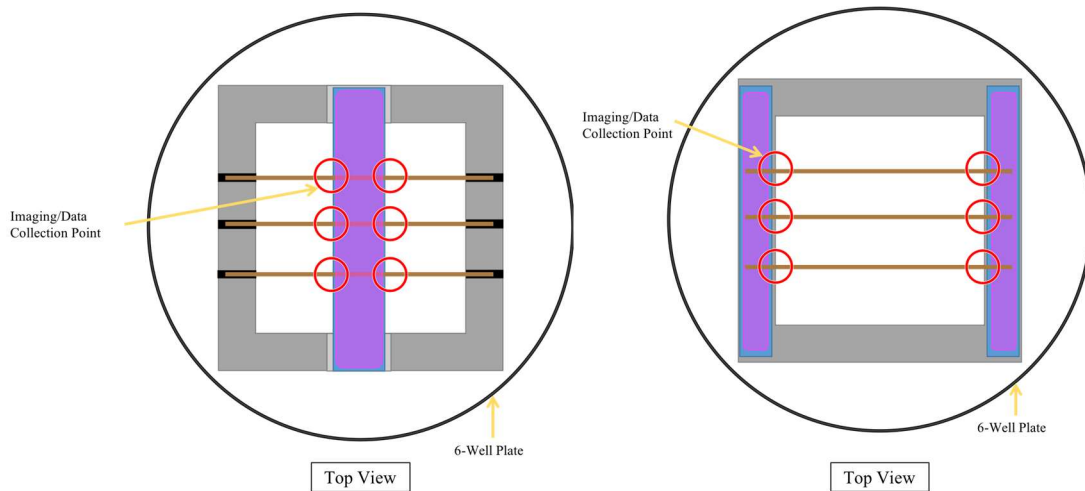


Figure 17. Location of data collection points (circled in red) to be images with Thermanox® in the middle of the PDMS frame (A, left) and on the sides of the PDMS frame (B, right).

4.3 Means Analysis

In order to compare the benefits of the different designs, a decision matrix was created. This decision matrix included the criteria discussed in Section 3.3. The weighting of each criteria was determined by combining the scores of the clients, the user, and the team as shown in Section 3.5. All of the potential designs were given a score from 1 to 3 in each category with a 1 representing the worst score and a 3 representing the best. The criteria for earning each score can be found in Appendix F. The designs were scored in each category independent of the other designs, based only on how successfully they met the outlined objective. The scores are shown in Table 18.

The scores were then multiplied by the predetermined weighting and summed to provide a weighted score. These overall scores provide a preliminary means of evaluating which design best meets all of the design objectives. Because the devices scored the same in many categories,

specifically the broad category of “Supports Cellular Characterization,” additional testing must be completed in order to compare which of the feasible design more effective.

The initial designs that were scored in this decision matrix were: The Grill, Sandwich, Grilled Cheese, and Weenie-on-a-stick along with the Pins Lab Model. The Grill, Sandwich, and Grilled Cheese were determined to be feasible and are described in the following section. The Weenie-on-a-Stick Model would have had threads suspended in clear tubing to allow for imaging on all sides of the threads. There was no determined method of fixturing the threads so the design was determined not to be feasible and was not explored further.

Table 18 : Decision Matrix

		Pugh Concept Decision Matrix	Design Concepts					weighted scores					
			"The Grill"	"Sandwich"	"Grilled Cheese"	"Weenie on a Stick"	Pins Model	Weight	"The Grill"	"Sandwich"	"Grilled Cheese"	"Weenie on a Stick"	Pins Model
Selection Criteria	Ease of Use	Minimal Preparation Time	2	2	1	1	2	0.5	1	1	0.5	0.5	1
		Easy to Clean	2	3	2	1	2	0.5	1	1.5	1	0.5	1
		Limited Monitoring Required	2	2	1	2	3	0.5	1	1	0.5	1	1.5
	Data Collection	Standardization Between Users	2	3	1	1	2	2.7	5.4	8.1	2.7	2.7	5.4
		Precision of Matrix	2	2	2	2	2	2.7	5.4	5.4	5.4	5.4	5.4
		in vivo Predictability	2	2	2	2	2	2.7	5.4	5.4	5.4	5.4	5.4
	Interface with 3D Scaffolds	Support Microthread Scaffolds	2	2	2	2	2	3.7	7.4	7.4	7.4	7.4	7.4
		Sustained Outgrowth	3	3	3	3	3	3.7	11.1	11.1	11.1	11.1	11.1
	Supports Cellular Characterization	Quantify Cell Migration	2	2	2	1	2	3.7	7.4	7.4	7.4	3.7	7.4
		Quantify Cell Proliferation	2	2	2	1	2	3.7	7.4	7.4	7.4	3.7	7.4
		Quantify Cell Confluence	2	2	2	1	2	3.7	7.4	7.4	7.4	3.7	7.4
		Observe Cell Alignment	2	2	2	1	2	3.7	7.4	7.4	7.4	3.7	7.4
		Maximize Data Collection Rate	2	3	2	1	2	3.7	7.4	11.1	7.4	3.7	7.4
	Cost Efficient	Materials Purchased Sustainably	3	2	3	2	3	0.3	0.9	0.6	0.9	0.6	0.9
		Equipment is Inexpensive or Provided	3	3	3	3	3	0.3	0.9	0.9	0.9	0.9	0.9
Minimize Use of Reagents		3	3	3	3	3	0.3	0.9	0.9	0.9	0.9	0.9	
High Throughput		2	3	2	1	2	0.3	0.6	0.9	0.6	0.3	0.6	

TOTAL SCORE	38	41	35	28	39
WEIGHTED SCORE	78	84.9	74.3	55.2	78.5

4.4 Feasible Designs

Based on the weighted scores assigned using the decision matrix, three feasible designs were chosen: “The Grill”, “The Sandwich”, and “The Grilled Cheese.” The fourth model included in the decision matrix, “Weenie-on-a-Stick” was discarded due to a low final score. Each design uses a combination of the means described in Section 4.2.

Figure 18 depicts The Grill design which consists of a rectangular PDMS frame with the fibrin microthreads running longitudinally across the frame. At each end of the frame a piece of Thermanox® plastic is fixed to the frame with sterile silicone glue. Threads are glued at the edges of the frame and the gel is seeded on the Thermanox® at each end of the “grill”. This design eliminates the need to create a separate Thermanox® stage, however it also eliminates any mechanical support at the center of the threads. Hydrated fibrin microthreads tend to sag, and they can only be a certain length without requiring support. The fixturing of the fibrin microthreads would also be difficult with this design because the Thermanox® and gel are located in the same area where the threads would be fixed. Threads would have to be glued to the sides or held in place using an external fixation method.

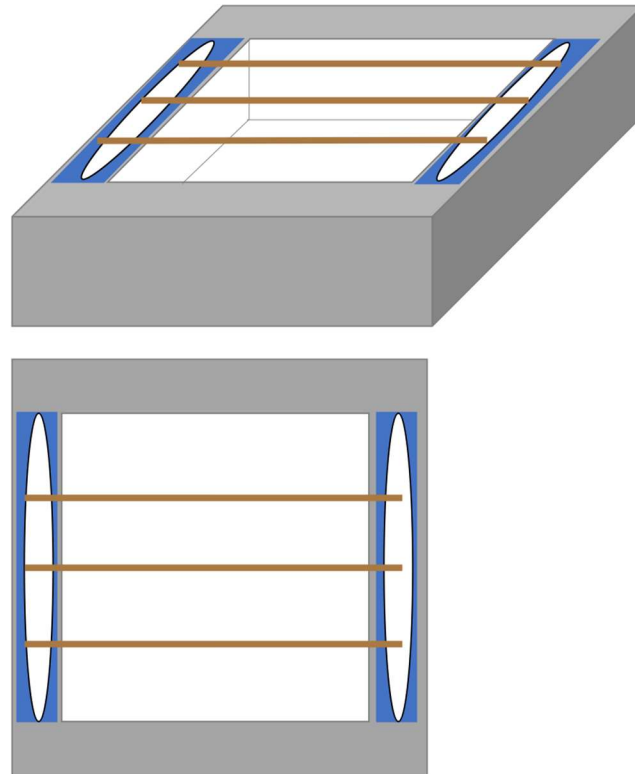


Figure 18. “The Grill” design. The frame is grey, the threads are brown, the Thermanox® is blue, and the glue is white.

The second feasible design is “The Sandwich” as shown in Figure 19. This design consists of a two-part 3D printed frame which snaps together to create a gasket. The fibrin microthreads run across the short dimension of the frame and are held in place using pressure created by the two sides of the sandwich. The Thermanox® seeded with the gel runs longitudinally across the center of the frame. Having a 3D printed reusable frame would eliminate the PDMS preparation and cutting time, however it would add to the cost and disassembly time. In order to use a 3D printed part, the chosen polymer would need to be non-cytotoxic and undergo repeat sterilization or be inexpensive enough to be single use. Using a pressure-based fixture system would also require some sort of preliminary fixturing system to align and hold the threads in place while the top piece of the frame was snapped on.

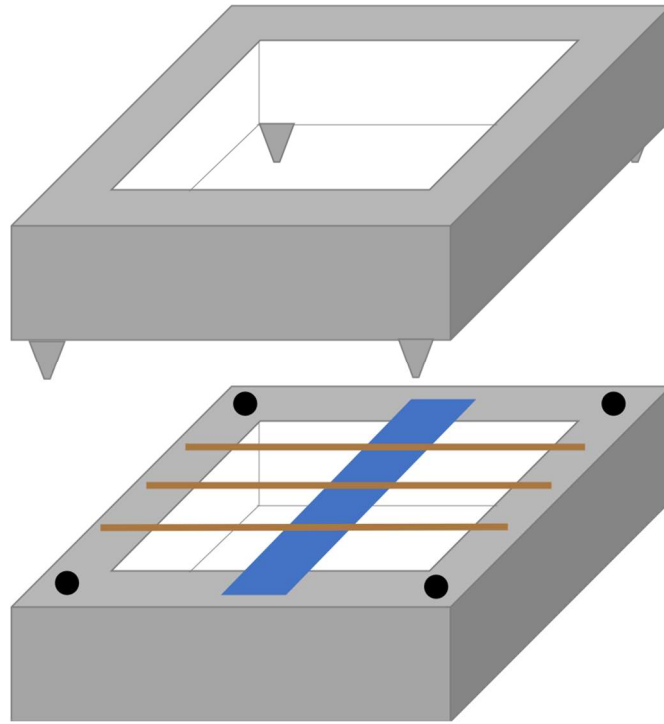


Figure 19. “The Sandwich” design. The frame is grey, the Thermanox® is blue, the threads are brown, and the gel is not pictured.

Figure 20 shows the third feasible design, “The Grilled Cheese,” which does not use Thermanox® or a frame. A plug is placed in the center of the well and gel is cast in a semi-circle at either end. The threads are added on top of the gel and more gel is cast on top to hold the threads in place. This design eliminates PDMS and Thermanox® assembly, however the placement and fixation of threads would be difficult. Additionally, there would be no mechanical support at the center of the threads and the assembly time would increase due to the two-step gel seeding process.

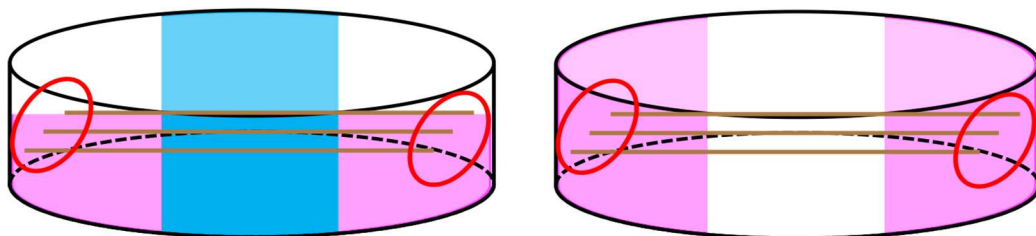


Figure 20. “The Grilled Cheese” design. The plug is shown in blue, the gel is shown in pink, and the threads are shown in brown.

4.5 Final Design

The final design combines aspects of “The Grill” and “The Sandwich” designs and was named the ML Model (Figure 18 and Figure 19). The design is based on a PDMS frame with the threads running longitudinally across. A Thermanox® coverslip will be placed across the center of the frame and seeded with the gel of cells. Threads will be fixed at both ends using slits cut into the PDMS frames. The PDMS frame will be formed in a 3D printed mold. The PDMS frame has an indentation for the Thermanox® to be placed across the PDMS frame. Figure 21 shows the top and side view of the ideal final design.

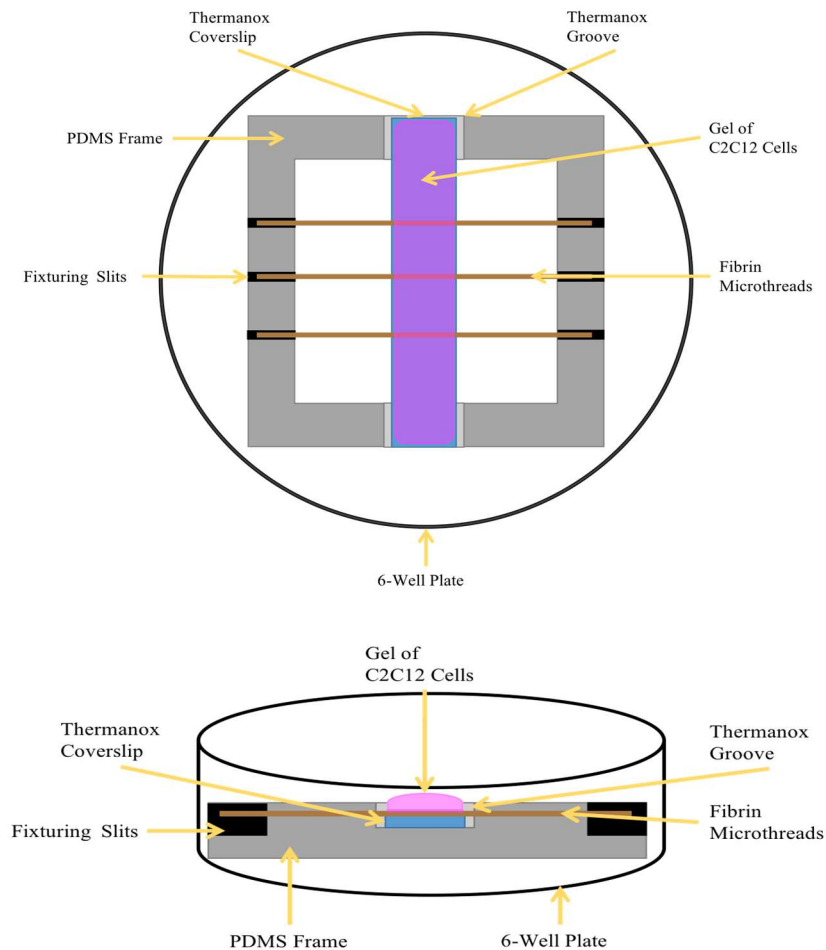


Figure 21. Overview of final design

5.0 Design Development and Validation Plan

In order to test the team's preliminary design, a series of experiments were performed to evaluate different components and validate the model's overall performance. These experiments and tests included assembly testing, reproducibility testing, sustainability testing, and cell outgrowth assay viability. The team compared setup times between the ML Model and the current Pins lab Model to optimize setup time. The team verified the ML Model decreased user-to-user variability. The team verified that our design is non-cytotoxic and compatible with the 6-well cell culture environment. Finally, the team quantified cellular outgrowth onto the fibrin microthread scaffolds.

5.1 Three-Dimensional *in vitro* Assay Development and Analysis

5.1.1 Mold for PDMS Frame

Initial prototypes of the mold were created using the Formlabs Form 2 SLA printer. The first iteration was created as a proof of concept using Durable resin (Figure 22). The first prototype of the mold was used to show design feasibility and to finalize PDMS frame dimensions. It contained the inverse of six frames with a slot for Thermanox®. Three of the wells had grooves for a glue fixturing system, and three were for a slit-based system. Prior to use, the wells of the mold were washed with 70% isopropyl alcohol to remove any uncured residual resin left behind from the fabrication process. PDMS was poured into the mold, vacuumed, and cured following standard procedure. The PDMS frames successfully released from the mold using a razor blade to separate the PDMS from the sides. This iteration of the mold was used to support the decision to use slits as a fixturing method instead of glue.

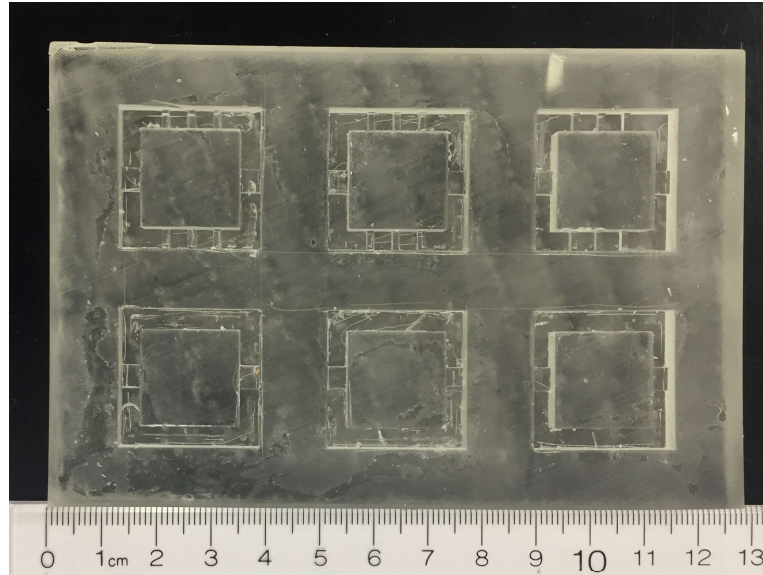


Figure 22. Durable resin mold

The second iteration of the mold was printed using Formlabs Biocompatible resin (Figure 23). This mold had six wells configured for the slit fixation method. Well dimensions were updated, and the overall mold dimensions were optimized to decrease material usage and manufacturing costs. Biocompatible resin was chosen to minimize the risk of any potentially cytotoxic resin components leaching into the PDMS. Prior to filling the wells with PDMS, the mold was soaked in 70% isopropyl alcohol for five minutes and thoroughly flushed with water to remove any uncured resin. However, after baking the PDMS for 2 hours at 60°C and letting it sit at room temperature for an extended period of time, the PDMS did not fully cure and would not cleanly release from the mold. The mold was given subsequent five-minute soaks in 70% isopropyl in an attempt to remove any residue that was interfering with the curing process that was not removed during the first wash. New batches of PDMS were also made to verify that the curing issue was not caused by improper mixing. These corrective measures failed to resolve the issue, and surfaces of the PDMS frame that were in contact with the biocompatible resin

continued not to cure properly. Once the frames were removed from the mold and allowed to sit for an extended period of time, full curing occurred, however the surface features were distorted with low resolution. This preliminary testing showed that biocompatible resin was not a feasible material choice for printing. In addition to preventing the PDMS from curing, printing with biocompatible resin is more than double the cost of printing with other resins.

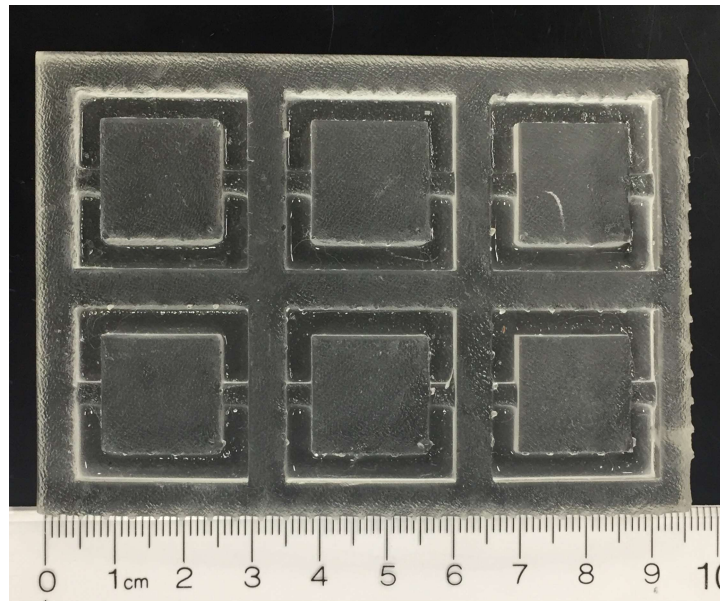


Figure 23. Biocompatible resin mold

The third iteration of the mold was created to decrease PDMS frame removal time. Instead of a 1-piece design, this mold had separate side and bottom components (Figure 24). A rubber gasket was placed between the side and bottom pieces to prevent PDMS from leaking out of the wells. Due to the project timeline and material availability, the two-piece mold was printed using Formlabs Tough resin. The Tough resin was found to be unsuitable for this application, as it was flexible and warped before heating. The team also anticipated having issues with PDMS curing, similar to what was experienced with the biocompatible resin. The complexity of this

design also created more potential for user error and variability. These factors caused the team to designate the two-piece design unfeasible and not proceed with further testing.

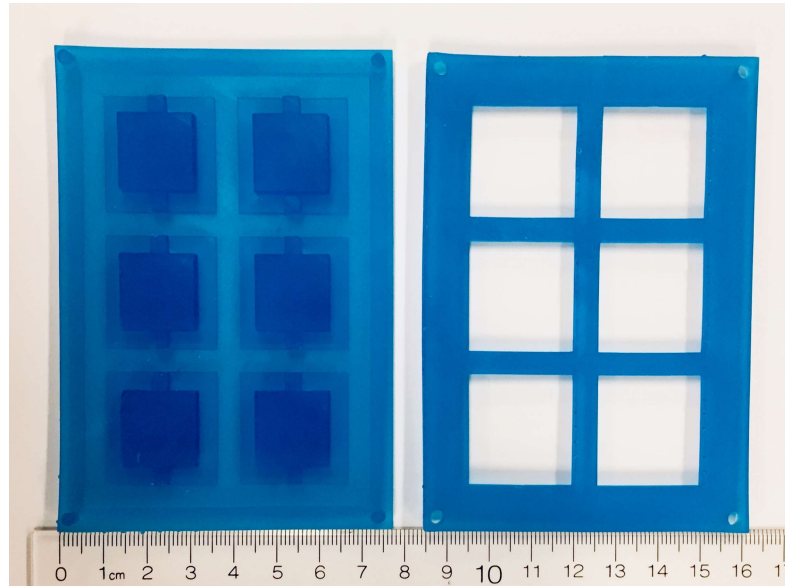


Figure 24. Tough resin two-piece mold. The sides of the mold press fit onto the bottom of the mold. When PDMS is cured, the frames can easily be released from the mold by removing the side piece.

Additive manufacturing using the Formlabs Form 2 SLA printer was chosen as the preliminary prototyping technique due to cost effectiveness, time, and the availability of a biocompatible material. Additionally, some features on the original prototype were too small to be machined accurately. After testing three mold prototypes created with SLA printing it was determined that the Form 2 resin post-print curing process was not consistent enough to be used reliably with PDMS. Each resin cured differently, and the amount of uncured resin left after post-processing varied between materials and print iterations. PDMS would not cure consistently and it was difficult to ensure that all uncured resin was removed from the part.

To avoid the issues associated with Form 2 mold prototypes, a 1-piece 6-well mold was machined from Delrin™ acetal plastic using a 3/32" end mill bit. A 3-degree draft angle was

added to the sides of the mold to facilitate easy removal of the frames. PDMS poured in the Delrin™ mold cured fully after one hour at 60°C and the frames lifted out of the mold cleanly. Figure 26 shows a frame made in the Delrin™ mold. This iteration of the mold was chosen as the team's final design and material because acetal plastic allowed the PDMS to fully cure and release from the mold. Additionally, the inclusion of a draft angle and the rounding of the corners facilitated easy frame removal. Acetal plastic has a heat deflection temperature higher than the PDMS curing temperature of 60 °C and does not leach cytotoxic elements into the PDMS. The feasibility of the Delrin™ mold was verified using testing described in the following sections and it was selected as the team's final design. Three more identical molds were machined to increase design validation data throughput.



Figure 25. Machined Delrin™ acetal plastic mold

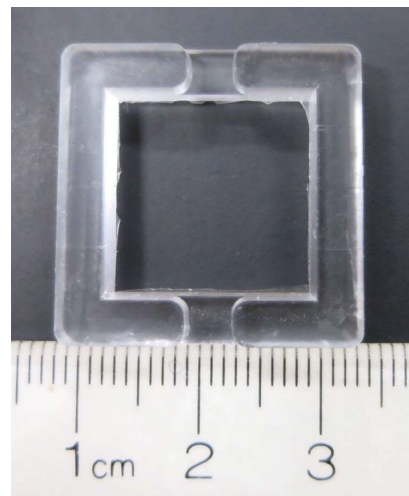


Figure 26. PDMS frame made in Delrin™ mold

5.1.2 Cutting Tool and Guide for Fibrin Microthread Fixturing Slits

To ensure that thread fixturing slits are made with uniform spacing and depth, a cutting tool and guide were designed. The cutting tool (Figure 27) consists of three equidistantly spaced blades. Three- and one-half inch paint scraper blades (Blue Hawk #0089625) were selected for

their two circular holes which allowed the blades to be secured at a fixed distance. This blade length also allows for three PDMS frames to be cut at once. Three blades were assembled onto 6-32 x 1" machine screws and spaced using a combination of nuts and washers. Blades were leveled and then all hardware was tightened to create the final 4.1mm cutting distance.

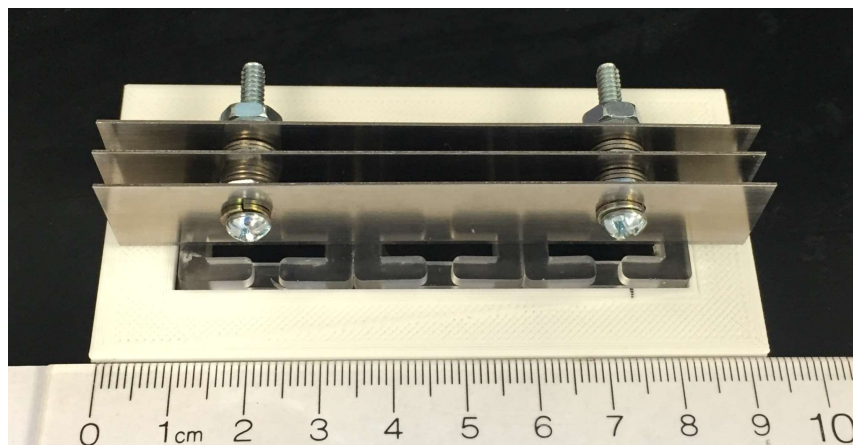


Figure 27. Cutting tool and PLA cutting guard with PDMS frames.

To standardize slit depth, a cutting guard was created to use with the cutting tool. Slits must be cut approximately halfway through the PDMS so that the threads are at the correct height to rest on the Thermanox®. A rectangular cutting guard with a thickness of 1.9 mm was printed using acrylonitrile butadiene styrene (PLA) polymer (Figure 27). The first iteration was created so that the slit depth would be exactly halfway through the 3.8 mm thick PDMS frame. The ends of the cutting guard were marked where the cutting tool should be lined up. The cutting guard was sized to accommodate three frames at once. Frames are placed in the guard (Figure 28) and the cutting tool is lined up with the marks on the guard. Once properly aligned, the cutting tool is pressed into the PDMS to create three evenly spaced cuts on either side of the frame. The combination of the mold, cutting tool, and cutting guide, was named the ML Model.

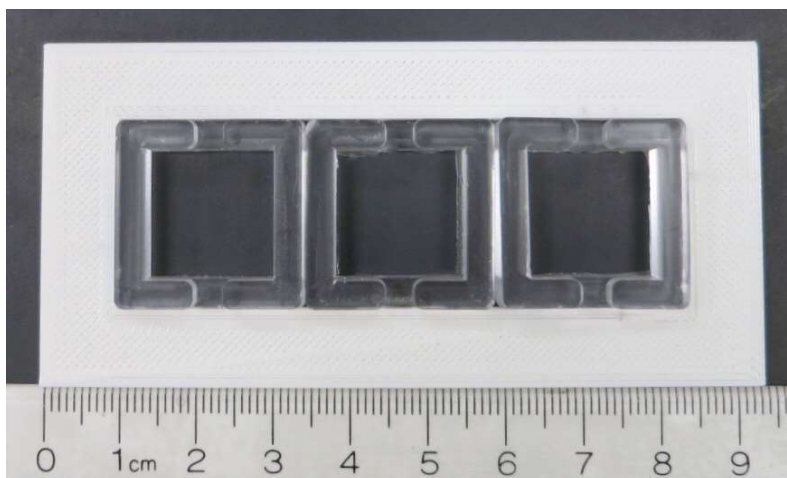


Figure 28. PDMS frames placed in PLA cutting guard

5.2 Three-Dimensional *in vitro* Assay Verification Studies

To verify that the ML Model met the design objectives stated in Section 3.3, the team completed assembly testing, reproducibility and sustainability testing, cell viability and sterility research, and cellular outgrowth assay validation.

5.2.1 Assembly Testing

Tests were performed to verify the amount of time it takes to construct the Pins Lab Model system in comparison to the amount of time it takes to construct the ML Model system. The Pins Lab Model system is constructed in three phases: construction of 6 PDMS rings, construction of the Thermanox® stage, and placement of fibrin microthreads onto PDMS rings. The ML Model system is constructed in four phases: removal of PDMS frames from mold, cutting of the fibrin microthread fixturing slits, placement of Thermanox® stage onto PDMS frame, and placement of fibrin microthreads into fixturing slits. To perform the assembly tests, four inexperienced users were timed when assembling each stage of the set up for the Pins Lab Model and the ML Model. These times were then compared to verify that the ML Model reduces

the assembly time. Assembly testing validates the ML Model is user friendly, standardized, and efficient.

5.2.1.1 Pins Lab Model Assembly Test

The three phases to construct the Pins Lab Model are construction of 6 PDMS rings, construction of the Thermanox® stage, and placement of fibrin microthreads onto PDMS rings. Each user followed a standard testing protocol (Appendix G) and was timed to determine how long it took to assemble each phase of the model. To create the 6 PDMS rings, cured PDMS was removed from a 11.7 cm by 7.5 cm plate and the edges of the PDMS rectangle were removed using a razor blade (Figure 29A). A $\frac{3}{4}$ inch diameter leather hole punch tool was used to make the inner diameter of 6 PDMS rings (Figure 29B). Then, a razor blade was used to cut out squares enclosing the punched-out hole in the center (Figure 29C). Once the 6 squares were created, the corners of the squares were removed using a razor blade to create an octagon shape and the sides were cut to ensure they are similar in width (Figure 29D).

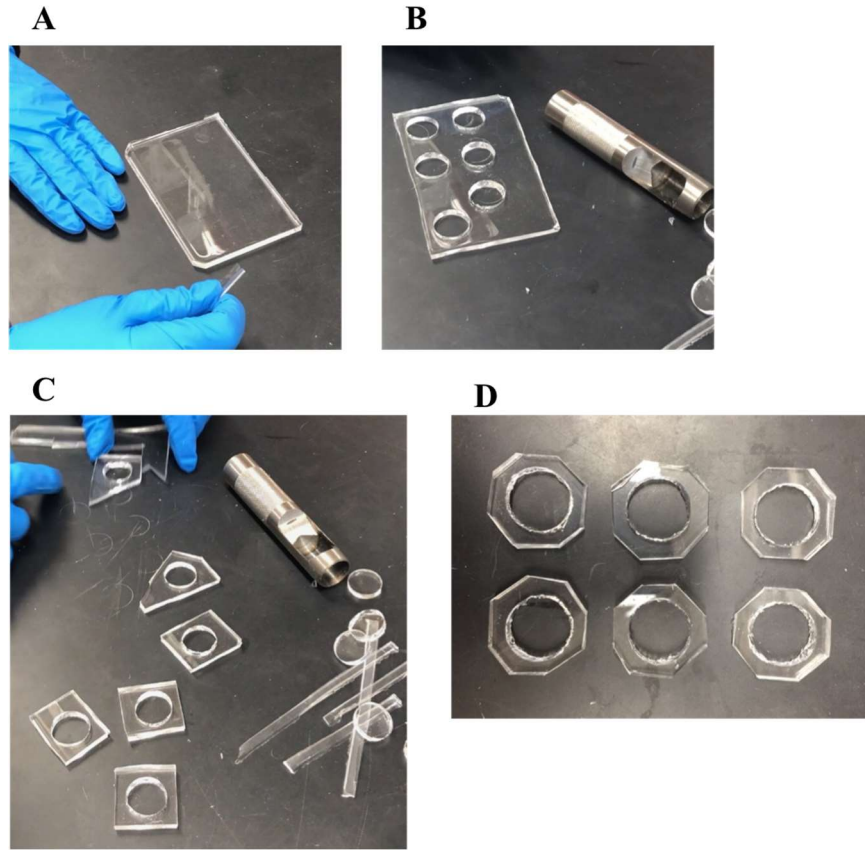


Figure 29. Steps taken to construct the 6 PDMS rings for the Pins Lab Model.

To create the Thermanox® stages, first, a syringe was filled with silicone glue. A leather hole punch tool with a 5/32-inch diameter was then used to punch 12 posts out of PDMS (Figure 30A). Thermanox® coverslips were cut into six 3mm by 13mm rectangles, ensuring that the cell treated side of the plastic was not touching the benchtop (Figure 30B-C). The user used the syringe filled with silicone glue to make two dots of glue in the center of the 6-wells (Figure 30D). Then the PDMS posts were placed on the dots of glue using forceps (Figure 30E). Dots of silicone glue were put on the top of the PDMS posts and forceps were used to lay the Thermanox® coverslips across the posts (Figure 30F).

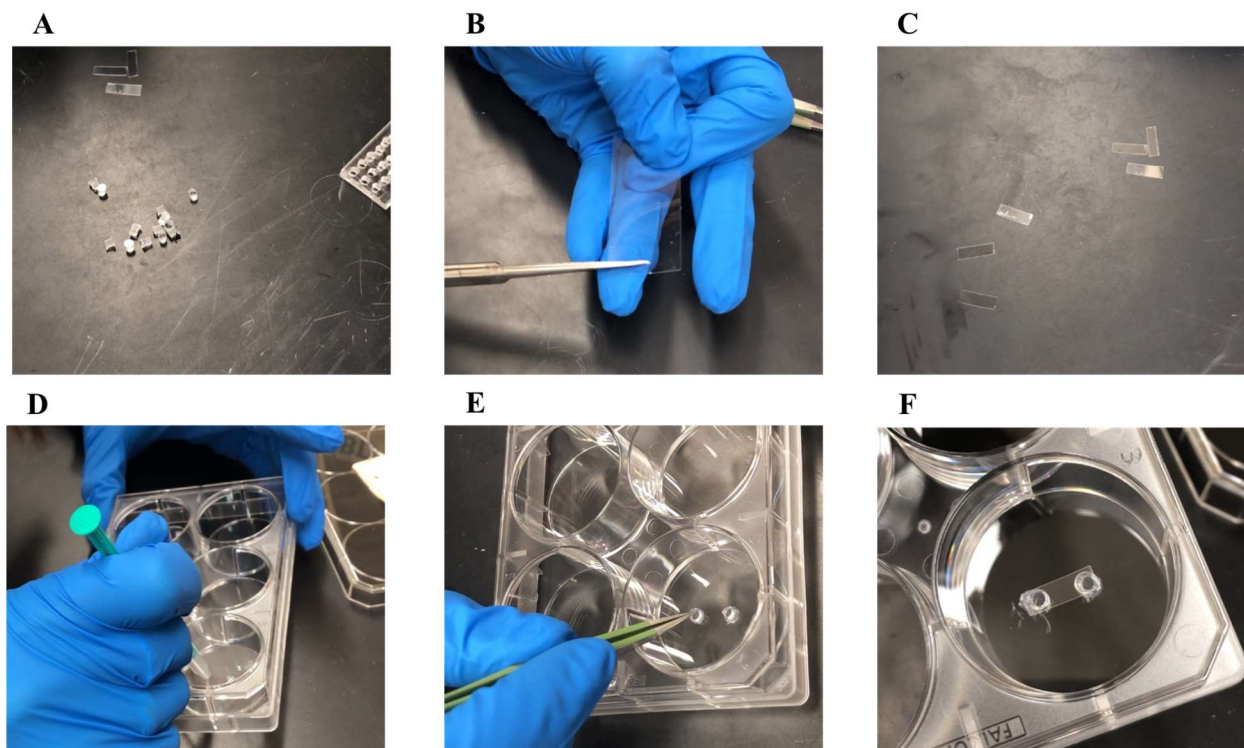


Figure 30. Steps taken to construct the Thermanox® stage for the Pins Lab Model.

In order to place the fibrin microthreads, a razor blade was used to create six parallel slits in the PDMS rings, three on each side of the ring (Figure 31A-B). Next a fibrin microthread was removed from the cardboard box, placed on the benchtop, and cut into three equal pieces using a razor blade (Figure 31C). A cut piece of the fibrin microthread is picked up using forceps. To place the fibrin microthread into the slit, the user pulls open the slit with one hand and places the fibrin microthread into the slit using forceps (Figure 31D). Each fibrin microthread was pulled taught on each side (Figure 31E).

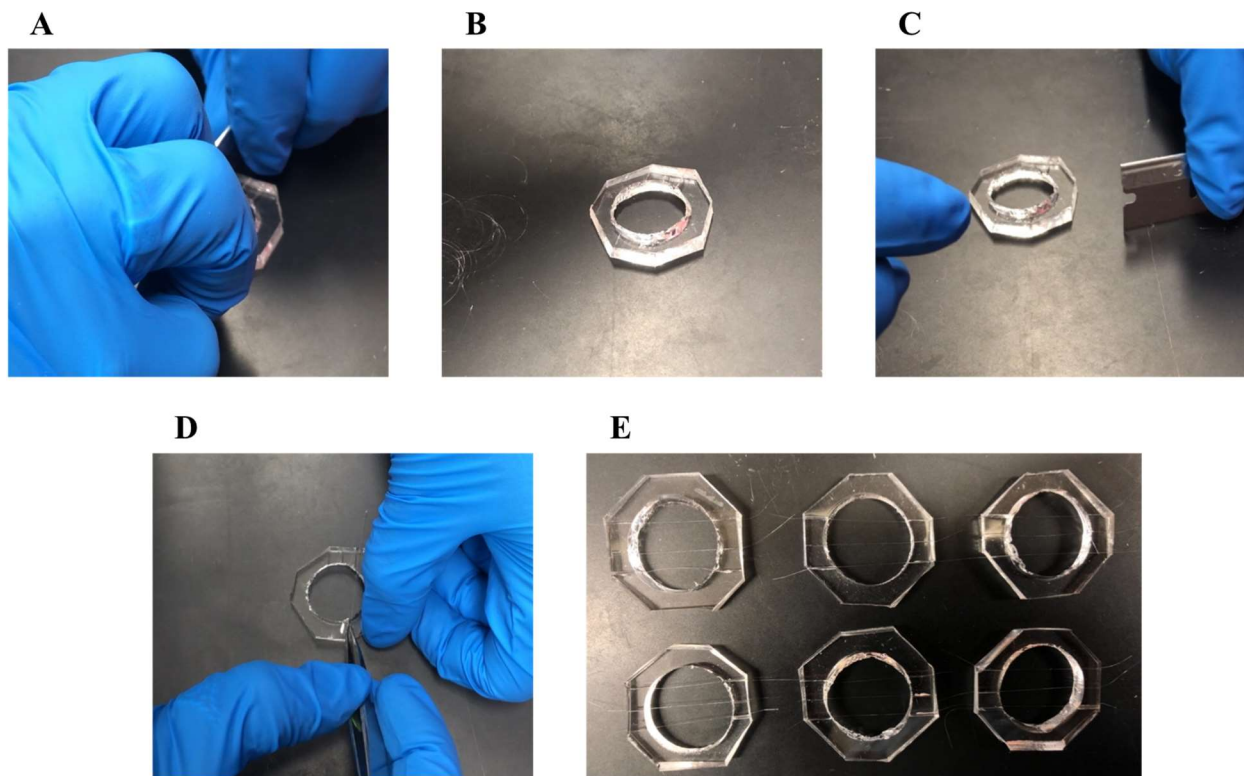


Figure 31. Steps taken to construct place fibrin microthreads for the Pins Lab Model.

5.2.1.2 ML Model Assembly Test

The four phases to construct the ML Model include removal of PDMS frames from the mold, cutting of the fibrin microthread fixturing slits, placement of the Thermanox® coverslips onto the PDMS frames, and placement of fibrin microthreads into the fixturing slits. Each user followed the standard testing protocol (Appendix H) and was timed to determine how long it took to assemble each phase of the model.

To remove the PDMS frames from the mold, a microspatula (scoopula) was used to trace the edges of the PDMS frame and lift it out of the mold (Appendix H, Part 3.2) (Figure 32A-C). This was completed for all six frames in the mold (Figure 32D). Each user was timed as they completed Part 1 of the assembly procedure.

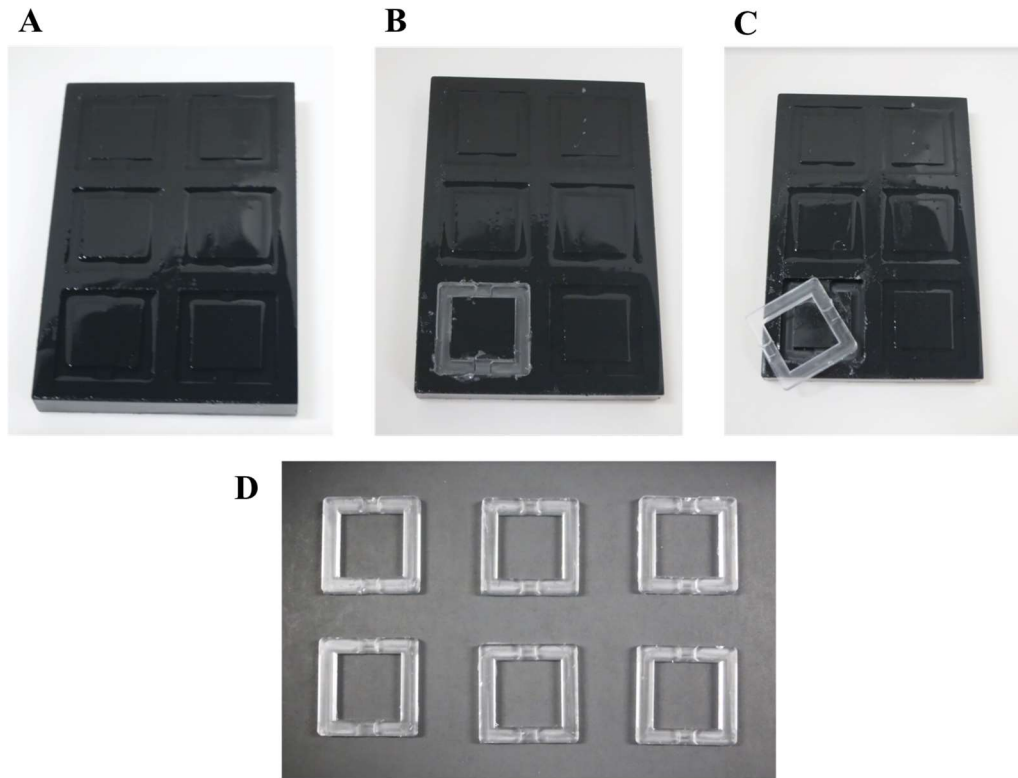


Figure 32. Steps taken to construct PDMS Frames for ML Model

The cutting guide and cutting tool were used to create the fibrin microthread fixturing slits in each PDMS frame. Three PDMS frames were aligned in the cutting guide (Figure 33A). Then, the cutting tool was aligned with the marks created on the cutting guide and pressed into the PDMS frames to create the fibrin microthreads fixturing slits (Figure 33B). This procedure was repeated for all six frames and each user timed themselves completing Part 2 of the ML Model assembly process (Appendix H, Part 3.3).

A**B**

Figure 33. Steps taken to construct fibrin microthread fixation slits using cutting guide and tool

The mold to create the PDMS frames creates a groove in the PDMS frames to hold the Thermanox® coverslips in place. Thermanox® coverslips are cut into 3 x 24.5 mm rectangles using a ruler and scissors, ensuring that the cell treated side of the plastic was not in contact with the benchtop (Figure 34A-B). To place the Thermanox® coverslip into the groove, the user first puts a drop of silicone glue in each groove to hold the Thermanox® coverslip in place (Figure 34C). Then, the user used forceps to place the Thermanox® coverslip into the groove (Figure 34D). This process is repeated for all six frames, and each user was timed to complete Part 3 of the ML Model assembly procedure (Appendix H, Part 3.4).

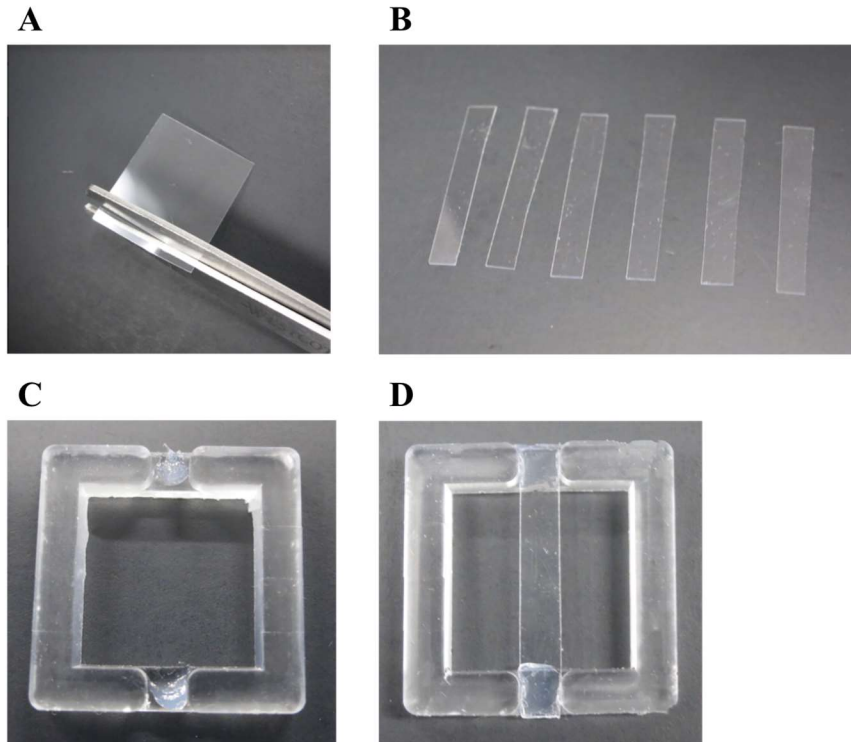


Figure 34. Steps taken to place Thermanox® stage

In order to place the fibrin microthreads, a fibrin microthread was removed from the cardboard box, placed on the benchtop, and cut into three equal pieces using a razor blade. A cut piece of the fibrin microthread was picked up using forceps. To place the fibrin microthread into the slit, the user pulls open the slit with one hand and places the fibrin microthread into the slit using forceps (Figure 35A). This was completed 3 times for each of the six frames. The fibrin microthreads were pulled taught on each side after placement (Figure 35B-C). Each user was timed to complete Part 4 of the ML Model assembly procedure (Appendix H, Part 3.5).

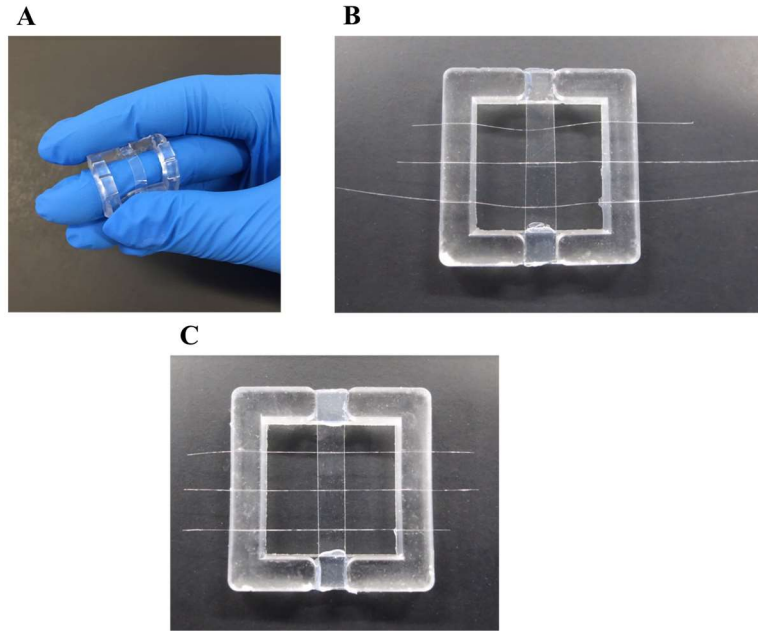


Figure 35. Steps taken to place fibrin microthreads

5.2.2 Reproducibility Testing and Sustainability Analysis

In order to determine the degree of reproducibility of the Pins Lab Model compared to the ML Model, user variability testing was completed. A power analysis was used to determine the necessary sample size and the corresponding assemblies were made following the protocols included in Appendix G-H. The reproducibility of the frame dimensions and fibrin microthread placement were tested for each model and the resulting data was used to measure reproducibility. Figure 36 shows the 6x8 array of reproducibility frames of the Pins Lab Model.



Figure 36. Pins Lab Model PDMS frames for reproducibility testing, $n=48$.

5.2.2.1 Pins Lab Model Reproducibility and Sustainability Tests

To complete the reproducibility and sustainability testing, the design team followed the protocols in Appendix I-J. Four plates of PDMS were poured to a thickness of approximately 4 mm and individually weighed to determine starting mass. Each plate was made into six rings following of the Pins Lab Model user variability protocol (Appendix G, Section 3.1) Excess PDMS not used to create the PDMS rings was collected for each plate and massed. The side width of each ring was measured in two positions (Figure 37 left) and the thickness was

measured across the diameter of the frame. Finally, each ring was individually weighed. Three slits were cut by hand across each ring approximately halfway through the ring's thickness. The distance between the slits was measured in two positions (Figure 37 right).

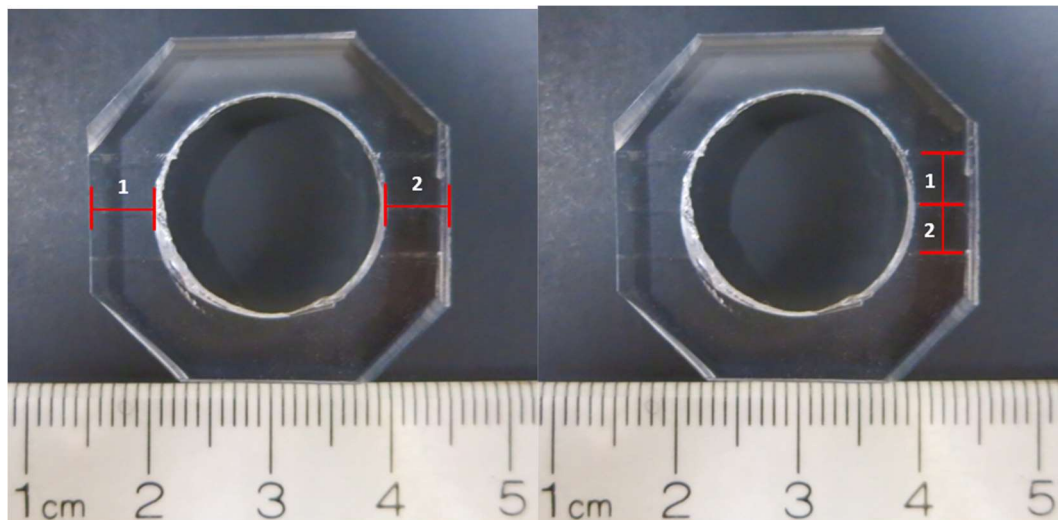


Figure 37. Side width measurement positions (left) and slit distance (right) on the Pins Lab Model

5.2.2.2 ML Model Reproducibility and Sustainability Tests

Testing was conducted on the ML Model following steps similar to those described in the section above (Appendix I-J). Twenty-four PDMS frames were made using the Delrin™ molds. The side width of each frame was measured in two positions (Figure 38 left) and the thickness was measured across the height of the frame. Finally, each frame was individually massed. Three slits were cut across the frame using the cutting tool and cutting guard. The distance between the slits was measured in two positions (Figure 38 right).

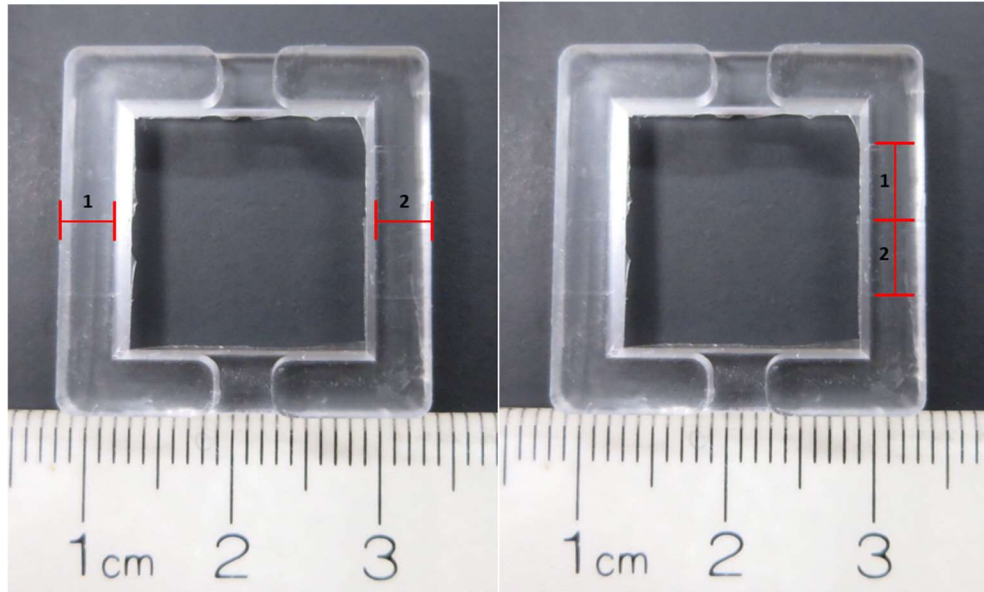


Figure 38. Side width measurement positions (left) and slit distance (right) on the ML Model

5.2.3 Cell Viability Research

The final mold was machined out of polyoxymethylene plastic (POM), commonly known as Delrin™. Delrin™ is used as a biocompatible material and has been used as a long-term medical implant in animal studies (Penick et al., 2005). Medical applications include cardiac valve prosthesis, dental implants and prosthetics, and orthopedic implants. Due to Delrin™'s mechanical, dimensional, and thermal stability along with its biocompatibility, the Penick et al. lab has used Delrin™ as a media-wetted component in a tissue engineered bioreactor to grow cartilage scaffold composite constructs. The Penick lab has obtained good results using Delrin™ as a component in the bioreactor (Penick et al., 2005).

A study was performed to assess the effects of media exposed to machined Delrin™ on cellular proliferation and chondrogenic differentiation of human mesenchymal stem cells (MSCs). Delrin™ was autoclaved to ensure that heating of the material did not have a cytotoxic effect on the MSCs. In the study, an assay was performed to evaluate the attachment of MSCs

onto Delrin™ blocks. A leaching assay was also performed to determine Delrin™'s effect on the proliferation of MSCs. MSCs were seeded at 80,000 cells per 60-mm diameter dish with 3 mL of medium. Twenty-four hours after seeding, the media was exchanged with a 1:1 ratio of fresh media to Delrin™ conditioned media. Cell proliferation was determined by creating a growth curve of the number of cells harvested on subsequent days. Researchers assessed the effects of Delrin™[®] on chondrogenic differentiation of MCSs by means of pellet culture. Chondrogenic differentiation of MCSs was evaluated through a series of histological and immunohistochemical assays on the pellets. Researchers concluded the use of Delrin™ conditioned media did not have a negative impact on the proliferation of MSCs over a one-week period, and Delrin™ conditioned media did not exhibit any chondrogenic differentiation after 3 weeks of culture (Penick et al., 2005).

Delrin™ is a biocompatible, medical grade, non-toxic plastic, making it suitable for biomedical applications. Its melting point is between 160°C and 184°C. Additionally, the maximum service temperature, the highest temperature at which the material can reasonably be used without oxidation, chemical change or excessive deflection or “creep” becoming a problem, of Delrin™ is between 76.9°C and 96.9°C. Autoclaves are typically programmed to reach a temperature of at least 121°C for 15 minutes to fully steam sterilize a material (CES EduPack, 2018).

The mold created by the design team must be able to withstand being in an oven at 60°C for one hour to thoroughly cure the PDMS frames. Because 60°C is well below the lower limit of the maximum service temperature, the Delrin™ will not leach any chemicals into the PDMS frames making them cytotoxic to the C2C12 cells. Evidence found in the Penick et al. paper defends Delrin™ as a safe material to be used in a cell culture environment. Therefore, the

design team did not need to complete a direct contact assay or leaching assay to assess the cell viability of the Delrin™ mold (Penick et al., 2005).

5.2.4 Sterilization Method

The existing model uses 70% ethanol as a sterilization method. After observing and interviewing the current user, and future user of the ML Model, the team determined that many failures occur during or after the ethanol disinfection. This is due to the several times that the wells are filled with liquid for the sterilization and subsequent rinses. This can cause the threads to become dislodged from the slits or dehydrated and break (Grasman, 2016). It was concluded that ethylene oxide gas (EtO) sterilization would be used in order to reduce the rate of failure.

5.2.4.1 Ethylene Oxide Sterilization

Dry scaffolds were sterilized by exposure to EtO for 12 hours using an Anprolene AN74i gas sterilizer. The scaffolds were aerated for a minimum of 24 hours to remove residual EtO molecules. Research supports that the mechanical strength and the chemical properties of fibrin microthreads are not compromised when using the EtO sterilization method. Both ethanol and EtO sterilization techniques are effective at preventing microbial or fungal growth in three days of observation (Grasman, 2016).

5.2.5 Cellular Outgrowth Assay Validation

Cellular outgrowth assay validation was performed as described in the Outgrowth Assay Protocol (Appendix K). Fibrin microthreads were made with standard protocol (Appendix A) and left to dry for at least 24 hours before they were used for assembly. The ML Model system was assembled 5-7 days before the first day of the experiment using the ML Model Protocol

(Appendix L). EtO sterilization was completed 4-5 days before the assay was run. The team completed four, 96-hour cellular outgrowth assay validation experiments. Each experiment consisted of one 6-well plate of fibrin microthreads and one 6-well plate of collagen microthreads. The collagen microthreads are another type of scaffold being explored by the Pins Lab (Cornwell, 2004). The collagen microthread plates were used as a negative control because the assay is run using a fibrin-based gel and therefore outgrowth would not occur onto the collagen threads.

6.0 Final Design and Results of Validation Testing

6.1 Overview of Final Design

A 6-well Delrin™ mold was selected as the final design for creating PDMS frames. To further standardize the assay process a cutting tool and cutting guide were designed in conjunction with the Delrin™ mold. Based on the studies described in Chapter 5, this final design achieved all of the objectives and functions described in Chapter 3, while following the set constraints and specifications. The detailed protocol for creating the ML Model can be found in Appendix L.

The four, 6-well Delrin™ molds can be re-machined using the part drawings found in Appendix M&N. A 3-degree draft angle on the mold sides is not necessary for frame formation, but facilitates easier frame removal. PDMS frames should be removed with a thin, blunt tool to prevent damage to the frame or the mold. A 20 mL syringe is used to fill the mold and a straight edge is used to level off excess PDMS. If any PDMS remains after frame removal, the mold can be cleaned using 70% isopropyl alcohol.

The cutting tool consists of three equidistant razor blades spaced approximately 4.1 mm apart using a combination of nuts and washers assembled onto machine screws. Three and a half inch blades were used because they allowed three PDMS frames to be cut simultaneously. Spacing hardware was chosen to account for decrease in distance when the washers were tightened. Before the final tightening occurred, the blades were leveled. To maintain blade spacing and prevent loosening a locking nut was added to the end of the screw.

To ensure the PDMS frames are cut to the correct depth, a rectangular cutting guide was 3D printed out of PLA using the part drawing found in Appendix O. The thickness of the cutting

guide was designed to be half the thickness of the PDMS. Cutting guide size and thickness can be adjusted based on the size of the cutting tool and the thickness of the PDMS frames.

6.2 Objectives Achieved

The following section describes how the final design components achieved the objectives set forth in Chapter 3: Project Strategy. This section includes details on how the PDMS mold, cutting guide, and cutting tool followed the specifications set and remained within the design space.

6.2.1 Ease of Use: Assembly

6.2.1.1 Mold for PDMS Frame

The defined objective was that the mold must be intuitive to researchers, regardless of experience level. One mold can make six PDMS frames in one round of PDMS curing. Common laboratory practice of making PDMS is intuitive, and a 10mL syringe can be used to inject the PDMS into each well. The mold is easy to handle, and can be moved from benchtop to oven, without concern. Compared to the current model assembly, the mold itself combines four steps into one. Previously, users had to start from a sheet of PDMS, trim the edges of the PDMS sheet, punch six evenly spaced holes, cut squares around each hole, and make those squares into octagons. With the PDMS mold, the user will only have to remove the PDMS frame and begin cutting slits and placing fibrin microthreads into the slits. The mold produces identical frames without relying on the user to properly shape them. The mold has a built-in groove for holding the Thermanox® coverslip, eliminating the need for the user to make the Thermanox® stage.

Once the PDMS frames are carefully removed from the mold using a microspatula, the mold can be cleaned and used again. Figure 39 displays the steps for both the Pins Model and ML Model.

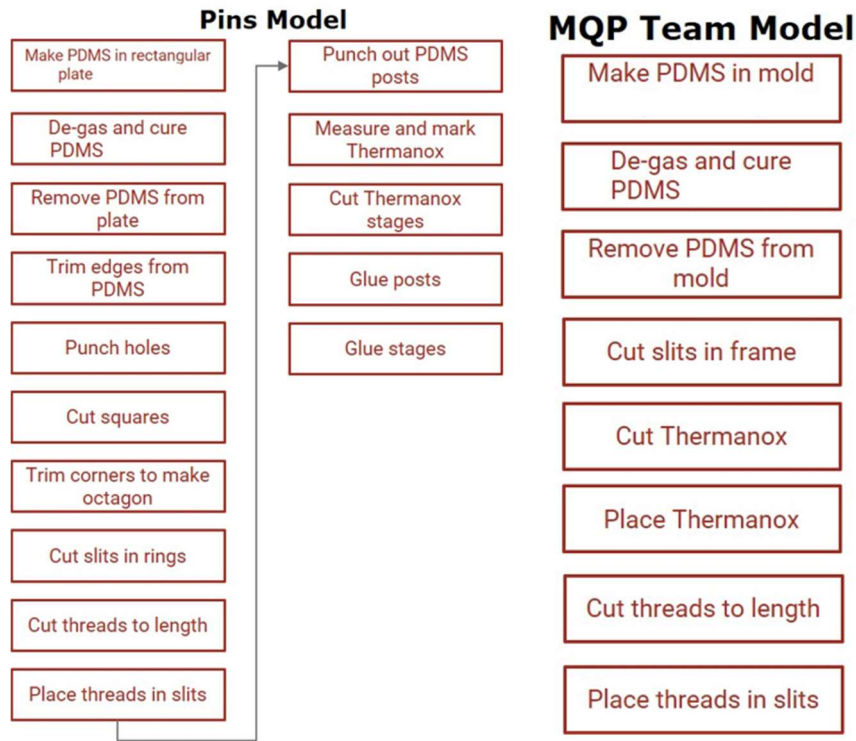


Figure 39. Steps of both the Pins Lab Model (left) and ML Model (right). The ML Model decreased number of steps from 15 to 8.

The assembly times to create the Pins Model and the ML Model were recorded and compared. Each of the members of the design team (N=4) were timed as they completed each part of the Pins Model assembly (Appendix G) and the ML Model assembly (Appendix H). The assembly steps were categorized into four different parts: PDMS frame fabrication, Thermanox® placement, fibrin microthread fixturing slit cutting, and fibrin microthread placement. Although times for all four steps were recorded, the team decided that only three parts, PDMS frame fabrication, Thermanox® placement, and fibrin microthread fixturing slit cutting, would be analyzed and compared between models. This is because the mold, cutting tool, and cutting

guide were designed to decrease user-to-user variability and ease of use in these steps, and did not address fibrin microthread placement.

The average time of each team member for assembly of the Pins Model and ML Model were recorded in Tables 19 and 20.

Table 19. Assembly times for four assembly steps: Pins Lab Model

Assembly Step	Team Member 1	Team Member 2	Team Member 3	Team Member 4	Average	Standard Deviation
PDMS Frame	6.5 min	8.5 min	9 min	8.2 min	8.05 min	± 1.08 min
Thermanox® Stage	11.9 min	12.2 min	12.5 min	12.7 min	12.3 min	± 0.35 min
Fixturing Slits	1.5 min	1.1 min	1.25 min	1.5 min	1.3 min	± 0.20 min
Thread Placement	33.12 min	19 min	22.2 min	26.4 min	25.2 min	± 6.09 min

Table 20. Assembly times for four assembly steps: ML Model

Assembly Step	Team Member 1	Team Member 2	Team Member 3	Team Member 4	Average	Standard Deviation
PDMS Frame	5 min	6 min	5.2 min	5.2 min	5.35 min	± 0.44 min
Thermanox® Stage	4.4 min	4.7 min	5.7 min	5.5 min	5.08 min	± 0.62 min
Fixturing Slits	1.4 min	0.9 min	0.8 min	0.75 min	0.96 min	± 0.29 min
Thread Placement	25.1 min	23.4 min	32.2 min	14.9 min	24.1 min	± 7.15 min

Figure 40 displays the average times for the three analyzed parts of the Pins and ML Model assemblies.

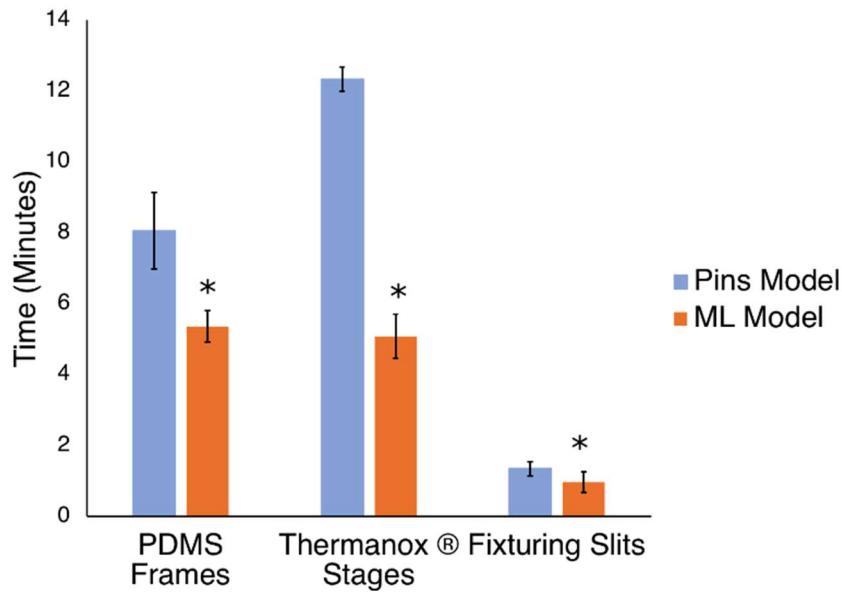


Figure 40. Assembly time differential between Pins Model and ML Model.

A paired one tail T-test was performed on the collected data to determine if the amount of time it took to assemble the different parts of the ML Model was significantly shorter than the time it took to assemble the Pins Model. A P-value of <0.05 (*) was considered to be statistically significant. The average times to create the PDMS frames for the Pins Model and ML Model were 8.05 ± 1.08 minutes and 5.35 ± 0.44 minutes, respectively. The P-value for the PDMS frame fabrication step is 0.00559. The average times to place the Thermanox® stages for the Pins Model and ML Model were 12.3 ± 0.35 minutes and 5.08 ± 0.62 minutes, respectively. The P-value for the PDMS frame fabrication step is 1.317×10^{-5} . Statistically, it takes significantly less time to create the PDMS frames using the ML Model. The average times to create the fibrin microthread fixturing slits for the Pins Model and ML Model were 1.3 ± 0.20 minutes and 0.96 ± 0.29 minutes, respectively. The P-value for the PDMS frame fabrication step is 0.0407. Statistically, it takes significantly less time to create the fixturing slits using the ML Model. A decreased assembly time will allow the user of the ML Model to create more models per day in preparation to run the

cellular outgrowth assay. In turn, this will increase data throughput of the assay results, expediting the *in vitro* testing process.

6.2.1.2 Cutting Guide and Cutting Tool for Fibrin Microthread Fixation Slits

The cutting guide makes cutting slits in the PDMS frame much more user-friendly and reproducible. The old model required the use of a single razor blade to cut three slits in each ring based on the user's best guess of where to place them and how deep to cut. The cutting tool cuts three slits (on each side of the frame) in three frames at once. The cutting guide ensures that all slits are the same depth. The tool/guide combo is intuitive and decreases the rate of failure caused when the PDMS is cut too deep and the frame breaks. With one motion and cut, the user is able to accomplish making identical slits (six slits per frame, three on each side) for three frames at once.

6.2.2 Reproducibility: Frame Fabrication

6.2.2.1 Mold for PDMS Frame

One of the highest ranked objectives during project strategy (Chapter 3) was reproducibility, meaning that the model must produce results that are consistent across technical replicates and multiple users. The mold creates six identical PDMS frames; 24.5 mm in length, 3.8 mm in height, with a width of 4 mm. Each frame provides a groove for the Thermanox® coverslip. The model currently used in the Pins lab has significant of variance in the length, height, and width of the model, which impacts the fibrin microthread placement and length. Figure 41 shows the location of the width measurements taken on each frame, and Figure 42 graphically displays the difference in variance between the two models.

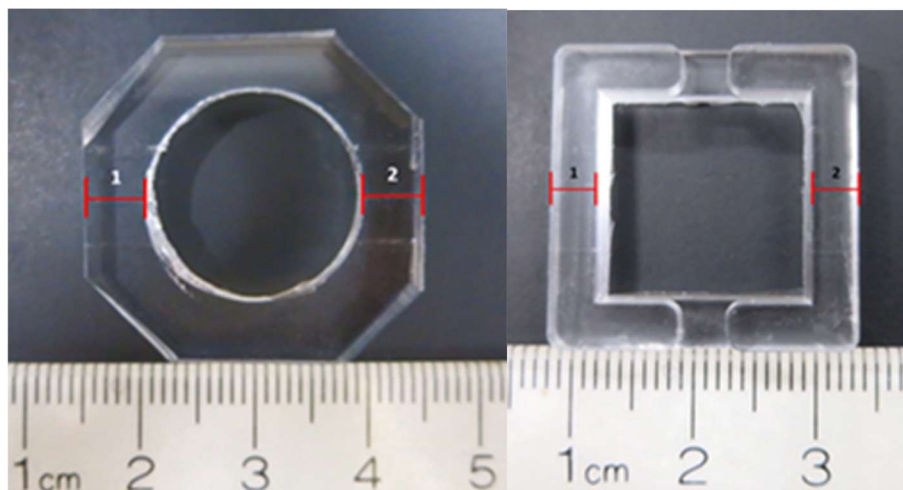


Figure 41. Width of PDMS frame measurement (red); Pins Model (left) and ML Model (right).

Reproducibility testing was conducted as described in Section 5.2.2. The team completed statistical analysis on the difference in the width of the PDMS frames created with the Pins Model assembly and the ML Model assembly. A total of 24 frames were created for each model (N=24; n=48). Two measurements of the width were taken and averaged for each frame (Figure 48). The standard deviation between the two measurements was calculated for each of the 24 frames for both models. In addition, the mean widths and overall standard deviations for the Pins Model and ML Model were calculated, 5.07 ± 0.896 mm and 3.74 ± 0.0505 mm, respectively. A paired T-test was performed on the standard deviations for each model to determine if the degree of user-to-user variability was reduced when using the ML Model. A P-value of <0.05 was considered to be statistically significant. The P-value was 2.78×10^{-6} (Figure 42).

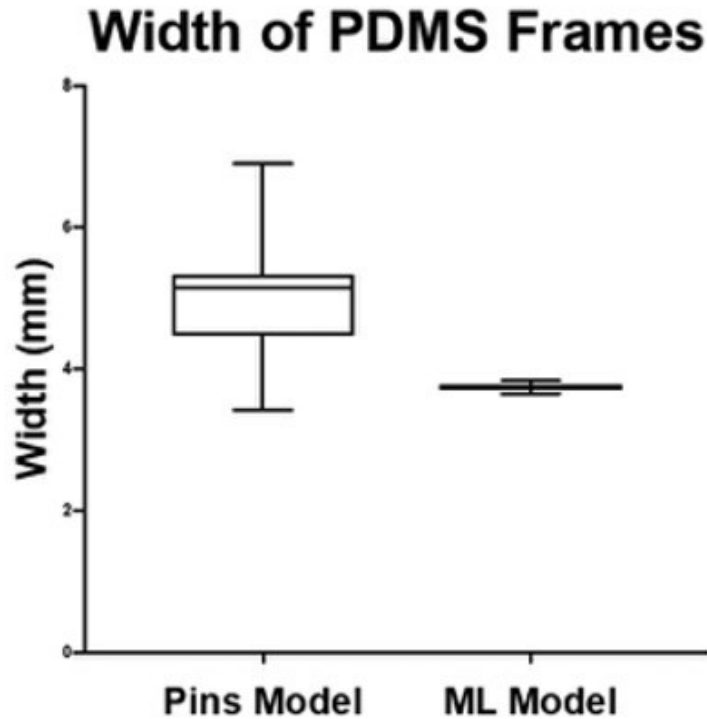


Figure 42. Statistically significant ($P < 0.05$) decrease in variation of PDMS frame dimensions in ML Model. Decreased user-to-user variability by 94.4%. Team used a paired T-Test, $n = 24$, $p\text{-value} = 2.78 \times 10^{-6}$

6.2.2.2 Cutting Guide and Cutting Tool for Fibrin Microthread Fixation Slits

The cutting guide/tool meets the reproducibility objective because it creates three equidistant slits in the PDMS frame, all with the same depth. The chance of failure (by PDMS frame breaking) decreases because the razor blade is stopped by the cutting guide at the bottom, preventing the user from cutting too deep. The cutting guide holds three PDMS frames, and the cutting tool can cut all of them at the same time. The cutting guide indicates where to place the cutting tool, improving reproducibility of the distance between slits and the depths of the slits, making each PDMS frame virtually identical. Figure 43 shows two models side by side and the measurements that were taken while the variation in these measurements is shown in Figure 44.

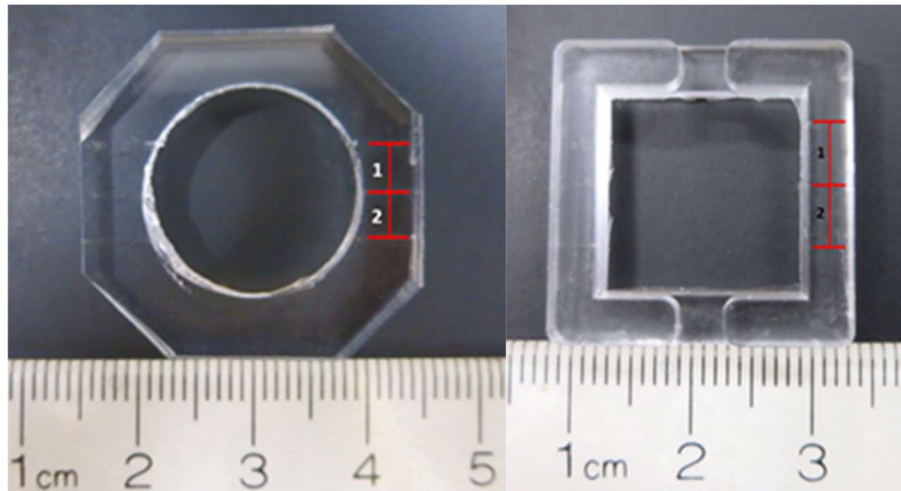


Figure 43. Distance between fibrin microthread fixturing slits measurement (red); Pins Model (left) and ML Model (right).

The team also completed statistical analysis on the difference in the distance between the fibrin microthread fixation slits created with the Pins Model assembly and the ML Model assembly. A total of 24 frames were created for each model (N=24; n=48). Two measurements of the distance between three slits were taken for each frame (Figure 43). The standard deviation between the two measurements was calculated for each of the 24 frames for both models. In addition, the mean distance between the fibrin microthread fixturing slits and overall standard deviations for the Pins Model and ML Model were calculated, 3.83 ± 0.533 mm and 4.51 ± 0.0854 mm, respectively. A paired T-test was performed on the standard deviations for each model to determine if the degree of user-to-user variability was reduced when using the ML Model. A P-value of <0.05 was considered to be statistically significant. The P-value was 9.20×10^{-6} (Figure 44).

Distance Between Fibrin Microthread Fixturing Slits

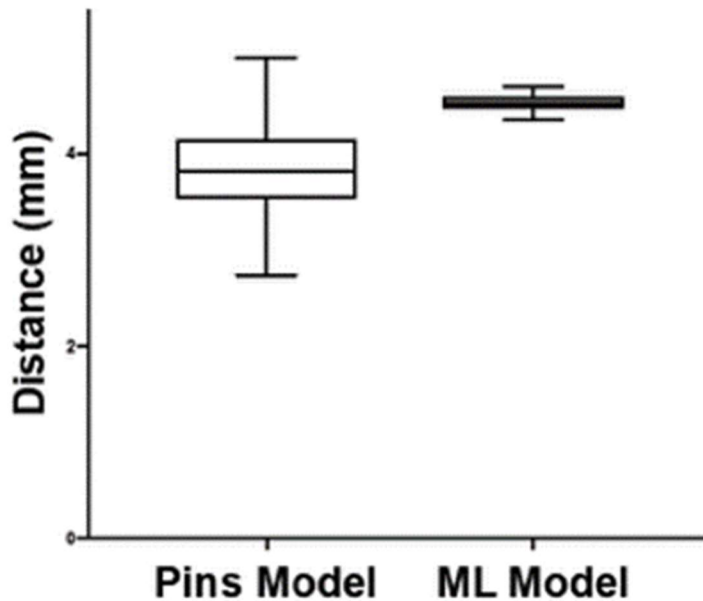


Figure 44. Statistically significant ($P < 0.05$) decrease in variation of fibrin microthread placement in ML Model. Decreased user-to-user variability by 83%. Team used a paired T-Test, $n=24$, $p\text{-value}=9.20 \times 10^{-6}$

6.2.3 Cost Efficient

6.2.3.1 Mold for PDMS Frame

The mold is a cost-efficient option to the current model because it is reusable. The dimensions of the Delrin™ mold are 3.681 in x 2.52 in x 0.228 in, and the cost for this volume of raw materials of Delrin™ plastic is about \$8 per mold. The cost of the 3/32 flute 3-degree draft end mill needed to machine the mold is \$20.57. The total estimated labor cost of four molds is about \$350. A single mold costs approximately \$102 [\$8 of material + ¼ (cost of tooling and labor)].

A sustainability analysis was performed to determine the amount of waste PDMS produced when creating the Pins Model and the ML Model. The Pins Model requires an 11x7 cm

sheet of PDMS to be created to hand-cut the frames out of, resulting in 70.4% of the PDMS sheet wasted. The Delrin mold creates a negligible amount of PDMS waste because a syringe is filled with the exact volume of PDMS needed to fill the six molds. As indicated in Figure 46, the total cost of PDMS needed to create 6 PDMS frames of the Pins Model is \$5.01, and the total cost of PDMS needed to create the ML Model is \$0.91. The ML Model decreases the cost of PDMS used by 81.8% (Figure 45).

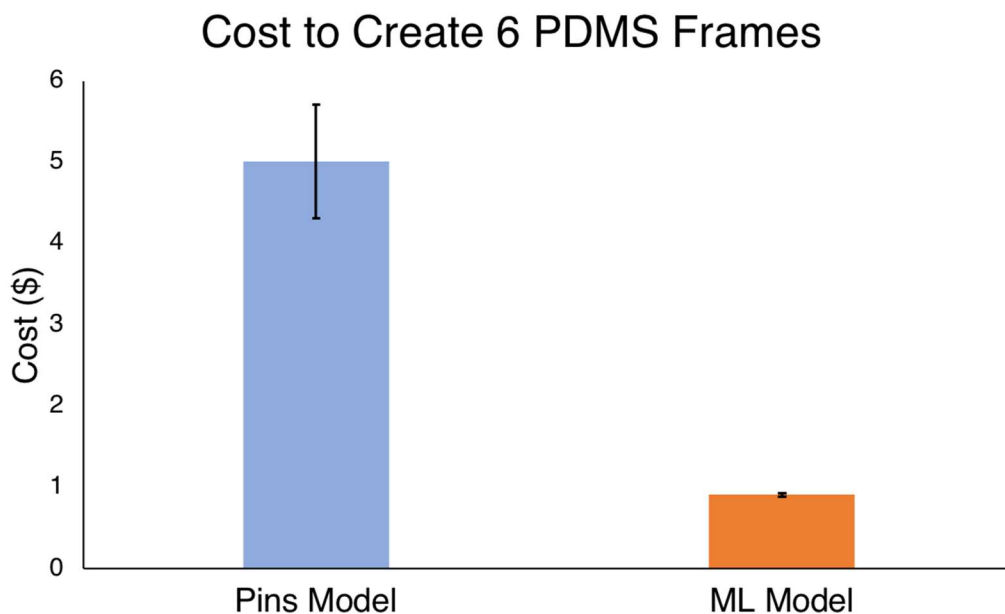


Figure 45. Cost to produce six PDMS frames for both the Pins Lab Model (left) versus the ML Model (right). The ML Model reduced cost of PDMS waste by 95%. This graph includes the mean and standard deviation. The team used a Paired T-test; $N = 4$; $P\text{-value} = 8.27 \times 10^{-7}$

6.2.3.2 Cutting Guide and Cutting Tool for Fibrin Microthread Fixation Slits

The cutting guide is a cost-efficient option to compliment the mold, as they are both reusable. The cutting is a one-time cost of \$0.18, 3D printed out of PLA in the WPI Rapid Prototyping Lab. This cost could change slightly depending on the dimensions the user needs for the cutting guide (i.e. if the user decided to create a cutting guide that held more or less than three PDMS frames at a time). The three razor blades used to create the cutting tool cost \$1.37,

and the cost of the washers and screws is \$1.50 making the total cost of the cutting tool \$2.87. All of the components used in the cutting tool were purchased at Lowes. These two design components combine for a one-time cost of \$3.08. The total cost of ML Model assembly kit is \$104.80 (Table 21).

Table 21. Cost analysis for ML Model assembly kit

Item	Cost
Cutting guide (PLA)	\$0.18
Cutting tool	\$2.87
Machined Delrin™ Mold (1)	\$101.75
ML Model total cost	\$104.80

It is important to note that the ML Model and Pins Lab Model require the same materials for the outgrowth assay, making these materials fixed and outside of the scope to investigate. This includes the biological materials needed to make cell culture media, create the fibrin gel, the C2C12 cells, and the several pipette and serological tips used throughout the cell culture procedures.

6.2.4 Interface with 3D Scaffold

6.2.4.1 Mold for PDMS Frame

The mold allows for the creation of PDMS frames which are able to interface with a 3D scaffold. PDMS is a biocompatible material that provides mechanical stability sufficient to

support fibrin microthreads. The Delrin™ Plastic, which was used to make the molds, has shown to not leach any toxins into a material like PDMS below a temperature of 76.9-96.9°C, known as the maximum service temperature (Penick, 2005).

6.2.4.2 Cutting Guide and Cutting Tool for Fibrin Microthread fixation slits

The cutting guide allows for the creation of identical and evenly spaced slits in the frame. This allows for the even thread fixation which is what allows the PDMS frames to interface with the 3D scaffolds. The PDMS frame is sterilized before contact with the C2C12 cellular gel, ensuring that any dust or fungus is eradicated before introduced to the cell culture environment.

6.2.5 Support of Cellular Outgrowth on 3D Scaffold

6.2.5.1 Cellular Outgrowth Assay Validation Experiment 1

On day 1 of experiment 1 (Exp1), a 6-well plate of the ML Model containing fibrin microthreads and a 6-well plate of the ML Model containing collagen microthreads was sterilized using the EtO sterilization method. The plates were left in the sterile packaging on the benchtop for at least 24 hours after EtO sterilization to degas. On day 2 of the experiment, C2C12 myoblast populated fibrin gels (20,000 cells) were dyed with DiI and seeded on the ML models, as written in the ML Model Outgrowth Assay Protocol (Appendix L). On days 3-4 of Exp2, both the fibrin and collagen plates were imaged at the 24hr and 48hr time points according to the imaging protocol discussed in ML Model Outgrowth Assay Protocol (Appendix L). Images were taken at using the Zeiss microscope at a 10X objective with the exposure times listed in Appendix P. The team was not able to image for days 5 and 6 of the experiment (3 and 4

of imaging) at the 72hr and 96hr time points, so the plates were bleached and properly disposed of following imaging on day 4.

6.2.5.2 Cellular Outgrowth Assay Validation Experiment 2

On day 1 of experiment 2 (Exp2), two 6-well plates of the ML Model containing fibrin microthreads were sterilized using the EtO sterilization method. The plates were left in the sterile packaging on the benchtop for at least 24 hours to degas. On day 2 of the experiment, C2C12 myoblast populated fibrin gels (20,000 cells) were dyed with DiI and seeded on the ML Models as written in the ML Model Outgrowth Assay Protocol in Appendix L. On days 3-6 of Exp2, both fibrin plates were imaged at the 24hr, 48hr, 72hr, and 96hr time points as stated in the imaging protocol detailed in Appendix L. After the 48hr imaging, the media was changed and the cells were re-dyed with DiI (Appendix L - after 48hr time point image). Images were taken at using the Zeiss microscope at a 10X objective at the exposure times listed in Appendix P.

6.2.5.3 Cellular Outgrowth Assay Validation Experiment 3

On day 1 of experiment 3 (Exp3), a 6-well plates of the ML Model containing fibrin microthreads and a 6-well plate containing collagen microthreads were sterilized using the EtO sterilization method. The plates were left in the sterile packaging on the benchtop for at least 24 hours to degas. On day 2 of the experiment, C2C12 myoblast populated fibrin gels (20,000 cells) were dyed with DiI and seeded on the ML Models as written in the ML Model Outgrowth Assay Protocol in Appendix L. On days 3-6 of Exp3, both the fibrin and collagen plates were imaged at the 24hr and 48hr time points as stated in the Imaging Protocol detailed in the outgrowth assay protocol in Appendix L. Images were taken at using the Zeiss microscope at a 10X objective at the exposure times listed in Appendix P.

A black substance was discovered on the Thermanox® coverslips on day 3 of the experiment (24-hour imaging time point) (Figure 46). Although the media was clear and red/pink, the team decided to bleach and dispose the plates so that they would not contaminate other items in the incubator. As a result, the team was only able to obtain one day of images.



Figure 46. Black substance observed in 6-well plate during Experiment 3.

6.2.5.4 Cellular Outgrowth Assay Validation Experiment 4

On day 1 of experiment 4 (Exp4), two 6-well plates of the ML Model containing fibrin microthreads were sterilized using the EtO sterilization method. The plates were left in the sterile packaging on the benchtop for at least 24 hours to degas. On day 2 of the experiment, C2C12 myoblast populated fibrin gels (20,000 cells) were dyed with DiI and seeded on the ML Models as written in the ML Model Outgrowth Assay Protocol in Appendix L. On days 3 of Exp4, both fibrin plates were imaged at the 24hr time points as stated in the imaging protocol detailed in Appendix L. Images were taken at using the Zeiss microscope at a 10X objective. Unfortunately, the 6-well plate used to perform the cellular outgrowth assay had a taller base/overall height than

the previous plates used. This made the model system and 6-well plate too tall to be able to be imaged within the working distance of the microscope. This can be attributed to restocking with a different 6-well plate in the WPI campus laboratories. As a result, the team decided to dispose of the Exp4 plates and stop the imaging process because the team was not able to obtain in focus images of the thread-gel interfaces.

6.2.5.5 Cellular Outgrowth Assay Validation: 96hr Outcome

The PDMS frames supported successful interaction between the C2C12 myoblast populated fibrin gel and fibrin microthreads. This is depicted in Figure 47 which shows assay results at the 96-hr time point. During the course of the outgrowth assay, the red-orange stained cells could be seen migrating/proliferating onto the fibrin microthreads.

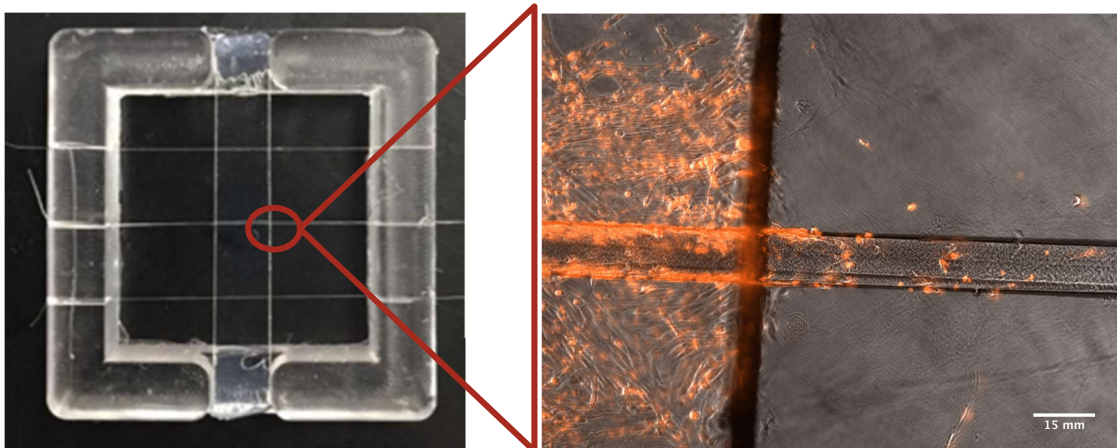


Figure 47. Cellular outgrowth assay viability results, $t=96\text{hr}$. DiI was used as a lipophilic membrane stain to provide a red-orange fluorescence.

6.3 Impact Analysis of PDMS Frame

The purpose of the following sections is to discuss the impact that the ML Model has on the surroundings; including economics, environment, health and safety, society, politics, ethics, manufacturing, and sustainability.

6.3.1 Economic Impact

The team designed a standardized 3D *in vitro* model of skeletal muscle regeneration onto fibrin microthread scaffolds to advance the research for a treatment for VML for use by biomedical engineers and researchers, specifically in the Pins Lab. The ML Model is a cost-efficient alternative to the current model used in the Pins lab, as there is virtually no PDMS wasted, as opposed to the wasted 76% of PDMS made to produce the previously used model. A standardized 3D *in vitro* model kit, containing the mold, cutting guide, and cutting tool is an off-the-shelf design that could be used for the testing of other 3D scaffolds, similar to fibrin microthreads (i.e. collagen microthreads). This ML Model kit would be a cost-effective competitor to the current designs in the biomedical engineering field (i.e. microfluidic models, etc.). Additionally, this model can support several types of microthread scaffolds (fibrin, collagen, etc.), making it useful for a wider range of labs. The ML Model would promote academic research, and eventual adoption by industries that focus on this developed treatment and its required materials.

This model improves the reproducibility and throughput of testing results of *in vitro* scaffolds, providing the researcher with confidence in which scaffolds would be successful *in vivo*. While *in vivo* testing is required to eventually approve this treatment by the FDA, the ML Model could decrease the number of animal subjects that have to be tested. By creating a reproducible model, it gives researchers more confidence moving into the *in vivo* testing phase, and would decrease the amount of “unnecessary” (or rushed) *in vivo* testing. As the researcher is able to be more confident in how the 3D scaffold would respond *in vivo*, the likelihood of the *in vivo* trials showing success increases. Eventually, this model could impact the rate at which an

implantable therapy is found to treat VML in soldiers, reducing the lifetime cost of disability for a soldier with a VML injury.

6.3.2 Environmental Impact

The designed ML Model (mold, cutting guide, and cutting tool) could have an impact on the environment. The 3D *in vitro* model is made using silicone (non-degradable), natural protein, fibrin, C2C12 cells and corresponding media, which would all be disposed of as biohazard waste. Once biohazard waste is transferred (by a diesel truck) to the appropriate facility, it is incinerated and dumped into landfills. Cellular environment byproducts and medium are required to follow safe biohazard disposal and be effectively harmless to the environment. Biohazard waste incinerators release one of the highest amounts of toxic and bioaccumulative pollutants into the Earth's ozone, along with mercury and dioxins as the materials burn. Diesel fuel is one of the most toxic pollutant fuels that vehicles use, and these pollutants are harmful to the public's and environment's health (Wormer, 2013).

The mold is made of Delrin™ Plastic and machined by a 3-degree draft angle screw. While the mold is reusable, it is made of a version of acetal plastic. Acetal plastic, like most other plastic materials, is a non-biodegradable material. Therefore, any plastic waste produced in the machining of this mold will sit in landfills for several of thousands of years, never re-entering the biologic cycle. This adds to humanity's current problem of waste pollution.

The cutting tool/guide is made of ABS, aluminum, and stainless-steel razor blades. PLA degrades over a long period of time, as it is non-biodegradable. Aluminum and stainless steel are not biodegradable, so similar to the acetal plastic, these parts will remain in landfills for virtually forever. However, this tool is reusable and would be used for a significant amount of time, rather than just being disposable, leading to less waste. Additionally, the ML Model will

decrease the amount of PDMS being thrown away and wasted. As stated previously, PDMS is not biodegradable, so the ML Model will decrease harm to the Earth.

6.3.3 Health and Safety Impact

The ML Model is a safe device for users. None of the components produce harmful chemical byproducts, as the different parts are composed of stable materials that are not reactive at room temperature (22°C). The two cautions that must be taken are the sharp edges on the cutting tool that are made of razor blades. If not carefully, and properly stored and handled, the razor edges could damage (puncture or cut) a person or important piece of lab equipment. While the cutting guide and cutting tool are reusable, when they have reached the end of their lifespan, or are broken, they must be disposed of following proper sharps disposal protocols. This model would eventually be used in a 6-well plate, which would include user exposure to cells and culture media.

The ML Model has the potential to be developed further and built upon to develop an implantable therapy for VML, which would greatly improve the muscle function and quality of life of soldiers. Once the ML Model is studied further in the Pins Lab, it must be approved by the FDA as a safe biomaterial for the majority of the population.

6.3.4 Societal Impact

The implementation of this device as a tool for modeling skeletal muscle regrowth on to fibrin microthreads *in vitro* will allow for an expedited timeline of scientific discovery. By decreasing user variability and increasing data throughput, this device allows researchers to answer a greater number of questions in a shorter period of time. This expedites the research timeline and will give researchers a more concrete idea of what constitutes success and failure *in*

vivo testing. Ultimately, this research will be used to implement fibrin microthread scaffolds as a means of treating VML and restoring function to the wounded tissue. This will improve the quality of life for those who have been affected by this injury. By restoring full function, VML patients will be able to perform activities at the same level they were able to before the injury. In the case of wounded veterans, this treatment may restore function at such a level that they are able to return to combat.

6.3.5 Political Impact

As the project currently stands, there are no immediate or foreseeable political impacts associated with it. As it currently stands, this project is very small-scale and will therefore not have any commercial or industrial impacts in the foreseeable future. If this product were to be made commercially available, it could become more widely used and therefore it would have to be revisited to analyze its broader effects. Potentially, the use of different components that are vital to the testing of this device could cause some controversy. The media used contains fetal bovine serum (FBS) which is taken from the blood of bovine fetuses. Additionally, fibrin is a blood component derived from animals. Both of these components could be cause for concern for animal rights activists and could lead to a political issue with the continued pursuit of this type of testing.

6.3.6 Ethical Impact

The ethical concerns directly associated with this project are minimal. An improved model of skeletal muscle regrowth onto fibrin microthreads will not likely have any large ethical ramifications. Although, the long-term goal of this research is to use fibrin microthread scaffolds as a treatment for VML. Fibrin and thrombin, which are needed to produce the fibrin

microthreads, are isolated from bovine sources which may raise some concern due to the use of animal material in scientific research. However, this project does not introduce any new need for these materials, rather suggests how to better utilize the materials that will already be used. An additional concern would be the risk of disease transfer from isolating these materials from animal sources, but they are processed in such a way so as to minimize this risk.

6.3.7 Manufacturing Impact

This project improved the manufacturability and assembly of the frames. With the new system designed by the team, the process of fabricating the frames has been streamlined and made more reproducible. The mold was machined from Delrin™ plastic and allowed for six identical PDMS frames to be created at once. The cutting guide and cutting tool ensure that all of the slits are equidistant and of the same depth. Using these three components allows for the consistent and user-friendly production and assembly of the frames. The average total hands-on time required is approximately 34 minutes for a set of six.

6.3.8 Sustainability

In order to create the mold for the frame, Delrin™ plastic was machined to fit the specifications of the team. Machining this material to the desired shape produces some waste, but not a significant amount due to the limited scale of production at this point in product development. If this mold were to become commercially available, material waste may become a factor that needs to be looked into.

The production and assembly of the frames designed in this project requires the use of energy through several steps in the process. After pouring the PDMS into the mold, it is put into a vacuum chamber for an hour and then cures in an oven for an hour at 60°C. Both of these steps

require the use of energy. By maximizing the number of frames that can be produced at one-time while minimizing the space that the molds take up, the amount of energy required to produce the frames is reduced.

By pouring the PDMS into molds for producing the frames, rather than cutting the frames from sheets of PDMS, there is less PDMS wasted in the process of making the frames. This is beneficial for the long-term commercialization of this product because it is more sustainable and produces far less waste.

7.0 Discussion of Results

This section highlights the overall results of validation testing and explanations as to why these results may have been achieved

7.1 Development of 3D *in vitro* Assay

7.1.1 Mold for PDMS Frame

The 6-well acetal plastic mold decreases user variability by standardizing the dimensions of the PDMS frames. Frames can be fabricated in fewer steps and in less time than the hand-cut frames used in the Pins Model. The three-degree draft angle on the mold enabled PDMS frames to be easily removed. The dimensions of the mold allow four molds to be vacuumed simultaneously in one chamber. PDMS can be easily removed from the acetal plastic, allowing for quick clean up.

7.1.2 Cutting Guide and Cutting Tool for Fibrin Microthread Fixturing Slits

The cutting tool creates equidistantly spaced thread fixation slits and allows the user to cut three frames at once. The cutting guide ensures uniform thread fixation split depth. It also prevents the slits from being too deep which would cause it to fail when it is bent during thread placement. By having all threads in the same viewing plane, imaging can be done more effectively because less time will be spent refocusing on a new plane. Additionally, uniform thread placement will help with the location and imaging of the leading cell.

7.2 Assembly Testing

Assembly testing performed by the team determined that the use of the Delrin™ mold, cutting guide, and cutting tool decreased overall assembly time of six frames by 48%. Both the PDMS frame removal/fabrication and Thermanox® stage steps saw the highest decrease in assembly time. This is attributed to the design components of the ML Model that standardize PDMS frame fabrication; specifically, the 6-well mold and built-in Thermanox® groove. The Thermanox® groove eliminated the need to create a separate stage, diminishing the assembly time considerably.

The assembly of both models were completed by all four members of the project team. We were all considered to be inexperienced for both models, and strictly followed the assembly protocol while creating both models. The thread placement step resulted in the minimal amount of time decreased, because the method of thread placement was identical between models (thread fixation slits). Additionally, manual thread placement can only be done so quickly and requires users to be careful with the PDMS frames and threads.

7.3 Reproducibility and Sustainability Analysis

Reproducibility testing performed by the team determined that the use of the Delrin™ mold, cutting guide, and cutting tool decreased overall user-to-user variability by 88.7%. In addition, sustainability analysis concluded that the use of the Delrin™ mold decreased the cost to create six PDMS frames by 81.8%.

7.3.1 Reproducibility Testing

The cutting guide and the cutting tool create equidistant slits of equal depth to fixture fibrin microthreads. These tools will decrease the user-to-user variability when creating the model and produce reproducible results when performing the cellular outgrowth assay to expedite the *in vitro* screening process. In addition, the cutting guide and the cutting tool improve the imaging process of the fibrin thread-gel interface. All of the threads will be located on the same plane, so the user will not have to adjust the focus of the microscope at each thread-gel interface.

The Delrin™ mold produces PDMS frames with equal widths independent of the user, decreasing user-to-user variability. Use of the ML Model mold will create each model in the cellular outgrowth assay to be virtually identical. Thus, the user's confidence in validation of the *in vitro* results of the outgrowth assay will be increased. Overall, an increased volume of reproducible *in vitro* data will also expedite the process of *in vitro* testing of fibrin microthreads. This will lead to successful fibrin microthread scaffolds to be tested *in vivo* sooner, bringing a treatment for VML closer to reality.

7.3.2 Sustainability Analysis

Sustainability analysis performed by the team determined that the use of the Delrin™ mold, cutting guide, and cutting tool decreased cost of PDMS used by 81.8%. A potential source of error is inaccuracy of the scale during the weighing process of the plates of waste PDMS for the Pins Lab Model. Additionally, the waste in the ML Model was negligible, but the remnant PDMS film on top of the mold could have added to the overall PDMS waste cost.

The cost of a 3.9 Kg set of base and curing agent to make PDMS in 3.8 the lab costs about \$500. Therefore, by decreasing the amount of PDMS used and wasted when creating the PDMS frames, the lab will be able to save money and use it towards other research. Additionally, by utilizing a reusable mold, the ML Model eliminates the need to use a new plate for pouring each sheet of PDMS.

7.4 Cell Outgrowth Assay Viability

The overarching goal of the outgrowth assay viability study was to show that the ML Model was able to sustain cellular outgrowth and be analyzed in the same manner as the Pins Lab Model. This study was completed four times, by means described in Section 5.2.5. The cellular outgrowth assay viability study was successful in showing that the ML Model can sustain cell culture conditions and the cellular reaction to fibrin microthreads resulted in alignment and outgrowth.

Experiment 1 only included the 24hr and 48hr time point images. Experiment 2 included the 24hr, 72hr, and 96hr time point images. This experiment provided the team with the most successful cellular outgrowth images. Experiment 3 was terminated due to contamination issues. Experiment 4 was assembled in a 6-well plate that was too tall to fit within the working distance of the Zeiss microscope. This made it impossible to take focused images without fear of damaging the objectives on the scope. Appendix Q is a composite of photos from 24hr, 48hr, 72hr, and 96hr taken during our experiments showing cellular outgrowth onto a fibrin microthread.

Several of the challenges that arose from this portion of design validation was due mostly to user inexperience; both in cell culture, staining procedures and troubleshooting the Zeiss when

the exposure times would differ. The results of the cellular outgrowth assay show that the ML Model is able to sustain cellular migration/proliferation and can be imaged using the Zeiss inverted fluorescence microscope.

7.5 Cost Analysis

The major costs required to create the ML Model assembly kit include the cost of the Delrin™ mold, cutting guide, and cutting tool. These tools can be easily cleaned for reuse, making the higher up-front cost a worthwhile investment. Additionally, the tooling for the mold and the labor cost for the time to set up the CNC machining program are one-time costs. Once the first mold is completed, the time and cost required to machine one mold decreases greatly.

At this point, the manufacturing of the three components has been done on a small scale, but in the long term, manufacturing could be outsourced, and all three components could be packaged as a kit. This would allow other labs to perform tests on microthreads in a reliable and consistent manner. Manufacturing the mold on a larger scale would also reduce the cost of producing each part.

7.6 Comparison to Existing Research

The design of a standardized *in vitro* model of skeletal muscle growth onto implantable fibrin microthreads presented in this paper was made using PDMS. A mold machined of Delrin™ acetal plastic allowed for the created on six identical frames which could then be cut using a cutting tool and gutting guide to produce evenly spaced slits of equal depth for thread fixation. As described in Chapter 2.4, there exist multiple 2D assays to model tissue growth. Because fibrin microthreads are a 3D scaffold, a model that can properly interface with them is

required. This is necessary in order to gather information that is as close as possible to what can be observed *in vivo*. The model currently used in the Pins Lab is hand-cut from sheets of PDMS in the shape of an octagon with a hole punched in the middle. A separate stage made of PDMS and Thermanox® is also constructed in the well plate (Grasman, 2015). This method has a lot of limitations as it is time consuming and results in a significant amount of user-to-user variability.

The ML Model has reduced both assembly time and user variability in comparison to the existing model. This makes the new model more consistent and easier to assemble. While the team did not compare the outgrowth distance of the leading cell to current data produced by the Pins Lab Model, we were able to observe cellular outgrowth onto the fibrin microthreads in the ML Model. In future, more in-depth comparisons can be performed to quantitatively compare outgrowth between the two models.

8.0 Conclusions and Future Work

This section summarizes the results and outcome of this MQP and potential future use of the ML Model.

8.1 Conclusions

The challenge proposed to the team was to design, develop, and characterize a 3D *in vitro* model of skeletal muscle tissue outgrowth. Through the design process, the team determined that the revised client statement/mission was that the model system used for the cellular outgrowth assay must be reproducible and standardized with less than 5% user variability. It must also be able to be assembled in half of the time required in the current protocol and must be able to be imaged to quantify proliferation, migration, and confluence of C2C12 cells in six, 35mm wells. Finally, the model must maintain structural integrity while submerged in media in a sterile environment for 96 hours. Overall, the main objectives of standardization of assembly, reproducibility of model, cost effectiveness, and support cellular characterization were achieved through the specified test methods. These objectives were validated through assembly testing, reproducibility testing, sustainability analysis, and cell outgrowth assay viability. From the data we were able to conclude that our design components combine to create a viable cellular outgrowth model to investigate treatments for VML and expedite the *in vitro* testing process.

8.2 Future Work

Further design recommendations include increasing the height of the groove in the mold created for the Thermanox® stage. This would reduce the number of threads floating off of the

Thermanox® coverslip and increase the number of thread-gel interfaces that are able to be imaged. To decrease the amount of time required to remove the frames, future work could be done to improve frame removal technique. The mold could be designed with a larger draft angle, tabs could be placed in the PDMS prior to curing for an easy removal point, or a better removal tool could be designed. Frame thickness could be increased to reduce the risk of PDMS rips during removal and the inner corners of each mold well could be rounded to decrease cracks at stress concentration points. Future improvements can be made to the cutting tool by creating a more user-friendly, ergonomic design with sharper blades. The dimensions of the cutting guide can be adjusted to create a higher tolerance on how the PDMS frames fit into the guide. The thickness of the cutting guide can also be adjusted based on PDMS frame dimensions and Thermanox® slot placement.

An additional step to validate the design would be to complete an experiment where the ML Model and Pins Lab Model are studied under identical conditions. This would allow the user to quantitatively compare the outgrowth of the cells onto fibrin microthreads. This would allow results obtained on the ML Model to be directly compared to Pins Lab Model data.

Outside of this project scope, but useful for the continuing use of PDMS for fibrin microthread fixation, is a device that could hold open the fixation slits while fibrin microthreads are placed. Automation of thread extrusion and placement onto the PDMS frame would also greatly improve the process of production for the ML Model.

Future *in vitro* ML Model research includes creating and testing a multi-cell design with muscle, nerve, and endothelial cells to better predict muscle tissue outgrowth *in vitro*. Muscle is a highly innervated tissue, and this multi-cell design will better reflect the healing response that fibrin microthreads would cause *in vivo*. To better compare the ML Model cellular outgrowth to

that of the Pins Lab Model, biophysical and biochemical properties of the threads should be modified; including growth factors and mechanical properties. This will work towards the ultimate goal of restoring muscle function in VML injuries.

References

- G. Agrawal, A. Aung, and S. Varghese, "Skeletal muscle-on-a-chip: an *in vitro* model to evaluate tissue formation and injury," *Lab on a Chip*, issue 20 pp. 3447-3461, 2017.
- B. Bianchi, C. Copelli, S. Ferrari, A. Ferri, and E. Sesenna, "Free flaps: Outcomes and complications in head and neck reconstructions," *Journal of Cranio-Maxillofacial Surgery*, vol. 37, no. 8, pp. 438, 2009.
- Biogelx. (2018) "A Simple Guide to 3D Cell Cultures"
- G. Bowlin, "Enhanced Porosity without Compromising Structural Integrity: The Nemesis of Electrospun Scaffolding," *Journal of Tissue Science & Engineering*, vol. 2, no. 103e, 2011.
- P. Brescia and P. Banks, "Investigation of Cell Migration using a High Density Cell Exclusion Assay and Automated Microplate Imager," *BioTek Application Note*, 2013.
- K. Cornwell, et al., "Characterizing fibroblast migration on discrete collagen threads for application in tissue regeneration" *Journal of Biomedical Materials Research Part A*, vol. 71(1), pp. 55-62, 2004.
- B. T. Corona, and S. M. Greising, "Challenges to acellular biological scaffold mediated skeletal muscle tissue regeneration" *Biomaterials*, vol. 104, pp. 238-246, 2016.
- Creative Bioarray. (2016) "3D Cell Culture Guide"
- D. I. Devore, T. J. Walters, R. J. Christy, C. R. Rathbone, J. R. Hsu, D. G. Baer, and J. C. Wenke, "For combat wounded: extremity trauma therapies from the USAISR." *Military medicine*, vol. 176, no. 6, pp. 660-663, 2011.
- J. Dziki, S. Badylak, M. Yabroudi, B. Sicari, F. Ambrosio, K. Stearns, N. Turner, A. Wyse, M. L. Boninger, E. H. P. Brown, and J. P. Rubin, "An acellular biologic scaffold treatment for volumetric muscle loss: results of a 13-patient cohort study," *NPJ Regenerative Medicine*, vol. 1, no. 1, pp. 16008, 2016.
- J. P. Fischer, R. M. Elliott, S. H. Kozin, and L. S. Levin, "Free Function Muscle Transfers for Upper Extremity Reconstruction: A Review of Indications, Techniques, and Outcomes," *Journal of Hand Surgery (American Volume)*, vol. 38, no. 12, pp. 2485, 2013.
- J. M. Grasman, M. P. O'Brien, K. Ackerman, K. A. Gagnon, G. M. Wong, G. D. Pins, "The effect of sterilization methods on the structural and chemical properties of fibrin microthread scaffolds," *Macromol Biosci*, vol. 16, no. 6, pp. 836-846, 2016.
- J. Grasman, D. Do, R. Page, and G. Pins, "Rapid release of growth factors regenerates force output in volumetric muscle loss injuries," *Biomaterials*, vol. 72, pp. 49-60, 2015.

- J. M. Grasman, R. L. Page, and G. D. Pins, “Design of an In Vitro Model of Cell Recruitment for Skeletal Muscle Regeneration Using Hepatocyte Growth Factor-Loaded Fibrin Microthreads,” *Tissue Engineering Part A*, vol. 23, no. 15-16, pp. 773-783, 2017.
- S. M. Greising, J. C. Rivera, S. M. Goldman, A. Watts, C. A. Aguilar, and B. T. Corona, “Unwavering Pathobiology of Volumetric Muscle Loss Injury,” vol. 7, no. 1, p. 13179, 2017.
- S. Grefte, A. Kuijpers-Jagtman, R. Torensma, and D. H. Von, “Skeletal muscle development and regeneration,” *Stem Cells and Development; Stem Cells Dev.*, vol. 16, no. 5, pp. 857–868, 2007.
- B. F. Grogan, and J. R. Hsu, “Volumetric muscle loss.(Report),” *Journal of the American Academy of Orthopaedic Surgeons*, vol. 19, no. 3, pp. s35, 2011.
- K. I. Hulkower and R. L. Herber, “Cell Migration and Invasion Assays as Tools for Drug Discovery,” *Pharmaceutics* vol. 3, no. 1. 2011.
- T. A. H. Jarvinen, T. L. N. Jarvinen, M. Kaarianen, H. Kalimo, and M. Jarvinen, “Muscle Injuries,” *The American Journal of Sports Medicine*, vol. 33, no. 5, pp. 745–764, 2005.
- M. Juhas, and N. Bursac, “Engineering skeletal muscle repair,” *Current Opinion in Biotechnology*, vol. 24, no. 5, pp. 880-886, 2013.
- M. Kheradmandi, E. Vasheghani-Farahani, A. Ghiaseddin, and F. Ganji, “Skeletal muscle regeneration via engineered tissue culture over electrospun nanofibrous chitosan/PVA scaffold,” *Journal of Biomedical Materials Part A*, vol. 104, no. 7, 2016.
- R. J. Korthuis, “Anatomy of Skeletal Muscle and Its Vascular Supply.” *Morgan & Claypool Life Sciences*, 2011.
- N. Kramer *et al.*, “In vitro cell migration and invasion assays,” *Mutation Research/Reviews in Mutation Research*, vol. 752, no. 1. pp. 10–24, 2013.
- B. Larson, “3D Cell Culture: A Review of Current Techniques” [white paper], *BioTek*, 2015.
- R. Lev, and D. Seliktar, “Hydrogel biomaterials and their therapeutic potential for muscle injuries and muscular dystrophies,” *Journal of Royal Society Interface*, vol. 15, no. 138, 2018.
- J. Liu, D. Saul, K. O. Boker, J. Ernst, W. Lehman, and A. F. Schilling, “Current Methods for Skeletal Muscle Tissue Repair and Regeneration,” *BioMed Research International*, vol. 2018, pp. e1984879, 2018.
- R. I. Litvinov, and J. W. Weisel, “What Is the Biological and Clinical Relevance of Fibrin?,” *Seminars in thrombosis and hemostasis*, vol. 42, no. 4, pp. 333-343, 2016.

J. Ma, S. Sahoo, A. R. Baker, and K. A. Derwin, "Investigating muscle regeneration with a dermis/small intestinal submucosa scaffold in a rat full-thickness abdominal wall defect model," *Journal of Biomedical Materials Research*, vol. 103, no. 2, pp. 355-364, 2015.

J. E. Morgan and T. A. Partridge, "Muscle satellite cells," *The International Journal of Biochemistry & Cell Biology*, vol. 35, no. 8, pp. 1151–1156, 2003.

R. Nigam, and B. Mahanta, "An Overview of Various Biomimetic Scaffolds: Challenges and Applications in Tissue Engineering," *Journal of Tissue Science & Engineering*, vol. 5, no. 2, pp. 1-1, 2014.

M. O'Brien, M. Carnes, R. Page, G. Gaudette, and G. Pins, "Designing Biopolymer Microthreads for Tissue Engineering and Regenerative Medicine," *Current Stem Cell Reports*, vol. 2, no. 2, pp. 147-157, 2016.

R. L. Page, C. Malcuit, L. Vilner, I. Vojtic, S. Shaw, E. Hedblom, J. Hu, G. D. Pins, M. W. Rolle, and T. Dominko, "Restoration of Skeletal Muscle Defects with Adult Human Cells Delivered on Fibrin Microthreads," *Tissue Engineering: Part A*, vol. 17, 2011.

J. A. Passipieri, H. B. Baker, M. Siriwardane, M. D. Ellenburg, M. Vadhavkar, J. M. Saul, S. Tomblyn, L. Burnett, and G. J. Christ, "Keratin Hydrogel Enhances In Vivo Skeletal Muscle Function in a Rat Model of Volumetric Muscle Loss," *Tissue Engineering: Part A*, vol. 23, pp. 556-571, 2017.

K. J. Penick, L. A. Solchaga, J. A. Berilla, and J. F. Welter, "Performance of polyoxymethylene plastic (POM) as a component of a tissue engineering bioreactor," *Journal of Biomedical Materials Research Part A*, vol. 75A, no. 1, pp. 168–174, 2005. *Plastic Sheet - 2.52x3.681x0.250*. [Online]. Available: [https://www.interstateplastics.com/Delrin-Black-Sheet-ACEBE5~SH.php?sku=ACEBE5 SH&vid=20190410181319-9p&dim2=2.52&dim3=3.681&thickness=0.250&qty=1&recalculate.x=65&recalculate.y=21](https://www.interstateplastics.com/Delrin-Black-Sheet-ACEBE5~SH.php?sku=ACEBE5%20SH&vid=20190410181319-9p&dim2=2.52&dim3=3.681&thickness=0.250&qty=1&recalculate.x=65&recalculate.y=21), n.d.

B. E. Pollot and B. T. Corona, "Volumetric Muscle Loss," *Methods in Molecular Biology*, vol. 1460, p. 19, 2016.

Polyoxymethylene (acetal, POM): CES EduPack, 2018.

T. Quazi, D. Mooney, M. Pumberger, S. Geissler, and G. Duda, "Biomaterials based strategies for skeletal muscle tissue engineering: Existing technologies and future trends," *Biomaterials*, vol. 53, pp. 502-521, 2015.

D. Sahar, "Total Posterior Leg Open Wound Management With Free Anterolateral Thigh Flap: Case and Literature Review", *Journal of Plastic Surgery*, vol. 13, e50, 2013.

S. Sanyal, "Culture and Assay Systems Used for 3D Cell Culture", *Corning Review Article*, 2014.

S. S. Segal, "Regulation of blood flow in the microcirculation," *Microcirculation*, vol. 12, no. 1, pp. 33–45, 2005.

B. M. Sicari, J. P. Rubin, C. L. Dearth, M. T. Wolf, F. Ambrosio, M. Boninger, N. J. Turner, D. J. Weber, T. W. Simpson, A. Wyse, E. H. P. Brown, J. L. Dziki, L. E. Fisher, S. Brown, and S. F. Badylak, "An Acellular Biologic Scaffold Promotes Skeletal Muscle Formation in Mice and Humans with Volumetric Muscle Loss," *Science Translational Medicine*, vol. 6, no. 234, 2014.

C. A. Staton, M. W. R. Reed, and N. J. Brown, "A critical analysis of current in vitro and in vivo angiogenesis assays," *International Journal of Experimental Pathology*, vol. 90, no. 3, pp. 195–221, 2009.

J. G. Tidball and S. A. Villalta, "Regulatory interactions between muscle and the immune system during muscle regeneration," *American Journal of Physiology - Regulatory, Integrative and Comparative Physiology*, vol. 298, no. 5, pp. 1173–1187, 2010.

N. J. Turner and S. F. Badylak, "Regeneration of skeletal muscle.(Report)," *Cell and Tissue Research*, vol. 347, no. 3, p. 759, 2012.

S. Varghese, A. Aung, and G. Agrawal, "Skeletal muscle-on-a-chip: an in vitro model to evaluate tissue formation and injury," *Lab on a Chip*, issue 20, pp. 3447-3461, 2017.

A. Vogt, "Advances in two-dimensional cell migration assay technologies," *European Pharmaceutical Review*, vol. 5 pp. 26-29, 2010.

Wormer, B. A., Augenstein, V. A., Carpenter, C. L., Burton, P. V., Yokeley, W. T., Prabhu, A. S., . . . & Heniford, B. T. (2013). The green operating room: simple changes to reduce cost and our carbon footprint. *The American Surgeon*, 79(7), 666-671.

K. M. Yamada and E. Cukierman, "Modeling Tissue Morphogenesis and Cancer in 3D," *Cell*, vol. 130, no. 4. pp. 601–610, 2007.

J. Zhang, Z. Q. Hu, N. J. Turner, S. F. Teng, W. Y. Cheng, H. Y. Zhou, L. Zhang, H. W. Hu, Q. Wang, and S. F. Badylak, "Perfusion-decellularized skeletal muscle as a three-dimensional scaffold with a vascular network template," *Biomaterials*, vol. 89, pp. 114, 2016.

J. Zhu and R. E. Merchant, "Design properties of hydrogel tissue-engineering scaffolds," *Expert Rev Med Devices*, vol. 8, no. 5, pp. 607–626, 2011.

Appendices

Appendix A: Fibrin Microthread Protocol

Fibrin Microthread Protocol

Materials:

- Fibrinogen aliquot (warmed to room temperature) **Do not shake!**
- Thrombin aliquot (warmed to room temperature)
- 40 mM CaCl₂ solution (warmed to room temperature)
- 100 mM HEPES buffer bath stock solution (**10X**) – prepared in previous lab session
- Deionized water
- Metal non-stick pan
- 25 Gauge blunt end needle (1)
- 0.86 mm I.D. polyethylene tubing (Intramedic PE90 427421)
- 1 mL syringes (2)
- Blending connector (SA-3670; Micromedics, MN)
- pH meter

Set Up Procedure:

1. Prepare 600 mL of 1X (10 mM) HEPES buffer solution (60 mL of stock solution and *540 mL diH₂O).
2. Place blunt end needle (25 gauge, BD) into 0.86 mm I.D. polyethylene tubing.

CAN REUSE THESE MATERIALS IF PREVIOUS USER WASHED PROPERLY

3. Luer lock the blunt end needle/tubing assembly onto the front end of blending connector.
4. Place a metal non-stick pan next to the syringe pump.
5. Fill pan with 600 mL HEPES buffer solution.
6. Do a “dry” run of the entire procedure, **before** loading the syringes with fibrinogen and thrombin, to make sure all materials and equipment are set up and working properly (as shown schematically in Figure 1 above). Make sure you know how to use the syringe pump and that when it is running the plungers are being depressed.

Co-extrusion Procedure:

1. Add 150 μL of thrombin aliquot to 850 μL of calcium chloride solution in a new 1mL microcentrifuge tube and mix well.
2. “Prime” both 1 mL syringes by moving the plunger. LABEL one as THROMBIN and one as FIBRINOGEN.
3. Collect all of the thrombin OR fibrinogen solution into the appropriate 1 mL syringes. **COLLECT THE FIBRINOGEN SOLUTION SLOWLY AND CAREFULLY, FAILURE TO DO SO MAY RESULT IN INSOLUBLE FIBRINOGEN FORMATION!! (it’s viscous!!!). Do not vortex or shake.**
4. Invert syringe, remove all bubbles, and ensure that both syringes have equal volumes.

5. Place each 1 mL syringe of fibrinogen and thrombin solutions into the back end of the blending applicator.

**ALWAYS PUT FIBRINOGEN SOLUTION IN THE BLENDING APPLICATOR
OPENING WITH THE CIRCLE ON IT.**

6. Secure syringe/blending applicator construct into syringe pump.
7. Press run on the syringe pump and wait for fibrin solution to flow out of the tip of the tubing.
8. Draw threads into the buffer solution, taking 6-10 seconds to draw each thread.
9. If the pump does not automatically stop when the syringes empty, press stop.
10. **Immediately wash tubing/blending applicator** with cold water and a 20 mL syringe, plugging the other opening with your thumb (at least 5 water rinses per blending applicator opening).
11. Flush water out of blending applicator/tubing repeating step 9 using an empty 20 mL syringe.
12. Fibers can be removed from the bath after 10-15 minutes (not longer than 15 minutes!!!).
13. Label a cardboard box with your team number and team member names.
14. Stretch threads and secure along the cardboard box (~7.5 inch threads).
15. Leave stretched fibrin threads to dry overnight.
16. After 16-24 hours (overnight), remove dried microthreads from the box. Make measurements immediately, or wrap dry microthreads in aluminum foil and store until use. **REMOVE MICROTHREADS FROM BOXES ASAP** after the lab to avoid disruption of your microthreads by other lab users.

Appendix B: User Interview Notes

User Interview Questions and Notes (Meagan, 9/6/18):

1. Can you tell us about the research you are currently working on?
 - a. Developing a scaffold to treat VML
 - b. Scaffold: fibrin microthread
 - c. Issue getting cells to infiltrate tissue to heal wound
 - d. GF - release kinetics, are cells multiplying
 - e. How to modify threads? Mechanical properties, degradation rate, crosslinking, surface features (generally smooth)
 - f. *In vitro* cell based assay
 - g. Cells: C2C12
 - h. Page: primary mouse
2. How do you currently model muscle regeneration with the microthread scaffold?
 - a. Assays - outgrowth paper in the email
 - b. 6 well plates with elevated cover slips (stage), align threads, add cells, culture cells
3. What do you like/dislike about similar devices you currently use?
 - a. Assays have long setup time, and long culture time
4. What is the most important aspect of the scaffold to you, as the user? Strength, cell proliferation, etc.?
 - a. Assay system:
 - i. **Reproducible and user friendly**
 - ii. Cost efficient (least)
 - iii. **Easy setup**
 - iv. **Easy image (fluorescent) - show infiltration, proliferate, migrate**
 - v. **3D!!** - figure out the limitations past research has faced
 1. Limitations of others: looking at 2D
 - vi. Use for different types of scaffolds - gel
 - vii. Work with desired cell types (myoblasts, endothelial, nerve)
 - viii. Co-culture system: multiple cell types (recommendations for future project)
 - ix. Migration, proliferation, stain, image (live imaging)
 - x. Multi-well format (lower)
 - xi. Cell culture - sterile
5. What will be the main application of this 3D scaffold? Soldiers, traumas, research?
 - i. Scaffolds themselves for any large-scale trauma
 - ii. Your assay: intermediate between *in vitro* and *in vivo*
 1. Better model that cuts down on the number of animals that need to be tested on

- b. Are there any other products/medical devices you wish to pair with this device?
(future things to do with assay)
 - i. Drug delivery
 - ii. Modeling musculoskeletal diseases
- 6. How would this model benefit you?
 - a. What information would it provide that you needed?
 - b. What would it make easier?
 - i. Setup
 - ii. Eventually be able to test all different scaffolds
 - c. What is your current model lacking?
 - i. Setup, time in culture
 - ii. **Outgrowth paper** - really looking for 3D, similar but improved?
- 7. What imaging technology/microscope do you use to image 3D models?
 - a. What imaging technology is available to us?
 - i. Confocal: 3D, fluorescent
 - ii. Zeiss: inverted fluorescence
 - iii. Keep in mind working distance
- 8. Is there anything we haven't asked you about that you think we should know?
 - a. Research: *in vitro* assays, cancer research for cell migration, scratch assay (limit: 2D), how can the scaffold be utilized in these assays, keep track of pros and cons and each assay,
- 9. Can we schedule another meeting with you, so you can give us a tour of the lab and what devices you are using specifically?

Extra Notes:

Will be making scaffold but not modifying them.

We are trying to develop an assay to look at cell outgrowth onto a scaffold.

Using threads as the scaffold.

Appendix C: Industry/Company Interview Notes

Company Interview Questions and Notes (Professor Whittington, 9/6/18):

1. What past experiences do you have working with any muscle regeneration devices in industry?
 - Cancer
 - Vascularization side
 - Collagen matrices microstructures
 - Change physical structures in microvessels
 - 3D cell culture tissue culture
2. What past models have been created for muscle regeneration that have been successful?
 - a. What were they lacking?
 - Things in body that aren't in the model (complexity)
 - Prevascularized or injection
 - Just cells and matrix for the model - missing key elements to make it *in vivo* like. Cannot put everything in *in vitro* model - would become too complex
 - b. What works well?
 - Can approximate some features that are best for the scope you are looking at
 - Looking at lumen on vessels
 - Able to generate a model to see measurable differences in mechanical properties
 1. Had the model for long enough to be able to measure these
 2. Platform technology for other research questions
3. **How would you like to see this 3D model used?**
 - a. Model with a functional component that would be able to be used for VML, or answer specific questions about regeneration
 - What elements could hinder or promote regeneration?
 - Be used in intermediate phases instead of just being able to replace muscle
 1. Vascularization, innervation
4. What would the needs of a company that would use/sell this model be?
5. What are your constraints for a model such as this?
6. How would this model benefit you?
 - a. What information would it provide that you needed?
 - b. What would it make easier?
 - c. What is your current model lacking?
7. From your experience, what are typical challenges when designing a model like this?
 - a. Identifying scope and components (How much is too much? How much is enough?)

- **REPRODUCIBILITY**

- b. Technical
 - c. Having your techniques down (sterile, cell culture, creating materials)
 - d. Make sure your **protocol** is good
 - e. **Determining appropriate outcomes (evaluating systems and what does success mean to you)**
 - Picking the correct output
 - Make sure your things line up - what is actually happening in what you are choosing to use
 - 1. Research about assays, cell types,
 - f. Don't forget about controls
8. Is there anything we haven't asked you that you think we should know?
- a. When we try to get more *in vivo* like having an idea what that means for us and your project
 - What aspects of muscle do we want to make it more *in vivo* like
 - Linking smaller scale outgrowth assays to how they correlate with *in vivo*
 - b. **Standardize Meagan's procedure**
 - **Make a universal protocol**
 - **REPRODUCIBILITY**
 - Rank which problems of Meagan's project are easiest to tackle first

Tumor model experience

- Who is going to actually be creating these models?
- How easy is it for someone to actually be able to do this?
 - Training time, feasibility
 - Are the assays equipped to handle 3D?
 - Too much information?
 - Can it penetrate depth?
 - Is dye working correctly?
 - Can it penetrate long enough?
 - Can incubation time be changed?
 - How with this "tool" actually be used?
 - How would the device be manufactured on a larger scale?
 - How many
 - Cost
- Collagen + 4 additives
 - Consolidated down to collagen + 1 additive
 - Makes much more accessible

Appendix D: Client Interview Notes

Client Interview Questions and Notes (Pins, 9/13/18):

1. Mechanisms of the *in vitro* 3D microscale outgrowth assay system in the journal article.
What could be improved on the current *in vitro* 3D microscale outgrowth assay system?
 - Extremely inefficient and time consuming because for any given plate you can only manipulate 1 condition → 1 well per condition

Version 1 → each island has 1 gel, threads go under it
Thermanox®

Carefully deposited drop of cells/gel

Well characterized *in vitro* model of wound healing

Fibroblast populated collagen lattices

Cells are going to outgrowth from the “wound margin” onto the thread

In vitro model is not as beneficial unless you can point to literature that says the same thing happens when you implant it

2. What would you like to see in the new 3D *in vitro* model?

- Lots of data points
- Easier set up
- Easy to handle

3. What would you like to change within the new 3D *in vitro* model?

- Really easy to contaminate (1 well), all or none
- Only imaging at one intersection of the thread and island
- Lifted from bottom in order to isolate threads from the bottom of the plate
- No 2 points are the same imaging wise
 - 80 data points if you have 20 threads
 - 1 well, 1 experiment, 1 time point, n=1
- only 1 condition per well
- Uses a lot of resources

Additional notes on this topic:

- “Outgrowth”
 - Cells growing onto the threads, define what that means to our project
 - Biological meaning
 - Cells are proliferating
 - Migrating
 - A front of cells is moving, not sure if they’re proliferating or migrating

- Want to be able to uncouple them
- Change focal point, some cells end up on the bottom of the plastic

4. How 3D is 3D? What is our scope/the size of the scaffold? (3D vs 2D)

- 3d is the fact that these cells are responding to a 3d biomaterial
 - Going all around the microthread
- Thinking about what we measure
- Tend to measure the distance to the leading cell
- Cells are all the way around the microthread (about 10% coverage)
- Thread is 3D, assay is 3D, implant will be 3D
- It's about the three-dimensional morphology of the structure
- Goal is to collect as much quality data as quickly as possible

5. What is the value of *in vitro*?

- Answer better questions more efficiently

6. Can we coculture with this type of model of just use one type of cell?

- Value to thread is oriented thread growth
- Guided topography

7. What is the most important aspect of the model to you, as the user?

- a. What are the major characteristics you want to measure? Strength, cell proliferation, etc.?
 - These threads are something with a growth factor coating on them, want to be able to pick up a bundle of them and put them into a muscle and see what happens
 - Interested in cellular responses to the biomaterial

Appendix E: Research Team Pairwise Comparison Chart

*before objectives were re-categorized

Totals for Pairwise Comparison for 3D <i>in vitro</i> Skeletal Muscle Regeneration					
	Team	Pins	Whittington	Carnes	Total
Ease of Use	0.5	0.5	0.5	0.5	2
Reproducible	3	4	3.5	2	12.5
Interface with 3D Scaffolds	4.5	4	3.5	4.5	16.5
Data Collection	4.5	4	3.5	4.5	16.5
Multi-Well Format	2	2	3.5	1.5	9
Cost Efficient	0.5	0.5	0.5	0	1.5

Appendix F: Decision Matrix Criteria

Criteria to Rank Decision Matrix				
	Objective	Criteria for Rank		
Ease of Use Metrics	Minimal Prep Time	1 = more than 1 hour to set up	2 = 30 min to 1 hour	3 = less than 30 min to set up
	"off the shelf"	1 = no	2 = yes	
	Easy to Handle	1 = no	2 = yes	
	Easy Data Collection	1 =		
	Easy to Clean	1 = required to clean up materials to make it, and whole assay	2 = required to clean one of the two items in #1	3 = can throw away whole assay
	Limited Monitoring required	1 = assay falls apart when media change	2 = assay stays together during media change	
Data Collection	Standardization between users	1 = extensive training required for setup and imaging	2 = some training required for set up and imaging	3 = minimal training required for set up and imaging
	Precision of matrix	1 = 100 - 66 % variance	2 = 66 - 33 % variance	3 = 33 - 0 % variance
	<i>in vivo</i> predictability	1 = 100 - 66 % variance	2 = 66 - 33 % variance	3 = 33 - 0 % variance
Interface w 3D scaffold	Support microthread scaffolds	1 = single fibrin threads	2 = bundles of threads + single threads	3 = threads + additional types of scaffolds
	Sustained outgrowth	1 = 50% of threads show sustained outgrowth	2 = 75% of threads show outgrowth	3 = 100% of threads show sustained outgrowth
Supports Cellular Characterization	Migration	1= migration is difficult to view	2= migration is viewable	3=migration is easily viewable
	Proliferation	1= proliferation is difficult to view	2= proliferation is viewable	3=proliferation is easily viewable

	Confluence	1= confluence is difficult to view	2= confluence is viewable	3= confluence is easily viewable
	Alignment	1= alignment is difficult to view	2= alignment is viewable	3=alignment is easily viewable
	Data collection	1= data is difficult to collect	2= data can be collected without much difficulty	3=data is easy to collect
	Maximize data collection	1 = less than 18 data points per 6 wells	2 = 18 data points per 6 wells	3 = more than 18 data points per 6 well
Cost Efficient	Materials purchased sustainably	1 = cost more than the budget	2 = some materials provided, some purchased	3 = all materials provided
	Inexpensive equipment	1 = cost more than budget	2 = some equipment provided, some purchased	3 = all equipment provided
	Minimize use of reagents	1 = cost more than budget	2 = some reagents provided, some purchased	3 = all reagents provided
	High throughput	1 = data collection time increases	2 = data collection time stays same	3 = data collection time decreases

Appendix G: User Variability Assembly Testing: Pins Lab Model

1. Purpose:

This test method is used to measure the difference in setup time for a 6-well plate between users of the Pins Lab Model.

2. Materials:

- PDMS sheet approximately 4mm thick
- PDMS sheet approximately 2mm thick
- Razor blade
- Tissue culture treated Thermanox® coverslip
- 3/4" diameter punch
- 5/32" diameter punch
- Silicone glue
- Forceps
- Fibrin microthreads
- Scissors
- Diamond tip tool

3. Methods:

NOTE: Before starting each section begin stopwatch. Record time it takes for user to create 6 individual assemblies.

3.1. PDMS Rings

- 3.1.1. Remove PDMS sheet from plate
- 3.1.2. Trim approximately 1/4" off each edge of the 4mm thick PDMS
- 3.1.3. Use the 3/4" punch to cut 6 holes in the PDMS sheet, leaving approximately 8 mm between holes
- 3.1.4. Cut around the circles to create squares with a wall thickness of approximately 4 mm
- 3.1.5. Cut the four corners off of each square to create 6 octagonal rings

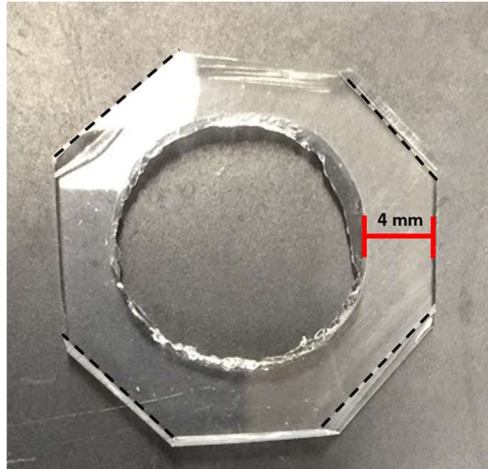


Figure 1. PDMS rings cut to octagonal shape

3.2. Thread Placement

- 3.2.1. Cut 3 sets of equidistant slits across the PDMS ring approximately halfway through the ring. Repeat on all 6 rings
- 3.2.2. Use the forceps to remove a fibrin microthread from the box
- 3.2.3. Cut a section of the microthread long enough to span the diameter of the ring. Make sure there is enough extra length to handle the threads.
- 3.2.4. Open one set of slits and use the forceps to place the microthread. Make sure that there is no excess slack.
- 3.2.5. Repeat steps 3.2.1 through 3.2.4 two additional times for each ring



Figure 2. PDMS ring with fibrin microthreads

3.3. Post and Stage Assembly

- 3.3.1. Use the 5/32" punch to cut 12 posts from the 2 mm thick PDMS sheet
- 3.3.2. Remove 1 sheet of Thermanox® from package with forceps. **NOTE: Ensure that Thermanox® remains oriented with the tissue culture treated side facing up**
- 3.3.3. Fill 1 ml syringe part of the way with medical grade silicone glue
- 3.3.4. Measure Thermanox® into six 3 mm x 13 mm rectangles and mark using a diamond tip tool
- 3.3.5. Use scissors to cut out the rectangles
- 3.3.6. Place two dots of silicone glue in the center of the well
- 3.3.7. Place a PDMS post on each glue dot
- 3.3.8. Place glue on top of the posts
- 3.3.9. Place one Thermanox® stage on the posts
- 3.3.10. Repeat steps 3.3.6 through 3.3.9 for the remaining five wells



Figure 3. Posts and stage placed in well

Appendix H: User Variability Assembly Testing: ML Model

1. Purpose: This test method is used to measure the difference in setup time for a 6-well plate between users of the ML Model.

2. Materials and Equipment:

Flat double-ended microspatula	Fibrin microthreads
3-blade cutting tool	Razor blade
Plastic cutting guide	Fine tipped-forceps
Thermanox® coverslip plastic	6-well plate
Silicone glue	

3. Methods

NOTE: Before starting each section begin stopwatch. Record time it takes for user to create 6 individual assemblies.

3.1. PDMS Frame Removal

- 3.1.1. Holding the microspatula perpendicular to the mold, gently run it around the edges of the frame (Figure 1A). You should be able to observe the PDMS turning opaque as it lifts from the plastic.
- 3.1.2. Use the microspatula to lift the four corners so that they are raised out of the mold (Figure 1B).
- 3.1.3. Gently peel the frame from the mold, **lifting perpendicular to the direction of the sides with the Thermanox® slot (Figure 1C).**
- 3.1.4. Repeat steps 3.1.1 through 3.1.3 on the remaining frames.

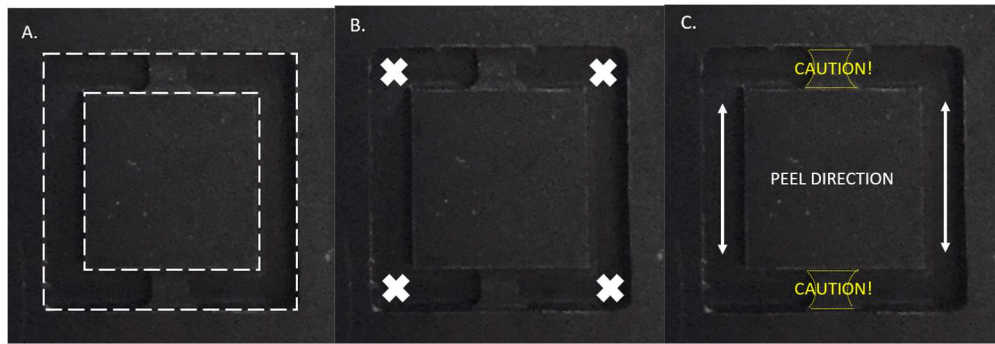


Figure 1. PDMS frame removal steps.

3.2. Thread Fixation Slits

- 3.2.1. Place three frames in the cutting guide as shown in Figure 2. Ensure that frames are level and fully in contact with the bench surface.
- 3.2.2. Place the cutting tool across the middle of the frames (Figure 3).
- 3.2.3. Press the cutting tool down into the frames until it touches the cutting guide. Make sure your weight is evenly distributed across the blades and you press perpendicular to the cutting guide.
- 3.2.4. Remove the frames from the cutting guide and repeat steps 3.2.1 through 3.2.3 on the remaining three frames.

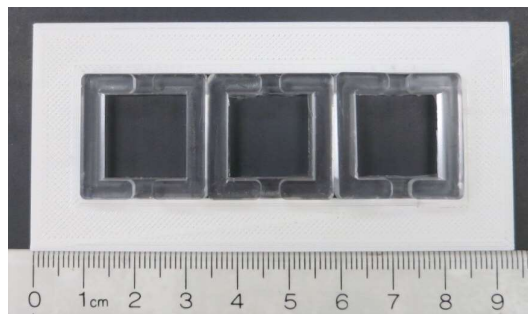


Figure 2. Frames placed in cutting guide

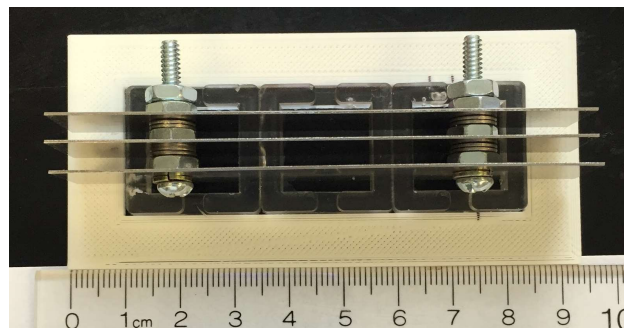


Figure 3. Cutting tool placed on cutting guide.

3.3. Thermanox® Placement

- 3.3.1. Cut a piece of Thermanox® approximately 3 mm x 24.5 mm. Ensure that the tissue culture treated side remains face up during handling.
- 3.3.2. Apply a small amount of silicone glue to each Thermanox® slot in the frame (Figure 4A).
- 3.3.3. Use forceps to place the Thermanox® into the frame (Figure 4B). Once placed, press gently at both ends to ensure the Thermanox® is properly seated in the slot.
- 3.3.4. Repeat steps 3.3.1 through 3.3.3 on the remaining frames.

NOTE: Glue must dry for at least 12 hours before beginning next step.

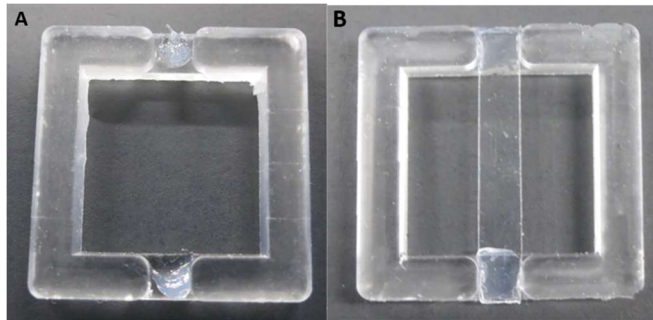


Figure 4. Silicone glue and Thermanox® placement

3.4. Thread Placement

- 3.4.1. Use a razor blade to cut a section of microthread approximately 1 ½ to 2 cm longer than the width of the PDMS frame (26-26.5 cm).
- 3.4.2. Use the thumb and pointer finger of your non-dominant hand to bend a PDMS frame around the curvature of your middle finger so the fixation slits are fully opened, as demonstrated in Figure 5.

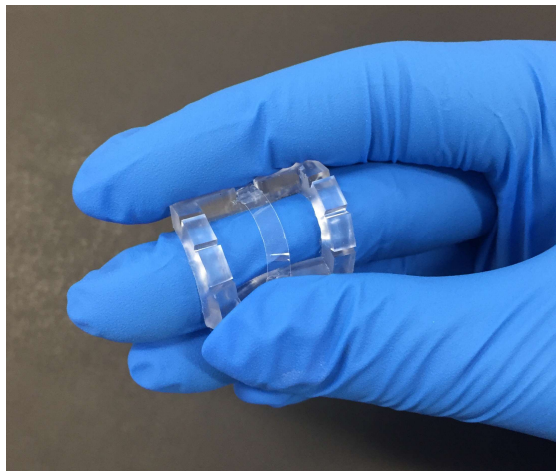


Figure 5. Technique for holding PDMS frame during thread placement.

- 3.4.3. With your dominant hand, use the fine tipped forceps to pick up the cut microthread length, and place it into horizontally adjacent thread fixation slits. (Figure 6). NOTE: Hold the thread close to the end to avoid damaging the center.

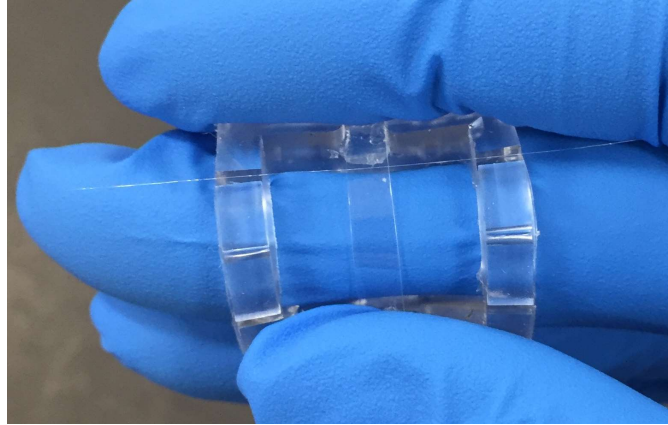


Figure 6. Thread placed in bent PDMS frame.

- 3.4.4. Repeat steps 3.5.1-3.5.3 until all three sets of thread fixation slits are filled.
- 3.4.5. Once threads are placed, release the PDMS frame. Adjust the tension of the microthreads until they appear taught. After tensioning the threads, use the razor blade to trim excess length from the ends. (Figure 7.)

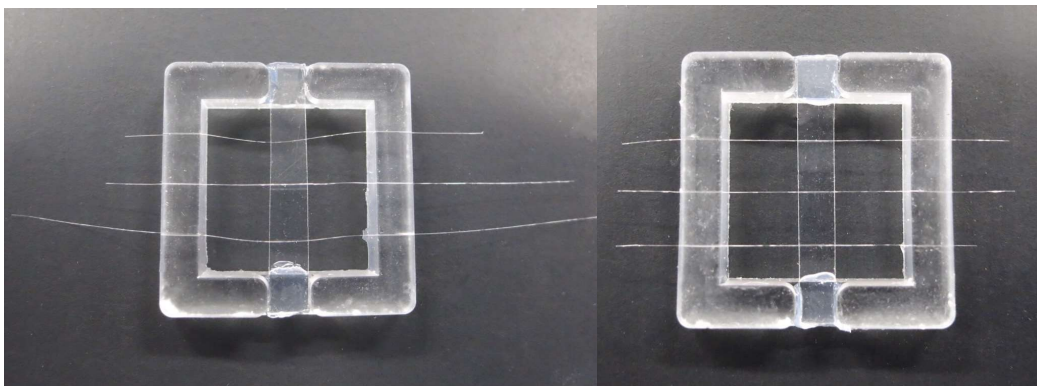


Figure 7. Microthreads before (left) and after (right) final adjustment.

Appendix I: Frame Reproducibility Testing Protocol

1. Purpose:

This test method is used to measure the variability in dimensions and mass between PDMS frames.

2. Materials:

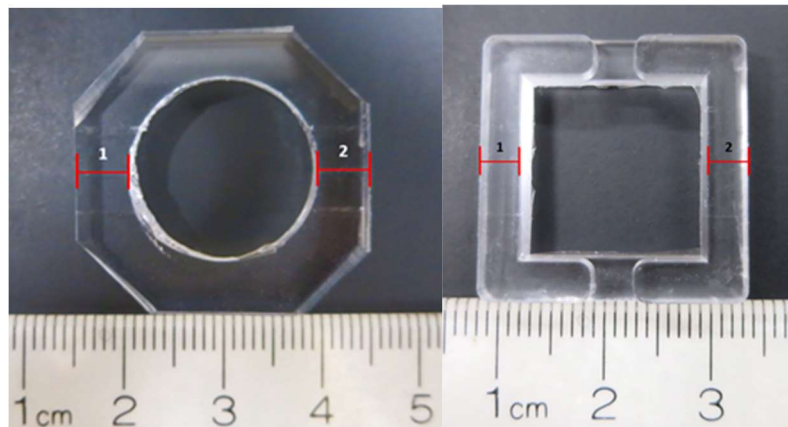
Calipers
Mass balance
PDMS frames

3. Methods:

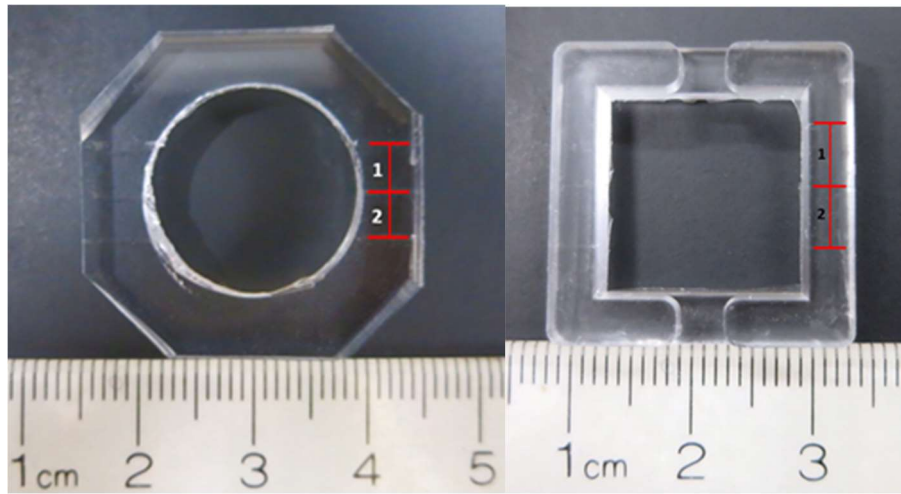
3.1. Dimensions

3.1.1. Measure the PDMS thickness in two areas on the frame and record on spreadsheet. Calculate the average PDMS thickness.

3.1.2. Measure the wall thickness in two areas and record on spreadsheet. Calculate the average wall thickness.



3.1.3. Measure the distance between the slits and record on spreadsheet.



3.2. Mass

3.2.1. Weigh the frame and record the mass on spreadsheet.

Appendix J: Sustainability Analysis Protocol

1. Purpose:

This method is used to test the amount of left over PDMS created when assembling the Pins Lab Model vs when assembling the ML Model.

2. Materials:

PDMS
Mass Balance
PDMS Frame

3. Methods:

3.1. Pins Lab Model

- 3.1.1. Using one sheet of PDMS, create 6 rings using the Pins-Grasman method.
- 3.1.2. Collect the scrap PDMS from the assembly.
- 3.1.3. Weigh the amount of leftover PDMS.
- 3.1.4. Record results in Excel spreadsheet.

3.2. ML Model

- 3.2.1. Weigh PDMS mold and record results in Excel spreadsheet.
- 3.2.2. Fill frames with PDMS.
- 3.2.3. Cure PDMS and remove frames from mold.
- 3.2.4. Weigh PDMS mold and record results in Excel spreadsheet.
- 3.2.5. Calculate the mass of PDMS left over on the mold.

Appendix K: “OG” Outgrowth Assay Protocol

“OG” Outgrowth Assay Protocol

Pre-experiment:

- Fibrin microthreads were made with normal protocol
1. 3 UNX threads were attached to a PDMS ring with inner diameter 3/4” by cutting 3 slats ½ way down through the thickness of the ring and wedging the thread in these slats so its taught across the ring opening
 2. Thermanox® coverslip stages were created in 6 well plates. This was done by adhering a small PDMS column (diam 5/32” and approx. 2 mm tall) with silicone glue to the bottom of a 6 well plate, and also to the non-tissue culture treated side of a Thermanox® coverslip. The Thermanox® coverslips were cut to be 3 x 13 mm rectangles. The glue was allowed to dry at least 12 hours.

Sterilization:

Day 1:

1. Custom 6 well plate with coverslip stages were sterilized in 70% Ethanol for 2 hours. Plates were rinsed 3 times for 5 minutes with diH₂O after Ethanol sterilization and allowed to dry in the laminar flow hood overnight
2. PDMS rings with fibrin microthreads were placed in 6 well plates. Rings were placed onto Thermanox® coverslip stages and adhered with 2 dots of sterile vacuum grease. Vacuum grease was dotted on the bottom of the 6 well plate and the ring was placed on top of that
3. Threads were hydrated in diH₂O for 1 hour prior to being 70% ethanol-sterilized for 2 hours. After Ethanol was removed, they were rinsed 3 times with diH₂O for 5 min each rinse

***** Alternative: Plates and threads could also be EtO sterilized which would be a lot less man hours/easier/threads less likely to break! But need to have samples prepped more in advance b/c rely on Gaudette lab to run the EtO

Experiment:

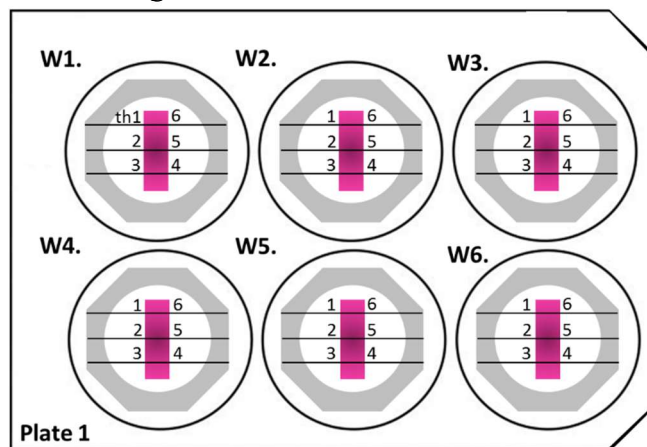
Day 2:

1. PDMS rings with threads were carefully removed from 6 well plates and carefully placed on top of the Thermanox® coverslip stages.
2. Threads (on rings) were hydrated in diH₂O for at least 1 hour prior to cell seeding
3. Calcium Chloride (31.25 mM) and thrombin (2.35 U/mL) were mixed on the benchtop
4. Fibrinogen (5.22 mg/mL) and thrombin +CaCl₂ aliquots were sterile filtered through 0.22 um filter in the hood into separate sterile microcentrifuge tubes
5. Cells: remove media, add trypsin+incubate, add media to trypsinized/detached cells. Add 0.5 mL of this to a new flask + 9.5 mL media. Add remaining cells (~9.5 mL) into conical tube. Spin down for 5 min. Resuspend in 1 mL media.
 - a. Add 5 uL of DiI cell labeling (Molecular probes DiI V-228888 Abs: 553, Em: 570) to the 1 mL of cells in media. (Follow manufacturer’s instructions)
 - b. Gently mix by pipetting and place cells into incubator for 20 minutes
 - c. Remove, centrifuge 5 min, and resuspend in 1 mL media.
 - d. Centrifuge 5 min, resuspend in 1 mL media
 - e. Remove centrifuge 5 min, and resuspend in 1 ml media

6. In sterile microcentrifuge tube, mix: fibrinogen (5.22 mg/mL) + CaCl₂/Thrombin (3.25 U/mL Th, 31.25 mM) + DiI-stained cell suspension (1,500,000 cells/mL) (8:2:2 ratio)
 - a. If wanted 1 mL of gel: 667 uL fibrinogen, 167 uL of CaCl₂ + thrombin mixture, 167 uL of cell suspension
 - b. **NOTE:** When seeding >12 wells, make the gels in two separate batches so you don't have an issue with it polymerizing before it is cast onto the stages
 - c. The final gel has a fibrinogen concentration of 3.5 mg/mL and a final cell concentration of 250,000 cells/mL → 20,000 cells within the 80 uL gel
7. Add **80 uL** of a C2C12-populated fibrin gel to each platform.
8. After gels were cast, the samples were placed in the incubator for 1 hour to facilitate gel formation
9. After 1 hour, wells were flooded with **6 mL** of proliferation media to completely cover the top of the gel

Day 3:

1. Image 24-hour timepoint on the Zeiss
 - a. EXPOSURE: Phase: _____ ms, Rho: _____ ms
 - b. Labeling: w1_th1
 - c. Labeling scheme



Day 4:

2. Imaged 48 hr timepoint on Zeiss
 - a. EXPOSURE: Phase: _____ ms, Rho: _____ ms
3. Re-loaded cells AFTER image 48 hr timepoint imaging with media/DiI
 - a. Add 1 mL media + 5 uL DiI to each 6 well
 - b. Incubate plate for 20 minutes
 - c. Remove 3 mL media from wells
 - d. Replace with 2mL fresh media
 - e. Agitate wells
 - f. Remove additional 2 mL media
 - g. Replace with 2 mL fresh media

Day 5:

10. Image 72 hr timepoint on Zeiss
 - a. EXPOSURE: Phase: _____ ms, Rho: _____ ms

Day 6:

1. Imaged 96 hr timepoint on Zeiss

- a. EXPOSURE: Phase: _____ ms, Rho: _____ ms
- After imaging 96 hr timepoint, fixed all the plates with 4% paraformaldehyde for 20 min
 - Can also do Ki67 staining of threads after fixation if want to see % cells proliferating on threads

Appendix L: ML Model Outgrowth Assay Protocol

1. **Purpose:** This document outlines the steps for assembling and performing one 6-well plate of the ML Model.

2. **Materials and Equipment:**

Assembly

Polydimethylsiloxane (PDMS) base and curing agent	Plastic cutting guide
20 mL syringe	Thermanox® coverslip plastic
1X 6-well acetal plastic mold	Silicone glue
Straight-edge leveling tool	Fibrin microthreads
Vacuum chamber	Razor blade
Low temperature oven	Fine tipped-forceps
Flat double-ended microspatula	6-well plate
3-blade cutting tool	Sterilization pouch

Outgrowth Assay

Fibrinogen (5.22 mg/mL)	10 mL conical tubes
Thrombin (2.35 U/mL)	Sterile vacuum grease
Calcium Chloride (31.25 mM)	Sterile forceps
Sterile diH ₂ O	0.22 µm sterile filter (x2)
DiI cell labeling (V-228888 Abs: 553, Em: 570)	1 mL sterile syringe (x2)
Sterile microcentrifuge tubes	Trypsin

Media Components: F12, DMEM, FBS, Pennstrep, Amp. B, Aprotinin

3. **ML Model Assembly**

3.1. **PDMS Frame Fabrication**

- 3.1.1. Mix 30 g of base with 3 g of curing agent and mix thoroughly (10:1 ratio).
- 3.1.2. Fill the syringe with PDMS.
- 3.1.3. Using the syringe, completely fill each well of the plastic mold.

- 3.1.4. Once all six wells have been filled, level off excess PDMS using a popsicle stick or other straight-edged tool.
- 3.1.5. Place the mold in the vacuum chamber until all air bubbles are removed (approximately one hour).
- 3.1.6. Move the mold into the low temperature oven and cure at 60°C for at least one hour.

3.2. PDMS Frame Removal

- 3.2.1. Remove mold from oven and let cool.
- 3.2.2. Holding the microspatula perpendicular to the mold, gently run it around the edges of the frame (Figure 1A). You should be able to observe the PDMS turning opaque as it lifts from the plastic.
- 3.2.3. Use the microspatula to lift the four corners so that they are raised out of the mold (Figure 1B).
- 3.2.4. Gently peel the frame from the mold, **lifting perpendicular to the direction of the sides with the Thermanox® slot (Figure 1C)**.
- 3.2.5. Trim any excess PDMS using a razor blade or X-acto knife.
- 3.2.6. Repeat steps 3.2.2 through 3.2.4 on the remaining frames.

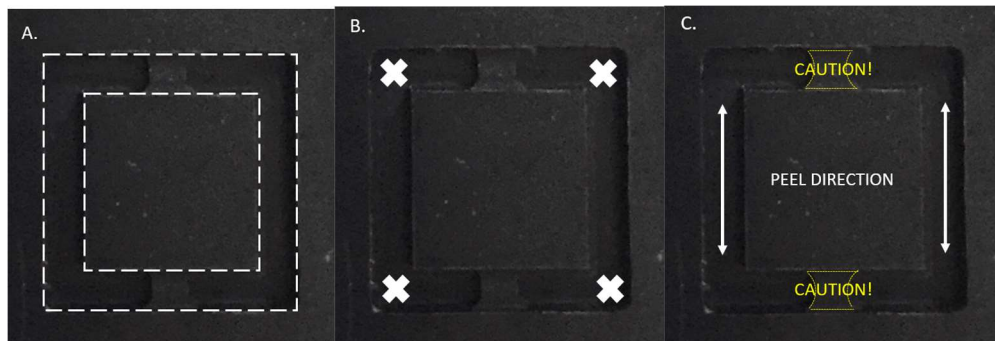


Figure 1. PDMS frame removal steps.

3.3. Thread Fixation Slits

- 3.3.1. Place three frames in the cutting guide as shown in Figure 2. Ensure that frames are level and fully in contact with the bench surface.
- 3.3.2. Place the cutting tool across the middle of the frames (Figure 3).
- 3.3.3. Press the cutting tool down into the frames until it touches the cutting guide. Make sure your weight is evenly distributed across the blades and you press perpendicular to the cutting guide.

- 3.3.4. Remove the frames from the cutting guide and repeat steps 3.3.1 through 3.3.3 on the remaining three frames.



Figure 2. Frames placed in cutting guide

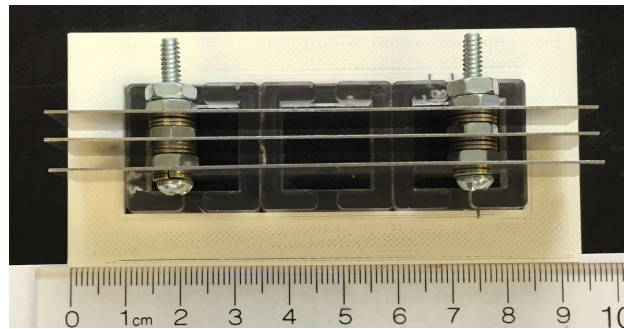


Figure 3. Cutting tool placed on cutting guide.

3.4. Thermanox® Placement

- 3.4.1. Cut a piece of Thermanox® approximately 3 mm x 24.5 mm. Ensure that the tissue culture treated side remains face up during handling.
- 3.4.2. Apply a small amount of silicone glue to each Thermanox® slot in the frame (Figure 4A).
- 3.4.3. Use forceps to place the Thermanox® into the frame (Figure 4B). Once placed, press gently at both ends to ensure the Thermanox® is properly seated in the slot.
- 3.4.4. Repeat steps 3.4.1 through 3.4.3 on the remaining frames.
- 3.4.5. Cover the frames and allow the glue to cure for at least 12 hours.

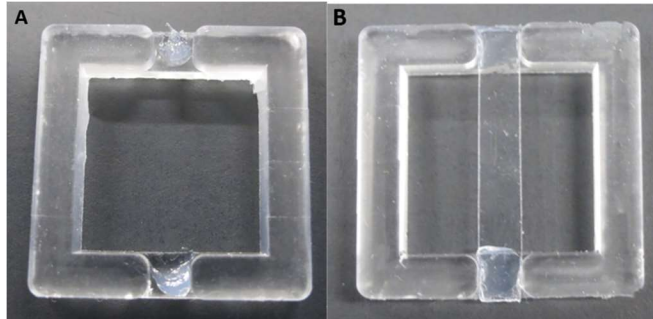


Figure 4. Silicone glue and Thermanox® placement

3.5. Thread Placement

- 3.5.1. Use a razor blade to cut a section of microthread approximately 1 ½ to 2 cm longer than the width of the PDMS frame (26-26.5 cm).
- 3.5.2. Use the thumb and pointer finger of your non-dominant hand to bend a PDMS frame around the curvature of your middle finger so the fixation slits are fully opened, as demonstrated in Figure 5.

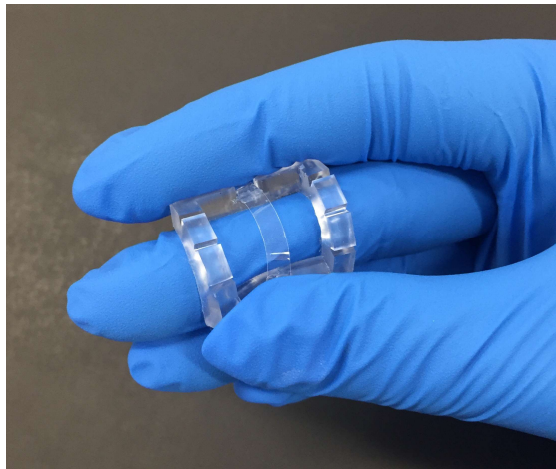


Figure 5. Technique for holding PDMS frame during thread placement.

- 3.5.3. With your dominant hand, use the fine tipped forceps to pick up the cut microthread length, and place it into horizontally adjacent thread fixation slits. (Figure 6). NOTE: Hold the thread close to the end to avoid damaging the center.

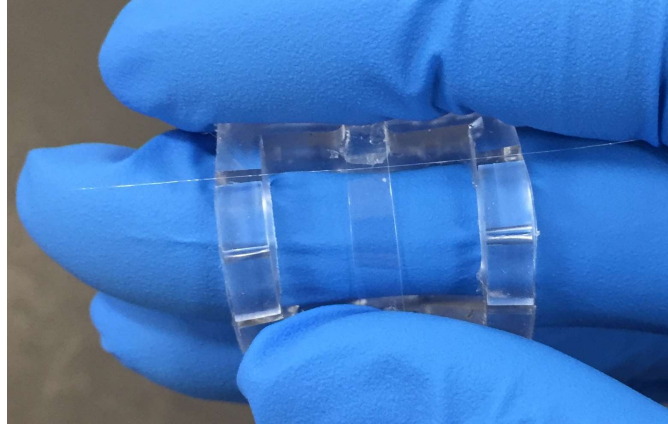


Figure 6. Thread placed in bent PDMS frame.

- 3.5.4. Repeat steps 3.5.1-3.5.3 until all three sets of thread fixation slits are filled.
- 3.5.5. Once threads are placed, release the PDMS frame. Adjust the tension of the microthreads until they appear taught. After tensioning the threads, use the razor blade to trim excess length from the ends. (Figure 7.)

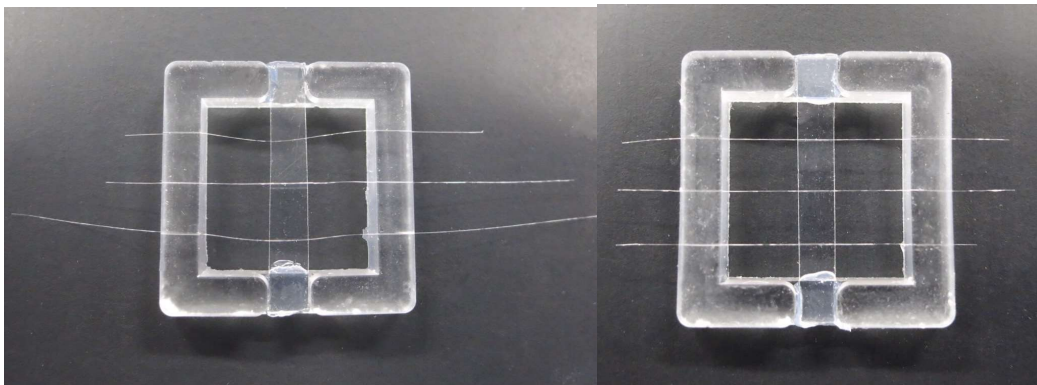


Figure 7. Microthreads before (left) and after (right) final adjustment.

3.6. Plate Assembly and Sterilization

- 3.6.1. Place the frames in a standard 6-well plate as shown in Figure 8.
- 3.6.2. Seal the 6-well plate in a single use sterilization pouch.
- 3.6.3. Sterilize the plate using Ethylene Oxide sterilization procedure.
- 3.6.4. Allow the plate to de-gas for at least 24 hours before using for outgrowth assay.

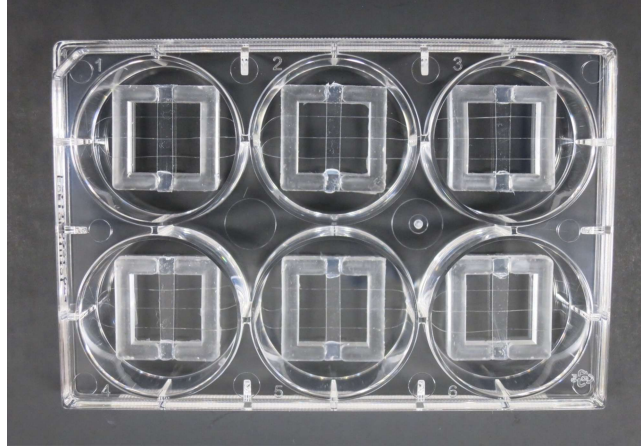


Figure 8. Frame orientation in 6-well plate.

4. Outgrowth Assay

4.1. Pre-experiment

- 4.1.1. Create 1mL aliquots of fibrinogen (5.22 mg/mL)
- 4.1.2. Create 0.5 mL aliquots of thrombin (2.35 U/mL) mixed with calcium chloride (31.25 mM) in a 1:1 ratio
- 4.1.3. Mix media components:

219 mL	F12
219 mL	DMEM
50 mL	FBS
5 mL	Pennstrep
5 mL	Amp. B
2 mL	Aprotinin

4.2. Experiment Setup

- 4.2.1. Bring the sterile plate into the hood and remove from sterilization bag.
- 4.2.2. Use the forceps to pick up each PDMS frame and place a small dot of sterile vacuum grease on the bottom surface under both sides of the Thermanox® groove. Replace frames in the orientation shown in Figure 8.
- 4.2.3. Hydrate the fibrin microthreads by pipetting 80 ul of diH₂O onto each of the Thermanox® stages and allowing the plate to sit for at least an hour.
- 4.2.4. During the thread hydration hour, prepare cells for seeding:

- 4.2.4.1. Remove plate from the incubator and check for confluence under the microscope.
 - 4.2.4.2. Bring plate into the hood and remove media.
 - 4.2.4.3. Add 5ml trypsin and incubate for 3 minutes. After the incubation period, check under microscope to ensure that all cells have detached from plate.
 - 4.2.4.4. Add 5 ml media to trypsinized/detached cells and pipet up and down to fully mix and remove any remaining attached cells.
 - 4.2.4.5. If the cells are being passaged, add 0.5 mL of the cell/media mixture and 9.5 mL media into a new flask.
 - 4.2.4.6. Centrifuge the remaining cell/media mixture down for 5 min at 1000 RPM. Resuspend cell pellet in 1 mL media.
 - 4.2.4.7. Add 5 uL of DiI cell labeling to the 1 mL of cells in media. (Follow manufacturer's instructions)
 - 4.2.4.8. Gently mix by pipetting and place cells into incubator for 20 minutes
 - 4.2.4.9. Centrifuge cells for 5 min at 1000 RPM and resuspend in 1 mL media.
 - 4.2.4.10. Repeat step 4.2.4.9 two more times.
 - 4.2.4.11. Resuspend the cells at a concentration of 1,500,000 cells/mL
- 4.2.5. Carefully aspirate the diH₂O off of the Thermanox® stages
- 4.2.6. Filter the fibrinogen and thrombin/CaCl₂ aliquots into separate **sterile** microcentrifuge tubes:
- 4.2.6.1. Rest a sterile filter in the top of the microcentrifuge tube.
 - 4.2.6.2. Use a 1mL syringe to draw up the aliquot.
 - 4.2.6.3. Fully inject the aliquot into the top opening of the filter.
 - 4.2.6.4. Remove the empty syringe, fill it with air, and firmly inject the air into the top opening of the filter to ensure that all of the aliquot gets filtered through.
 - 4.2.6.5. Remove the syringe and filter and dispose.
 - 4.2.6.6. Repeat steps 4.2.6.1 through 4.2.6.5 to filter the second aliquot into a separate microcentrifuge tube.
- 4.2.7. Make the cell seeded gel in a **sterile** microcentrifuge tube:

For one 6-well plate: 80 uL gel per well x 6 wells = ~ 500 uL total
Gel is made in an 8:2:2 ratio:
8 parts fibrinogen : 2 parts cell suspension : 2 parts thrombin/CaCl₂
333 uL : 83 ul : 83 ul

- 4.2.7.1. Add 333 ul fibrinogen
- 4.2.7.2. Add 83 ul cell suspension
- 4.2.7.3. Add 83 ul thrombin/CaCl₂
- 4.2.7.4. Mix directly after combining
- 4.2.8. Add 80 mL of gel to each Thermanox® stage
- 4.2.9. Place the plate in the incubator for 1 hour to facilitate gel formation.
- 4.2.10. After 1 hour, flood each well with 6 mL of media to completely cover the top of the gel.
- 4.2.11. Place the plate in the incubator.

5. Imaging

5.1. 24 Hours

- 5.1.1. Image plate on the Zeiss. Take images using the phase contrast 1 channel, overlaid with rhodamine fluorescence. Keep track of the well and thread imaged using the labeling scheme shown in Figure 9.
- 5.1.2. Record the image exposure [phase (ms) and Rho (ms)] and save the image file using the following naming convention:

exp#_plate#_w#_t#_thread type.czi

(experiment #, plate #, well #, thread #, thread type)

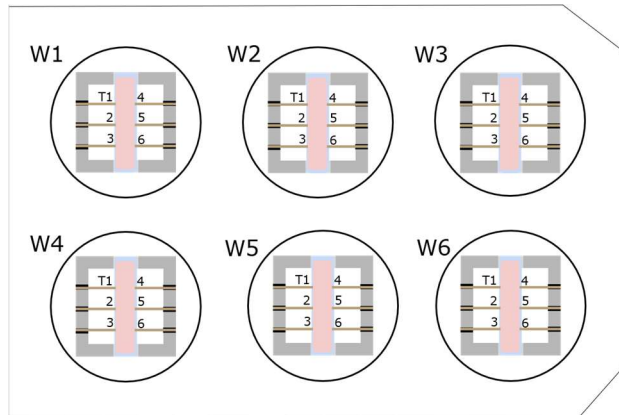


Figure 9. 6-well plate imaging scheme

5.2. 48 Hours

5.2.1. Image plate on the Zeiss using the same protocol specified in the 24 Hour instructions

5.2.2. **After** imaging, re-dye cells:

5.2.2.1. Add 1 mL media and 5 uL DiI to each well

5.2.2.2. Incubate plate for 20 minutes

5.2.2.3. Remove 3 mL media from each well

5.2.2.4. Replace with 2mL fresh media in each well

5.2.2.5. Agitate wells

5.2.2.6. Remove additional 2 mL media from each well

5.2.2.7. Replace with 2 mL fresh media in each well

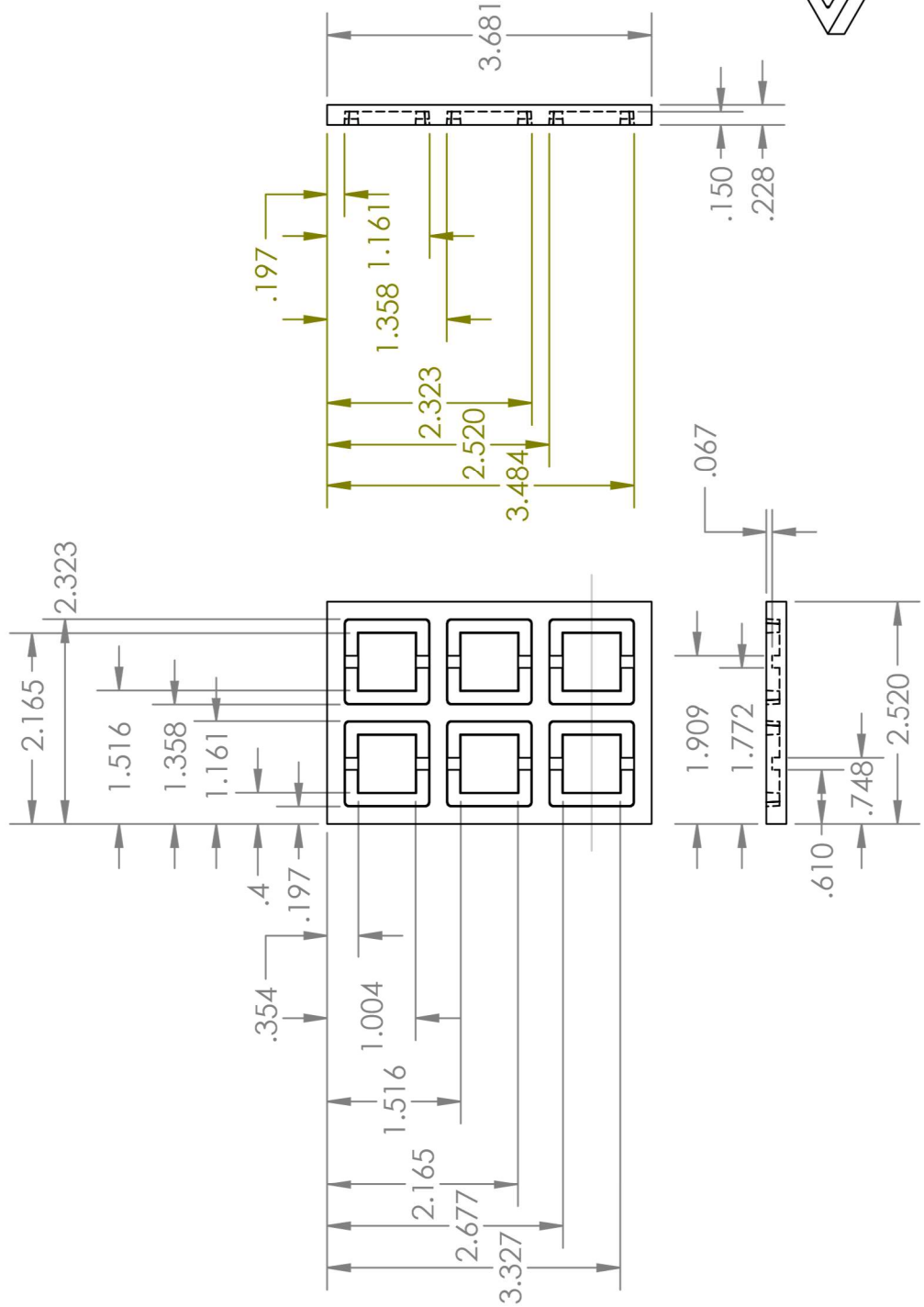
5.3. 72 Hours

5.3.1. Image plate on the Zeiss using the same protocol specified in the 24-Hour instructions.

5.4. 96 Hours

5.4.1. Image plate on the Zeiss using the same protocol specified in the 24-Hour instructions.

Appendix M: PDMS Mold
 Drawing for Machining



A

DRAWN		NAME		DATE	
CHECKED		E. Morra		2/7/19	
ENG APPR.					
MFG APPR.					
Q.A.					
COMMENTS:					
3 degree draft angle					
UNLESS OTHERWISE SPECIFIED:		DIMENSIONS ARE IN INCHES		TOLERANCES:	
		FRACTIONAL ±		ANGULAR: MACH ± BEND ±	
		TWO PLACE DECIMAL ±		THREE PLACE DECIMAL ±	
		INTERPRET GEOMETRIC TOLERANCING PER:		MATERIAL	
				Delrin Acetal Plastic	
				FINISH	
				USED ON	
				NEXT ASSY	
				APPLICATION	
				DO NOT SCALE DRAWING	

TITLE:
 PDMS Mold (6 Well)

SIZE DWG. NO. **A** REV **0**

SCALE: 1:2 WEIGHT: SHEET 1 OF 1

PROPRIETARY AND CONFIDENTIAL
 THE INFORMATION CONTAINED IN THIS DRAWING IS THE SOLE PROPERTY OF <INSERT COMPANY NAME HERE>. ANY REPRODUCTION IN PART OR AS A WHOLE WITHOUT THE WRITTEN PERMISSION OF <INSERT COMPANY NAME HERE> IS PROHIBITED.

172

B

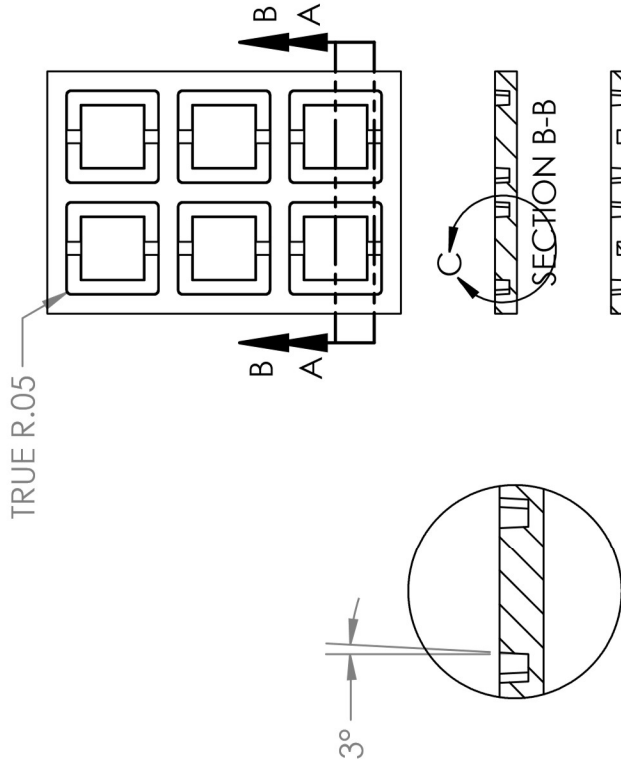
B

1

2

Appendix N: PDMS Mold

Drawing for Machining



PROPRIETARY AND CONFIDENTIAL
 THE INFORMATION CONTAINED IN THIS DRAWING IS THE SOLE PROPERTY OF <INSERT COMPANY NAME HERE>. ANY REPRODUCTION IN PART OR AS A WHOLE WITHOUT THE WRITTEN PERMISSION OF <INSERT COMPANY NAME HERE> IS PROHIBITED.

173

UNLESS OTHERWISE SPECIFIED:		NAME	DATE
DIMENSIONS ARE IN INCHES	DRAWN	E. Morra	2/15/19
TOLERANCES:	CHECKED		
FRACTIONAL ±	ENG APPR.		
ANGULAR: MACH ± BEND ±	MFG APPR.		
TWO PLACE DECIMAL ±	G.A.		
THREE PLACE DECIMAL ±	COMMENTS:		
INTERPRET GEOMETRIC TOLERANCING PER:	MATERIAL	PDMS Mold (6 well) (Section View)	
	Delrin Acetal Plastic	SIZE	DWG. NO.
	FINISH	A	0
	USED ON	SCALE: 1:2	WEIGHT:
	APPLICATION	SHEET 1 OF 1	

1

2

B

B

A

A

1

2

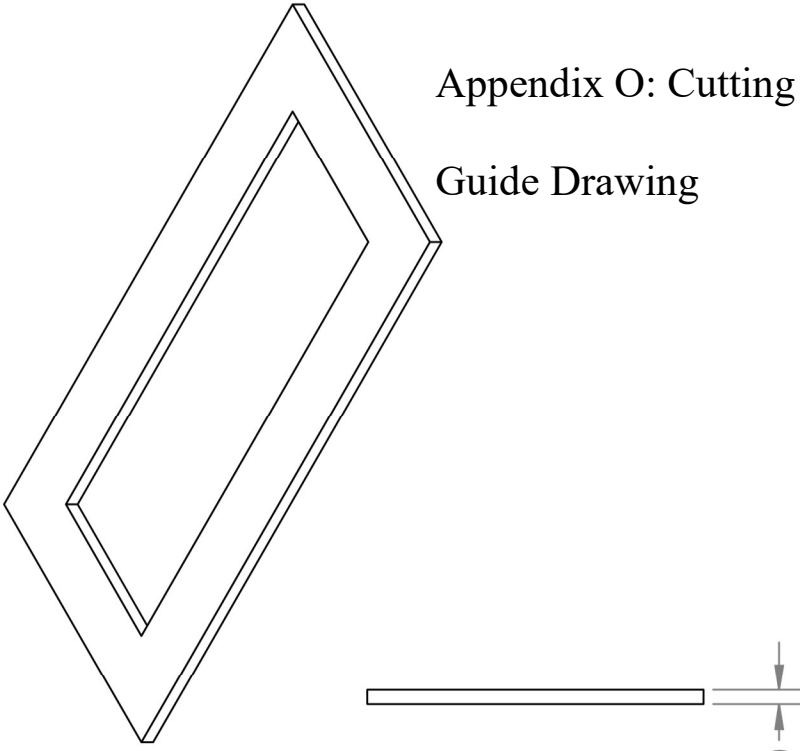
1

2

B

B

Appendix O: Cutting Guide Drawing



1.90

A

A

DRAWN		NAME		DATE	
E. Morra		E. Morra		2/28/19	
CHECKED					
ENG APPR.					
MFG APPR.					
Q.A.					
COMMENTS:					
UNLESS OTHERWISE SPECIFIED:					
DIMENSIONS ARE IN MM					
TOLERANCES:					
ANGULAR: 0°20'					
ONE PLACE DECIMAL ±.1					
TWO PLACE DECIMAL ±.01					
THREE PLACE DECIMAL ±.005					
INTERPRET GEOMETRIC TOLERANCING PER:					
MATERIAL PLA					
FINISH					
NEXT ASSY		USED ON			
APPLICATION				DO NOT SCALE DRAWING	

TITLE:

Cutting guard

SIZE DWG. NO. REV

A

SCALE: 1:1 WEIGHT: SHEET 1 OF 1

PROPRIETARY AND CONFIDENTIAL
 THE INFORMATION CONTAINED IN THIS DRAWING IS THE SOLE PROPERTY OF <INSERT COMPANY NAME HERE>. ANY REPRODUCTION IN PART OR AS A WHOLE WITHOUT THE WRITTEN PERMISSION OF <INSERT COMPANY NAME HERE> IS PROHIBITED.

1

2

Appendix P: Imaging Exposure Settings

Experiment 1:

Imaging Time Point	Phase 1 Exposure	DiI Exposure
24hr	319 ms	2000 ms
48hr	358 ms	1088 ms

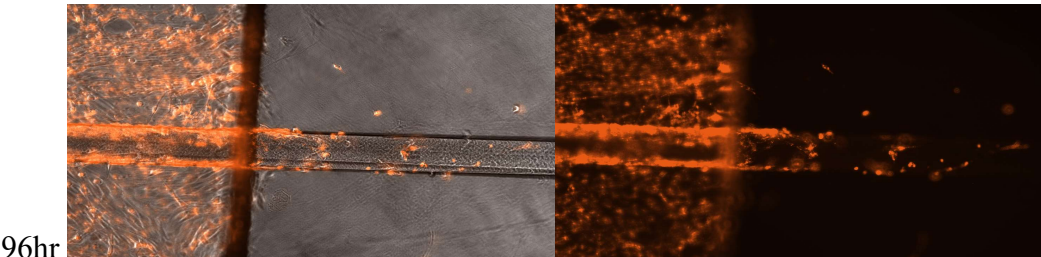
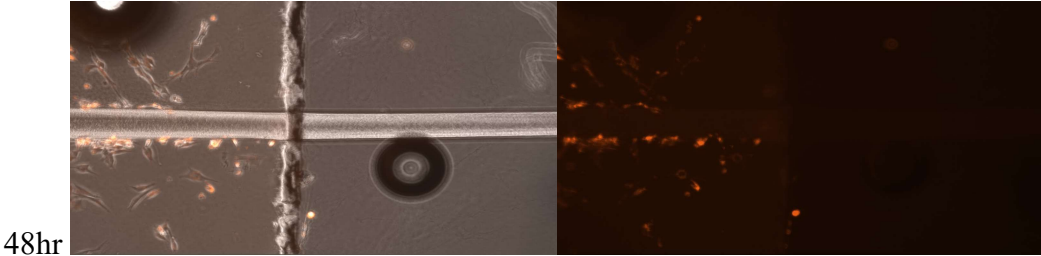
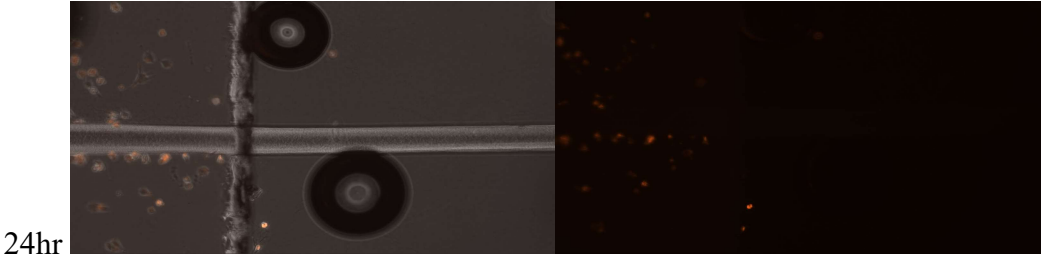
Experiment 2:

Imaging Time Point	Phase 1 Exposure	DiI Exposure
24hr	31 ms	727 ms
72hr	314 ms	514 ms
96hr	430 ms	1378 ms

Experiment 3:

Imaging Time Point	Phase 1 Exposure	DiI Exposure
24hr	350 ms	3000 ms
48hr	260 ms	3000 ms

Appendix Q: Outgrowth Images: 24-96hr



Appendix R: Gantt Chart

A Term

Week	A-Term						
	1	2	3	4	5	6	7
Item							
Introduction							
Literature Review							
Project Strategy							
Gantt Chart							
Alternative Designs							
Test Alternative Designs							
Finalize Design							
Fabricate Final Design							
Test Existing Design (Meg's)							
Test Final Design							
>>> Assembly Testing							
>>> Cell Viability Testing							
>>> Throughput Testing							
Analysis and Recommendations							
MQP Report							
Introduction							
Background							
Methodology							
Design Overview							
Design Verificiation							
Final Design and Validation							
Conclusions and Recommendations							
Final Presentation							
Value Creation							
Lab Notebook							
Self & Team Evaluations							
Emily Morra							
Erin Heinle							
Alyssa Paul							
Emily Mossman							

B Term

Week	B-Term						
	1	2	3	4	5	6	7
Item							
Introduction							
Literature Review							
Project Strategy	█						
Gantt Chart							█
Alternative Designs	█	█	█	█			
Test Alternative Designs				█	█	█	█
Finalize Design							█
Fabricate Final Design							
Test Existing Design (Meg's)							
Test Final Design							
>>> Assembly Testing							
>>> Cell Viability Testing							
>>> Throughput Testing							
Analysis and Recommendations							
MQP Report							
Introduction							
Background	█						
Methodology	█	█	█	█			
Design Overview		█	█	█	█	█	
Design Verificiation							█
Final Design and Validation							
Conclusions and Recommendations							
Final Presentation				█	█	█	█
Value Creation							
Lab Notebook	█	█	█	█	█	█	█
Self & Team Evaluations							█
Emily Morra							
Erin Heinle							
Alyssa Paul							
Emily Mossman							

C Term

Week	C-Term						
	1	2	3	4	5	6	7
Item							
Introduction							
Literature Review							
Project Strategy							
Gantt Chart							
Alternative Designs							
Test Alternative Designs							
Finalize Design							
Fabricate Final Design							
Test Existing Design (Meg's)							
Test Final Design							
>>> Assembly Testing							
>>> Cell Viability Testing							
>>> Throughput Testing							
Analysis and Recommendations							
MQP Report							
Introduction							
Background							
Methodology							
Design Overview							
Design Verficiation							
Final Design and Validation							
Conclusions and Recommendations							
Final Presentation							
Value Creation							
Lab Notebook							
Self & Team Evaluations							
Emily Morra							
Erin Heinle							
Alyssa Paul							
Emily Mossman							

D Term

Week	D-Term						
	1	2	3	4	5	6	7
Item							
Introduction							
Literature Review							
Project Strategy							
Gantt Chart							
Alternative Designs							
Test Alternative Designs							
Finalize Design							
Fabricate Final Design							
Test Existing Design (Meg's)							
Test Final Design							
>>> Assembly Testing							
>>> Cell Viability Testing							
>>> Throughput Testing							
Analysis and Recommendations							
MQP Report							
Introduction							
Background							
Methodology							
Design Overview							
Design Verificiation							
Final Design and Validation							
Conclusions and Recommendations							
Final Presentation							
Value Creation							
Lab Notebook							
Self & Team Evaluations							
Emily Morra							
Erin Heinle							
Alyssa Paul							
Emily Mossman							

Appendix S: Expense Report/Budget Analysis

Starting Budget	\$1,000
- Lab Fee	- \$400
- McMaster	- \$12.29
Remaining Budget	\$587.71

Appendix T: Bill of Materials

Name	Quantity	Details	Cost
Delrin™	1	½"x 4"x 12" bar McMaster-Carr #8662K46	\$24.27 per foot
End-mill (for machining mold)	1	3 Flute, 3 Degree Taper, 3/32" Mill Diameter, 1" Long Cut McMaster-Carr #8936A48	\$20.57
PDMS	30g base and 3g curing agent used per mold	Sylgard® 184 Silicone Elastomer Kit (3.9 kg) Material # 2065622	\$503.79 for 3.9 kg kit
PLA	5.90g	Cutting guide printed on Ultimaker 3D printer	\$0.03/g
Cutting tool blades	3	Blue Hawk™ 3.5 in Scraper Blades Product # 0089625	\$2.28 for package of 5
Cutting tool screws	2	Hillman 6/32 x 1 in machine screws Product # 491282	\$1.28 (5 screws and 5 nuts)